PB82-237934

Validation and Application of the SEASAT-SMMR Geophysical Algorithms

Washington Univ., Seattle

Prepared for

National Oceanic and Atmospheric Administration
Rockville, MD

Feb 82

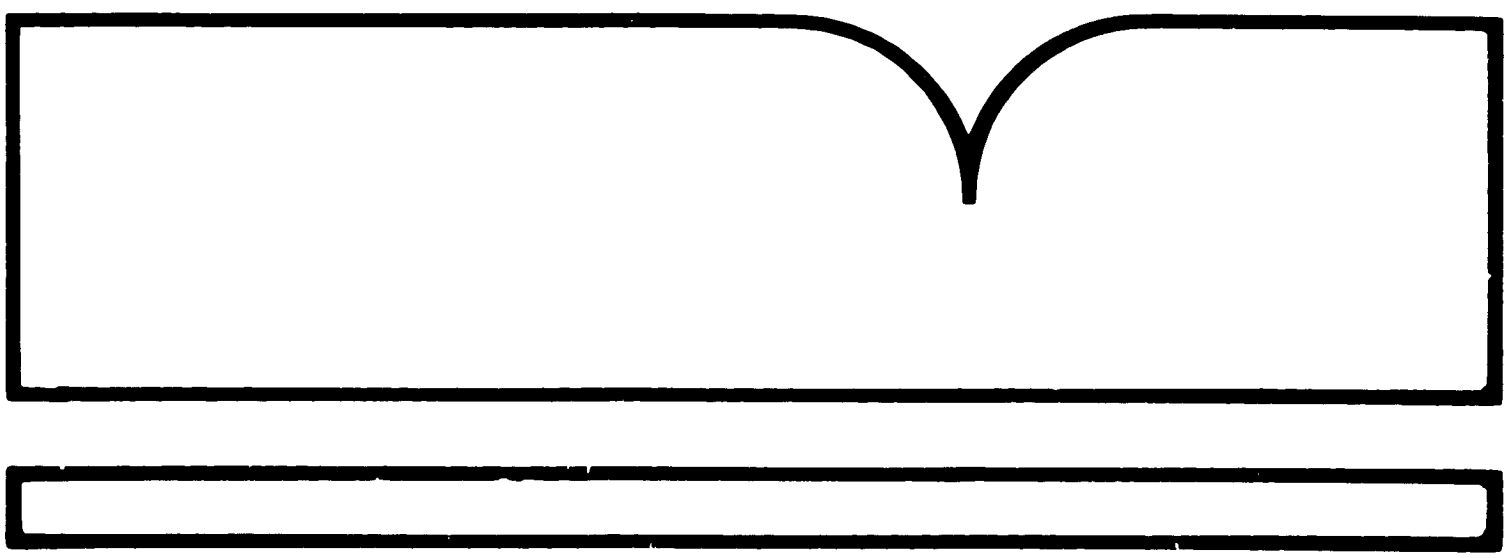

FINAL REPORT NOAA CONTRACT NA 78-SAC-04102

VALIDATION AND APPLICATION OF THE SEASAT-SMMR GEOPHYSICAL ALGORITHMS

KRISTINA B. KATSAROS

LYNN A. MCMURDIE

DEPARTMENT OF ATMOSPHERIC SCIENCES
UNIVERSITY OF WASHINGTON
SEATTLE, WASHINGTON 98195

FEBRUARY 1982

Atmospheric Sciences Contribution Number 616

FINAL REPORT NOAA CONTRACT NA 78-SAC-04102

VALIDATION AND APPLICATION OF THE SEASAT-SMMR GEOPHYSICAL ALGORITHMS

KRISTINA B. KATSAROS

LYNN A. MCMURDIE

DEPARTMENT OF ATMOSPHERIC SCIENCES
UNIVERSITY OF WASHINGTON
SEATTLE, WASHINGTON 98195

FEBRUARY 1982

Atmospheric Sciences Contribution Number 616

NOAA FORM 25-13 (1-78)

BIBLIOGRAPHIC DATA SHEET

U. S. DEPARTMENT OF COMMERCE
NATIONAL OCEANIC AND ATMOSPHERIC ADMINISTRATION

1. NOAA ACCESSION NUMBER	2.	3. RECIPIENT'S ACCESSION NUMBER
NOAA-82051012		PB82-237934

4. TITLE AND SUBTITLE
Validation and Application of the SEASAT-SMMR Geophysical Algorithms

5. REPORT DATE
Feb 1982

6.

7. AUTHOR(S)
Kristina B. Katsaros and Lynn A. McMurdie

8. REPORT NO.
UW/AS Contrib. 616

9. PERFORMING ORGANIZATION NAME AND ADDRESS
Washington University, Seattle, 98195,
Department of Atmospheric Sciences

10. PROJECT/TASK NO.

11. CONTRACT/GRANT NO.
NA 78-SAC-04102

12. SPONSORING ORGANIZATION NAME AND ADDRESS
National Oceanographic and Atmsopheric Administration,
Rockville, MD 20852

13. TYPE OF REPORT AND PERIOD COVERED
Final Rept.

14.

15. PUBLICATION REFERENCE Washington University, Department of Atmsopheric Sciences, Final Report to NOAA, February 1982. Atmospheric Sciences Contribution No. 616. 94 p, 23 fig, 1 tab, 27 ref, 4 append.

16. ABSTRACT

The work was concentrated on verification of the atmospheric water channels on Seasat's Scanning Multichannel Microwave Radiometer (SMMR). Data from the Gulf of Alaska Experiment (GOASEX), tropical island stations, and particularly from the Joint Air Sea Interaction (JASIN) experiment have been used to compare with the SMMR algorithm predictions. SMMR's water vapor has been found to be at least as accurate as conventional radiosondes. Liquid water and rain rate have insufficient comparisons for statistical results, but can be said to show promise in a qualitative sense. The Seasat SMMR maps of the atmospheric water components were found to be very useful in helping to locate fronts and cloudy and rainy areas in the JASIN experiment. Continuing work on applying Seasat SMMR data in analyzing Pacific midlatitude cyclones is also reported and some speculation on future uses of this totally new marine atmospheric information are offered. (Author modified)

17. KEY WORDS AND DOCUMENT ANALYSIS

17A. DESCRIPTORS

*Remote sensing, *Air water interactions, Verifying, Water vapor, Algorithms, Marine atmospheres, Cyclones

17B. IDENTIFIERS/OPEN-ENDED TERMS

*Air-sea interaction, Seasat, Scanning Multichannel Microwave Radiometer (SMMR), Gulf of Alaska Experiment (GOASEX), Joint Air Sea Interaction experiment (JASIN)

17C. COSATI FIELD/GROUP

4B

18. AVAILABILITY STATEMENT
Released for distribution:

19. SECURITY CLASS (This report) UNCLASSIFIED

21. NO. OF PAGES 95 p.

20. SECURITY CLASS (This report) UNCLASSIFIED

22. PRICE

NOAA FORM 25-13 (1-78) SUPERSEDES ALL PREVIOUS EDITIONS.

FOREWORD

The work reported here was sponsored by a joint program of the National Aeronautics and Space Administration and the National Oceanographic and Atmospheric Administration. The purpose of this program was to validate the products of the many experimental remote sensing systems on the Seasat satellite and to show their usefulness in applications to atmospheric and oceanic studies.

Our research has addressed both validation and application of three of the geophysical products from the Seasat Scanning Multichannel Microwave Radiometer (SMMR), viz. integrated atmospheric water vapor, integrated liquid water and rain rate over the oceans.

The contract was administered through the office of Dr. John W. Sherman III, with Dr. John C. Alishouse as contract monitor. The work has benefited from very efficient management. We would also like to express sincere appreciation to Dr. Alishouse for invaluable cooperation in many aspects of the research.

Kristina B. Katsaros

Principal Investigator

TABLE OF CONTENTS

ABSTRACT

The work during this two year contract has been concentrated on verification of the atmospheric water channels on Seasat's Scanning Multichannel Microwave Radiometer (SMMR). Data from the Gulf of Alaska Experiment (GOASEX), tropical island stations, and particularly from the Joint Air Sea Interaction (JASIN) experiment have been used to compare with the SMMR algorithm predictions. SMMR's water vapor has been found to be at least as accurate as conventional radiosondes. Liquid water and rain rate have insufficient comparisons for statistical results, but can be said to show promise in a qualitative sense. The Seasat SMMR maps of the atmospheric water components were found to be very useful in helping to locate fronts and cloudy and rainy areas in the JASIN experiment. Continuing work on applying Seasat SMMR data in analyzing Pacific midlatitude cyclones is also reported herein, and some speculation on future uses of this totally new marine atmospheric information are offered.

I. INTRODUCTION

The original aim of this work was to use sea surface temperature data obtained by our group during the Joint Air Sea Interaction Experiment 1978 (Royal Society, 1979) in the North Atlantic for verification of the surface temperatures produced from the Seasat Scanning Multichannel Microwave Radiometer (SMMR)[1]. Soon SMMR surface temperatures in this region were found to be greatly contaminated by radio frequency interference and land in the side lobes of the antennae. Our interest has therefore turned instead to the atmospheric water parameters produced by SMMR algorithms. Not much attention was given to these channels at first. They were mainly on the instrument to provide corrections for the long wave channels of SMMR and the radar type sensors (Gloersen and Barath, 1977).

However, interest in remote sensing of the atmospheric water parameters dates back to the 1960's. Deirmendjian (1963, 1968) made thorough calculations of Mie parameters for liquid water spheres and ice spheres of absorption, scattering and phase matrix coefficients for various wavelengths and drop size distributions. He showed that these coefficients varied with wavelength, drop size distributions, temperature, and phase of the hydrometeors. Savage (1976) made simil. alculations for wavelengths in the microwave region, and then applied th. values of these coefficients to a radiative model. By changing atmospheric parameters such as cloud temperature, rainfall rate, lapse rates, etc., he calculated brightness temperatures that would be received by a satellite radiometer. Other models have also appeared in the literature (Weinmann and Davis, 1978; Jung, 1980).

---

[1] Information about the Seasat satellite and the SMMR instrument can be found in Lipes, et al. (1979) and Njoku, Stacey and Barath (1980).

Since there are an infinite number of possible atmospheric conditions that could be modeled, the inverse problem (deducing atmospheric parameters from given brightness temperatures) is not so easily solved. Nevertheless, based on these earlier studies and further empirical studies, algorithms have been constructed which can retrieve atmospheric parameters from the brightness temperatures of SMMR's channels at 18, 21, and 37 GHz (Bierman et al., 1978; Wilheit and Chang, 1979).

There are differences in approach between the two algorithms referenced above, both in the way they are formulated and in the numerical techniques used. For these reasons the Seasat project processed the SMMR data using both algorithms during the evaluation period. In the first SMMR verification workshop (GOASEX I Report, 1979) the two algorithms, "Wentz" and "Wilheit" named after their originators, performed reasonably well in midlatitudes, where the total water vapor content was less than 35 kg/m^2 and the rain rates were low, typically < 3 mm/hr. To test a wider range of conditions, we sought radiosonde data from tropical regions. Such data is available from weather ship Tango and atolls in the Pacific. We only used data from atolls small enough so that the emission by the land does not contaminate the SMMR signals (SMMR Mini I and II, 1979).

II. VALIDATION OF SMMR ALGORITHMS

In 1980 a Seasat-JASIN workshop was held (Businger et al., 1980). Many more data points were contributed to our intercomparisons because of the frequent radiosonde schedule at a 200 km triangle of meteorological ships. The results of this work was presented at the COSPAR/SCOR/IUCRM Colloquium in Venice, Italy in May of 1980 (Katsaros et al., 1981, see

Appendix A). Further work on radiosonde intercomparisons has been performed by Alishouse (1982).

During the Seasat-JASIN workshop, the potential contributions of SMMR's products to the objectives of the JASIN program became evident and were brought to the attention of our European colleagues through a short article in *Nature* (Taylor et al., 1981, see Appendix B). It was particularly valuable to have the areal coverage of integrated water vapor in establishing locations of surface fronts. The prevalence of research ships on the water also allowed more detailed comparison between surface based observations and SMMR produced rain rates. This study where SMMR products were applied to analyze the meteorological situation is found in Taylor et al. (1982, see Appendix C).

III. APPLICATIONS OF SMMR GEOPHYSICAL PARAMETERS

Those of us involved in looking at the atmospheric water informa ion provided by SMMR (vapor in kg/m^2, liquid in kg/m^2, and rain rate in mm/hr) feel that it has great potential both for atmospheric and oceanic research and in the future for operational purposes as well. Because the atmospheric water products were not the main motivation for Seasat, an optimistic presentation of the potential of this information was given at a workshop in Wisconsin (Katsaros, 1981, see Appendix D).

There is still much work to be done to put SMMR products of liquid water and rain rate on a really firm quantitative basis. A new algorithm based on Wilheit's has been offered by Chester (1981), which appears to be more accurate. However, the comparison data remain very limited for these two parameters and we will probably only be able to use Seasat SMMR's data

in a qualitative sense. Nonetheless, they give us a totally new perspective on the atmosphere over the ocean.

The integrated atmospheric water vapor signals are, however, already competitive with the same information from radiosondes, and by SMMR's spatial coverage provide both dependable and totally new information. We are still keeping a watchful eye on problems which may be present when evaluating water vapor content in the presence of rain.

With the encouraging results of the verification phase of the work, we are now applying SMMR information to a study of the evolution of mid-latitude cyclones during their passage across the North Pacific Ocean. This work is continuing under a new contract, but a case study of a single storm is reported below.

IV. ONGOING WORK STUDYING PACIFIC CYCLONES

A. Background and Objectives

Nimbus E Microwave Spectrometer (NEMS), Electrically Scanning Microwave Radiometer (ESMR), and Scanning Microwave Spectrometer (SCAMS), satellite microwave radiometers, have been reasonably successful in determining atmospheric water parameters of water vapor, liquid water, and rain rate (Savage, 1976; Staelin et al., 1976; Chang and Wilheit, 1979). By using two-week averages, Grody et al. (1980) defined the Intertropical Convergence Zone (ITCZ) in terms of precipitable water and liquid water. However, these previous radiometers did not have spatial resolutions commensurate with the scale of phenomena such as frontal rainbands of the order of 30 km. With Seasat's SMMR on the other hand, we have the opportunity to examine in more

detail the atmospheric distribution of rain, liquid water, and water vapor by virtue of the resolutions being 27 km, 54 km and 54 km respectively.

The birthplace of Pacific northwest storms is in the Gulf of Alaska. As they cross the ocean, they develop and change and often reach the west coast of North America in an occluded form (Nuss, 1980; Overland and Heister, 1980). Traditionally, the strength and structure of these storms was examined by merchant and weather ships, and buoy reports. More recently GOES-W geosynchronous satellite pictures in the infrared and visible wavelengths have improved the synoptic analyses over the Pacific Ocean. Although these data sources provide information on areas of cloudiness, surface pressure, temperature, and wind speeds, information on the mesoscale structure is lacking. A SMMR type instrument can possibly fill this gap. This project examines the possibilities of studying the mesoscale structure of storms at different stages (i.e. initial, developing, and mature) in terms of integrated atmospheric water vapor, integrated liquid water, and rainfall rate as seen by the Seasat SMMR.

Fields of atmospheric water vapor, liquid water, and rainfall rate are drawn for particular revolutions and are correlated qualitatively with visible and IR satellite pictures, National Meteorological Center analysis, and ship reports. Questions we are addressing include: How do these fields change with the development of a Gulf of Alaska storm? Does SMMR aid in location of fronts? Can SMMR be used to increase weather forecasting ability over the oceans and in the landfall regions of these storms?

B. Methods and Data Analysis

Since the Seasat satellite was only operating during the months July

through September 1978, the possible number of storms to study was limited. During the summer months the storms that do develop tend to be weak, disorganized and occlude rapidly before reaching the west coast of North America (Nuss, 1980). Nevertheless, there were some storms in the Seasat lifetime that are adequate.

The criteria used in selecting storms was fairly subjective. It was desired to study storms that exhibited a definite life cycle with initial, developing, and mature stages, so National Meteorological Center surface and 500 mb maps for the Seasat period were studied. Then storms with a definite life cycle, well developed surface low, and reports of some rain were chosen. On the basis of visible and infrared GOES-W satellite pictures and intersection with SMMR swaths, the storms were given varying priority.

Characteristics of the different stages of a storm are based on Wallace and Hobbs (1977) and are shown schematically in Figure 1. Also shown in Figure 1 are criteria used in determining which region is sampled by Seasat. The categories were defined as follows: SMMR samples a "prefrontal" region when it just crosses the warm front, or is on the warm side of the cold front. The "frontal region" is sampled when SMMR passes over the apex of the frontal wave. This includes the surface low in the case of the initial and developing stages of a storm. The "postfrontal" region is sampled when SMMR passes over the cold front or behind it. This includes the surface low in the case of the mature stage.

Table 1 lists the chosen storms with a brief description of each storm and the revolutions that sample them. They are listed in order of priority based on criteria outlined above. Also included are the region and the stage of the storm that is sampled by each revolution with a statement of the quality.

C. A Case Study

So far, only the storm in the period 16-20 September has been studied in any detail. Like many storms that track across the North Pacific (Nuss, 1980), this storm began as a wave that formed in the cold front region of a very old system with the low center over the Aleutian Islands. It was analyzed at 1200Z, Saturday, 16 September as a stationary front stretching from 145°W to the dateline at 30°N, and a separate mature system located over the Aleutian Islands (see Figure 2a). But in the satellite pictures for this time, the two systems are hard to distinguish. By 0600Z, Sunday, 17 September (Figure 3b) a surface low had developed in the vicinity of 50°N and 160°W with a thick cloud shield as seen by GOES-W satellite ahead of the storm. The upper level flow became westerly-southwesterly during this time. During 17 September the system began to occlude and join up with an old surface low at 55°N and 175°W. By 1200Z, 18 September (Figure 4b) the upper level low had deepened and moved eastward, producing a southwesterly flow in the region of the storm system. The system was in a mature stage at this point with an occluded front stretching along the north British Columbia and Alaskan coast. At 1800Z, 18 September (Figure 4c) a wave developed along the cold front at 48°N and 150°W. At 0000Z, 19 September it is evident that the system had become "vertical" with the surface low and upper level low at the same location (see Figures 5a,b). The system rapidly occluded and wound up, and by 1800Z, 19 September this system had reached the British Columbia coast (Figure 5c). Surface and 500 mb charts for 16-20 September are presented in Figures 2-6.

Two revolutions that sample this storm, rev 1198 and rev 1212, have been analyzed. Figures 7a, b, c correspond to integrated water vapor,

liquid water, and rainfall rates, respectively, for rev 1198 (1830Z, 18 September); and Figures 8a, b, c correspond to the same fields for rev 1212 (1810Z, 19 September). Also shown in these figures are the visible and infrared GOES-W satellite pictures and NMC surface analysis for the time of the Seasat pass. The dashed lines on these figures enclose the SMMR swath. A few ship reports are included on Figures 7c and 8c.

Figure 7c, rainfall rate for rev 1198, shows that the areas of rain are concentrated along the cold front. Although there is no measure of rainfall rate in ship reports, weathership C7P at 50°N 145°W (indicated with a P on Figure 7c) reported steady rain from 1500Z to 2100Z. Two other ships located outside the SMMR swath reported light drizzle.

Like the rainfall rate field, the integrated liquid water field (Figure 7b) shows the heaviest concentration along the front. Behind the cold front, north of 50°N and from 140°W - 150°W, there are two areas of intermediate concentration of liquid water. As expected, they coincide with areas of bright clouds.

Like the previous two fields, Figure 7a of the integrated water vapor shows maxima along and slightly ahead of the frontal region. South of the front the contour lines of water vapor in kg/m^2 are widely spaced; whereas to the north of the front, the contour lines are closely packed. This corresponds well with the idea that a front is a boundary between two air masses, one warm and moist, the other cool and dry.

In Figure 8c rainfall rate for rev 1212, there are again three distinct rain areas located along and slightly ahead of the cold front. The middle rain area shows an intensity greater than 3 mm/hr. There are four ship

reports plotted in the vicinity of the area, all of which are reporting rain. This field does not differ radically from the rainfall rate field of rev 1198.

The liquid water field (Figure 8b) again shows maxima along the front. There appears to be a large amount of liquid water at 48°N 133°W in the same spot as the strongest rainband. There is an area of integrated liquid water greater than .2 kg/m^2 behind the occluded portion of the frontal system that corresponds well with the satellite picture. This pattern is somewhat different from what was seen in Figure 7b.

The water vapor field of rev 1212 (Figure 8a) shows a stronger gradient behind the front than is seen in Figure 7a, rev 1198. The water vapor seems to be much more concentrated along the front. In Figure 8a behind the occluded portion of the system, the air is much drier and has a more uniform moisture field, as evidenced by the 15 kg/m^2 line.

As Figures 7a, b, c and 8a, b, c show, the patterns derived from SMMR correspond well qualitatively with the visible and infrared satellite pictures. Also brought out by these patterns are features that cannot be distinguished on the satellite pictures. These include rain areas and areas of large amounts of liquid water. The atmospheric water vapor field may prove to be a useful tool in determining how much precipitable water is available in a storm. This could then be used towards improving quantitative precipitation forecasts.

The other revolutions listed in Table 1 for this storm will be analyzed in a similar fashion. Therefore, the storm will be sufficiently sampled at all stages to follow its evolution. Further plans include constructing a composite storm from the six listed in Table 1.

REFERENCES

Alishouse, J. 1982: Total precipitable water and rainfall determination from the Seasat Scanning Multichannel Microwave Radiometer (SMMR), *J. Geophys. Res.* (submitted).

Bierman, G. J., R. G. Lipes, F. J. Wentz, 1978: Paper presented at the Twelfth Annual Asilomar Conference on Circuits, Systems, and Computers, Pacific Grove, California, 6-8 November, 1978.

Businger, J. A., R. H. Stewart, T. Guymer, D. B. Lame and G. H. Born, 1980: *Seasat-JASIN Workshop Report, Volume 1: Findings and Conclusions.* JPL Publication 80-62, Jet Propulsion Laboratory, Pasadena.

Chang, A.T.C. and T. T. Wilheit, 1979: Remote sensing of atmospheric water vapor, liquid water, and wind speed at the ocean surface by passive microwave techniques from Nimbus 5 satellite, *Radio Sci., 14*, 793-802.

Chester, T. J. 1981. Final changes in SMMR geophysical data production algorithm, *SMMR Mini Workshop IV*, JPL-622-234-NASA, Jet Propulsion Laboratory, Pasadena.

Deirmendjian, D. 1963: *Complete Microwave Scattering and Extinction Properties of Polydispersed Cloud and Rain Elements*, The Rand Corporation, R-422-PR.

Deirmendjian, D. 1968: *Electromagnetic Scattering on Spherical Polydispersions*, Elsevier Press, New York, 290 pp.

GOASEX I Report, 1979: *Seasat Gulf of Alaska Workshop Report*, JPL-622-101-NASA, Vol. 1, Jet Propulsion Laboratory, Pasadena.

Gloersen, P. and F. T. Barath, 1977: A scanning multichannel microwave radiometer for Nimbus G and Seasat-A, *IEEE J. of Oceanic Engineering, OE-2*, 1172-1178.

Grody, N. C., A. Gruber and W. C. Shen, 1980: Atmospheric water content over the tropical Pacific derived from the Nimbus-6 scanning microwave spectrometer, *J. Appl. Meteorol., 19*, 986-996.

Jung, H. J. 1980: The determination of rainfall rates from satellite measurements of the thermal microwave emission, *Atmos. Physics, 53*, 366-388.

Katsaros, K. B. 1981: Seasat SMMR's atmospheric water determinations, in *Proceedings of a Workshop on Applications of Existing Satellite Data to the Study of the Ocean Surface Energetics, 19-21 November 1980, University of Wisconsin-Madison*, Ed. C. Gautier, 145-149.

Katsaros, K. B., P. K. Taylor, J. C. Alishouse and R. G. Lipes, 1981: Quality of Seasat SMMR (Scanning Multichannel Microwave Radiometer) atmospheric water determinations, in *Oceanography from Space*, Ed. J.F.R. Gower, Plenum Publishing Corporation, 691-706.

Lipes, R. G., R. L. Bernstein, V. J. Cardone, K. B. Katsaros, E. G. Njoku, A. L. Riley, D. B. Ross, C. T. Swift and F. J. Wentz, 1979: Seasat scanning multichannel microwave radiometer: Results of the Gulf of Alaska Workshop, *Science, 204*, 1415-1417.

Njoku, E. G., J. M. Stacey and F. T. Barath, 1980: The Seasat Scanning Multichannel Microwave Radiometer (SMMR): Instrument description and performance, *IEEE J. Oceanic Engineering, OE-5*, 100-115.

Nuss, W. 1980: Analysis of Past Data in STREX Area, distributed to STREX Principal Investigators by International STREX Office, Pacific Marine Environmental Laboratories, NOAA, Seattle, October 1980.

Overland, J. E. and T. R. Heister, 1980: Development of a synoptic climatology for the northeast Gulf of Alaska, *J. Appl. Meteorol., 19*, 1-14.

Royal Society, 1979: *Air-Sea Interaction Project.* Summary of the 1978 Field Experiment (JASIN, 1978), The Royal Society, London, 139 pp.

Savage, R. C. 1976: The Transfer of Thermal Microwaves through Hydrometeors. Ph.D. Thesis, University of Wisconsin-Madison, 147 pp.

SMMR-Mini I, 1979: *Seasat SMMR-Mini Workshop I*, JPL-622-208-NASA, Jet Propulsion Laboratory, Pasadena.

SMMR-Mini II, 1979: *Seasat SMMR-Mini Workshop II*, JPL-622-212-NASA, Jet Propulsion Laboratory, Pasadena.

Staelin, D. H., K. F. Kunzi, R. L. Pettyjohn, R.K.L. Poon, R. W. Wilcox and J. W. Waters, 1976: Remote sensing of atmospheric water vapour and liquid water with the Nimbus 5 microwave spectrometer, *J. Appl. Meteorol., 15*, 1204-1214.

Taylor, P. K., T. H. Guymer, K. B. Katsaros and R. G. Lipes, 1982: Atmospheric water distributions determined by the Seasat multichannel microwave radiometer, in *Proceedings of the Global Water Budget Symposium, 10-15 August 1981, Oxford, England* (in press).

Taylor, P. K., K. B. Katsaros and R. G. Lipes, 1981: Determinations by Seasat of atmospheric water and synoptic fronts, *Nature, 294*, 737-739.

Wallace, J. M. and P. V. Hobbs, 1977: *Atmospheric Science: An Introductory Survey*, Academic Press, Inc., New York.

Weinmann, J. A. and R. Davis, 1978: Thermal microwave radiances from horizontally finite clouds of hydrometeors, *J. Geophys. Res., 83*, 3099-3107.

Wilheit, T. T. and A.T.C. Chang, 1979: *An Algorithm for Retrieval of Ocean Surface and Atmospheric Parameters from the Observations of the Scanning Multichannel Microwave Radiometer (SMMR)*, NASA Technical Memorandum 80277, NASA Goddard Space Flight Center, Greenbelt, MD.

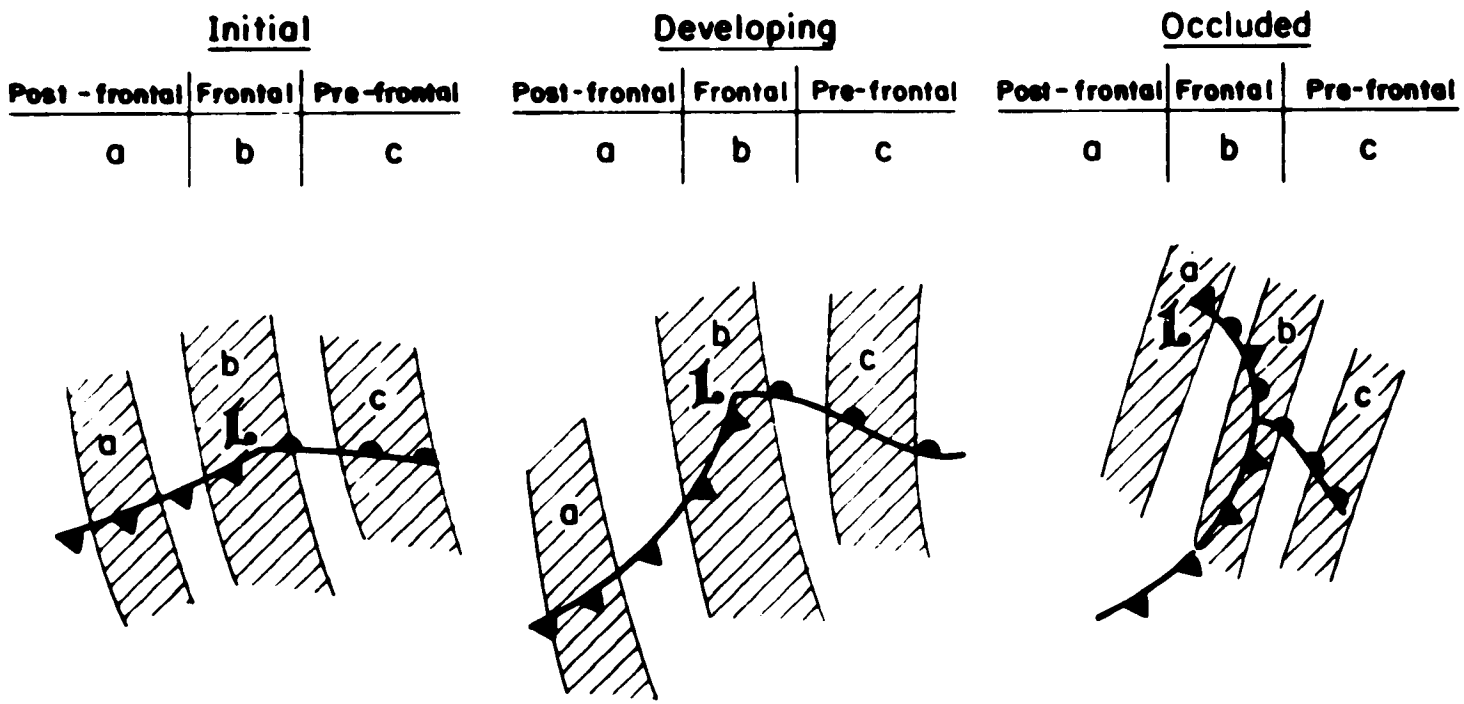

Figure 1. Criteria in determining the stage of a storm (based on Wallace and Hobbs, 1977), and which portion is sampled by Seasat SMMR. a, b, c refer to possible SMMR swaths.

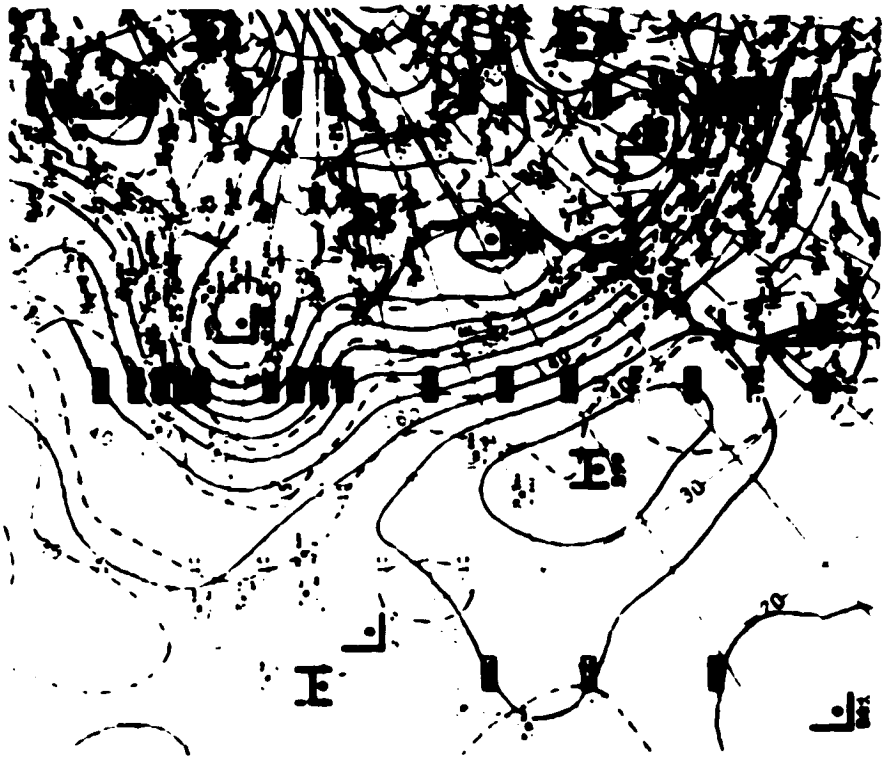

Figure 2a. NMC surface analysis for 1200Z 16 September 1978

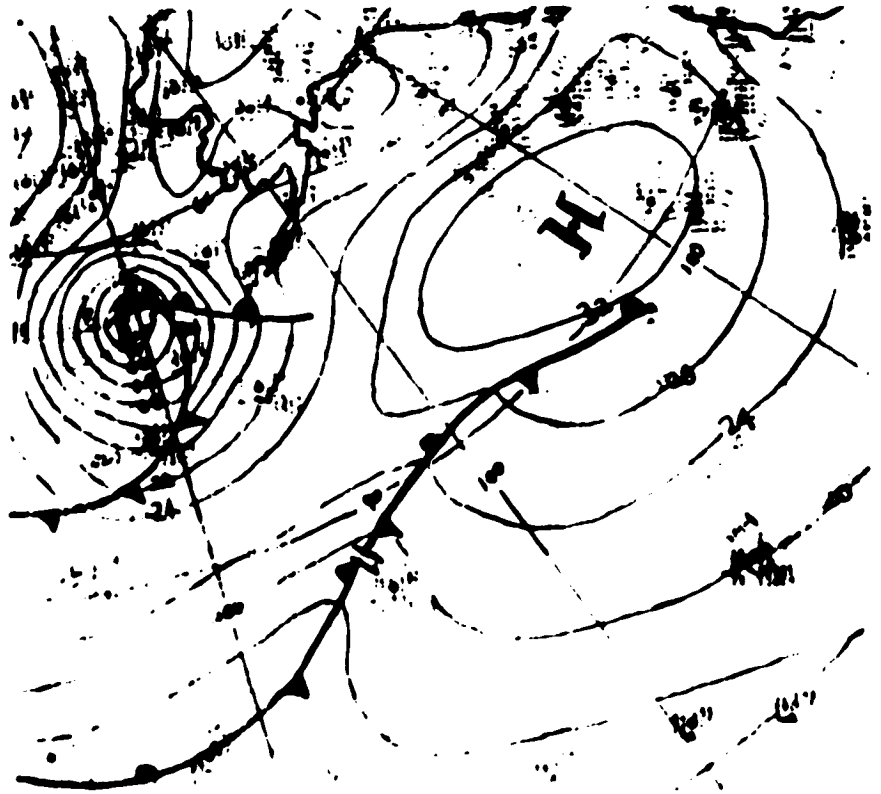

Figure 2b. NMC 500 mb analysis for 1200Z 16 September 1978

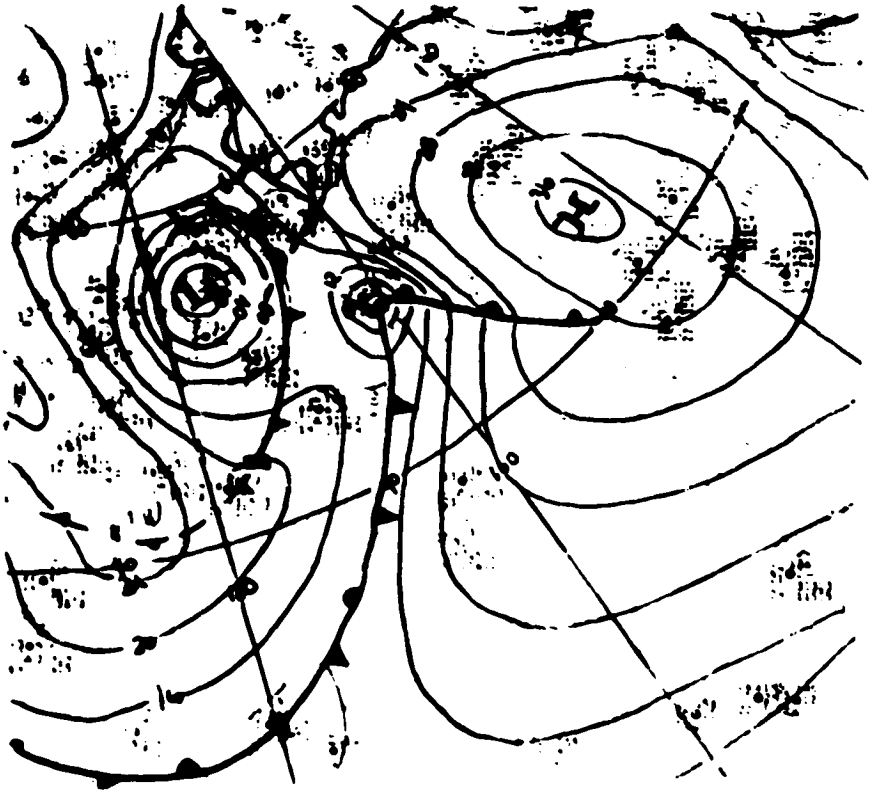

Figure 3b. NMC surface analysis for 0600Z 17 September 1978

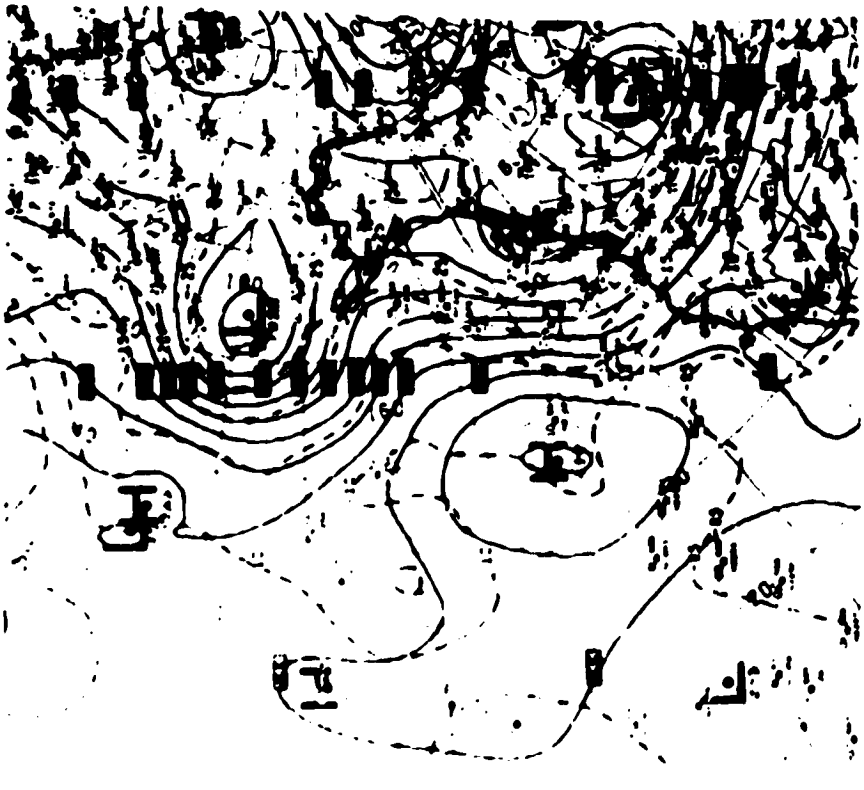

Figure 3a. NMC 500 mb analysis for 0000Z 17 September 1978

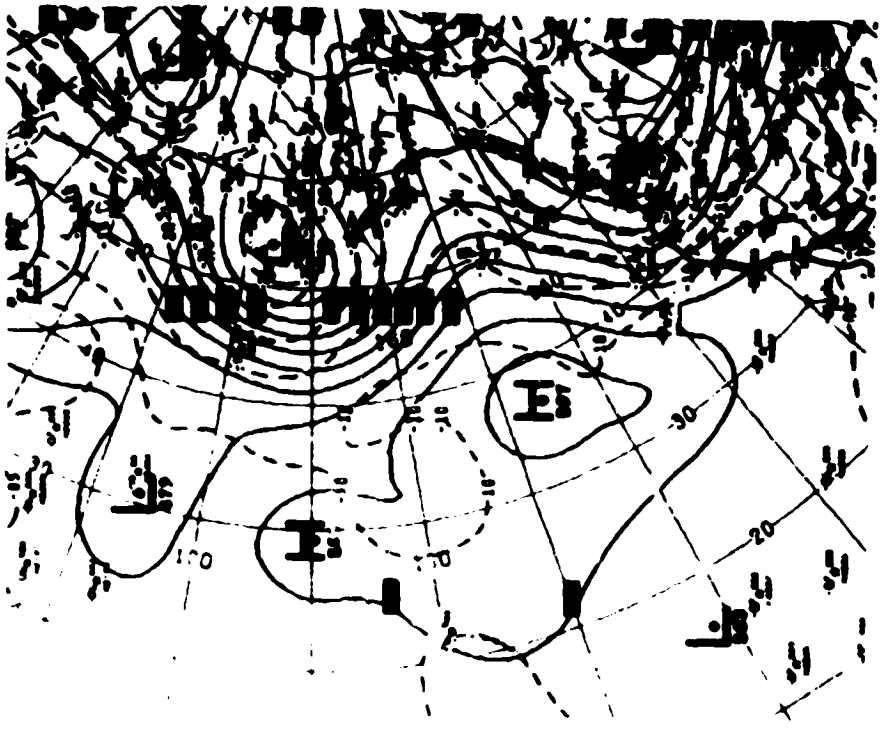

Figure 3d. NMC 500 mb analysis for 1200 Z
17 September 1978

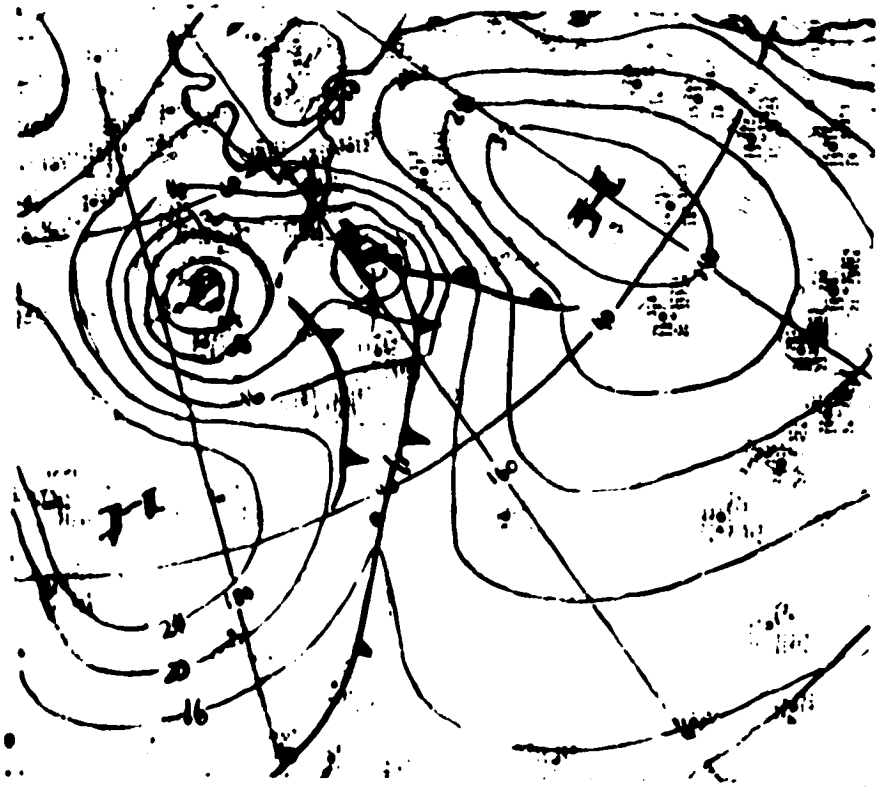

Figure 3c. NMC surface analysis for 1200Z
17 September 1978

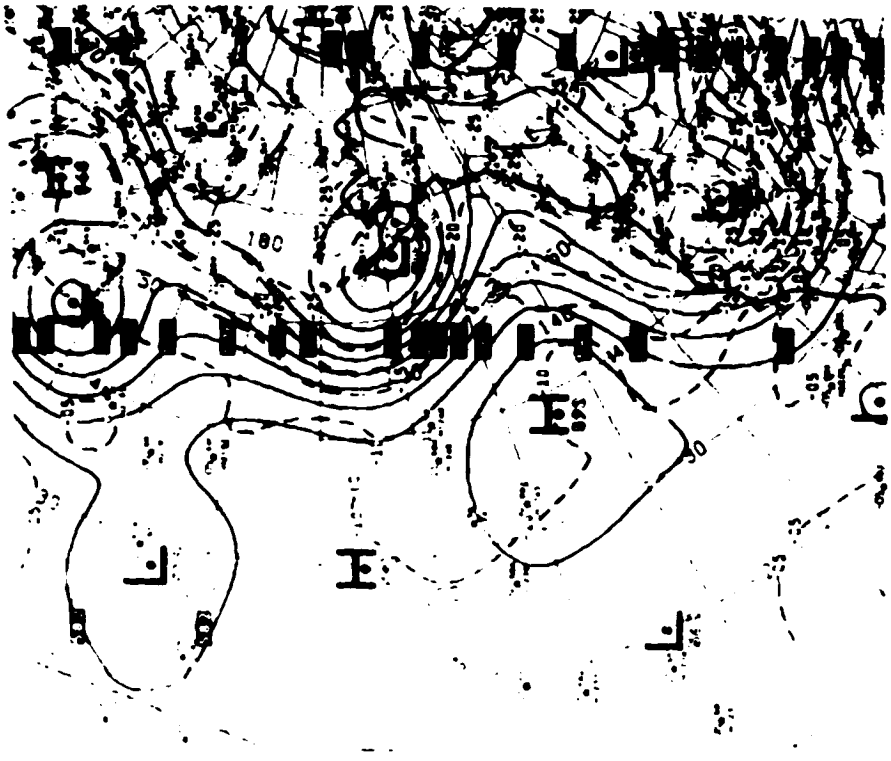

Figure 4b. NMC 500 mb analysis for 1200Z 18 September 1978

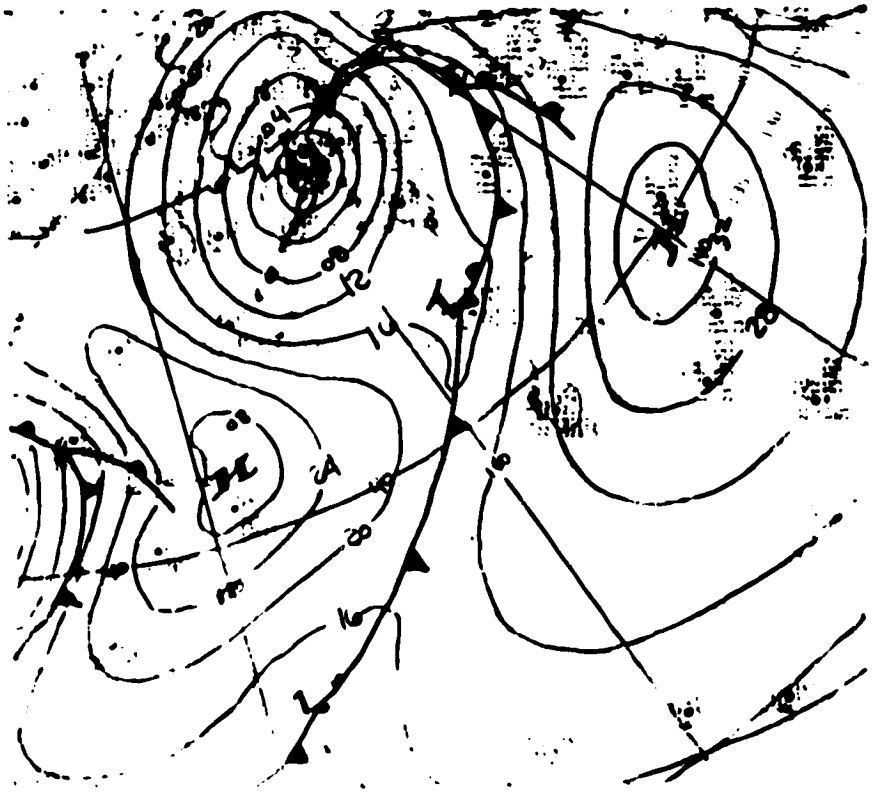

Figure 4a. NMC surface analysis for 1200Z 18 September 1978

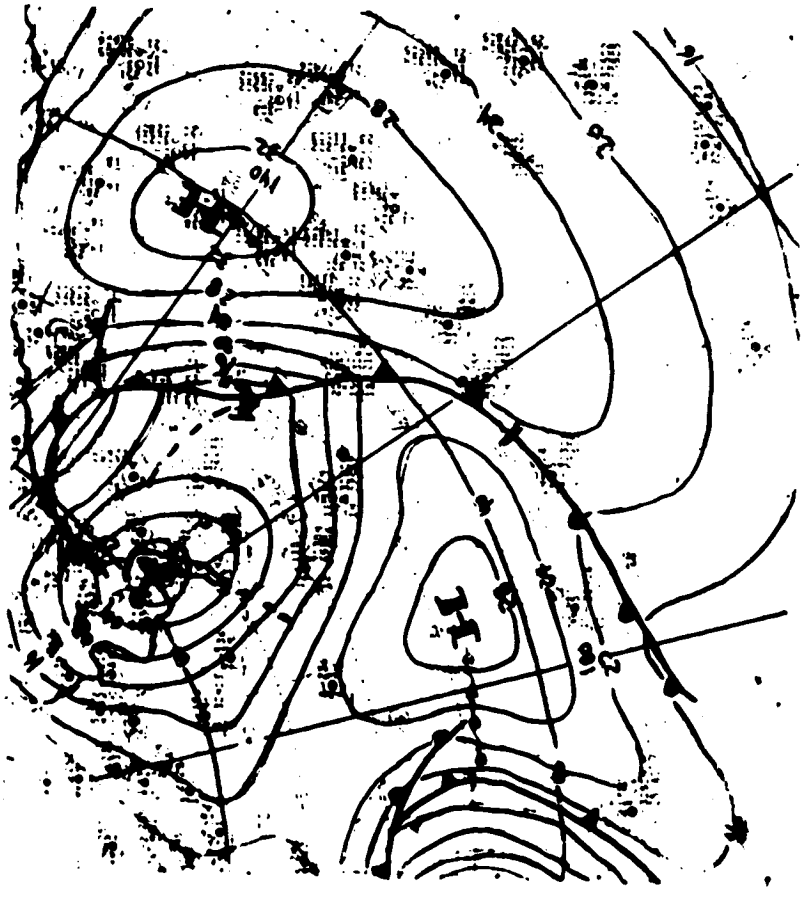

Figure 4c. NMC surface analysis for 1800Z
18 September 1978

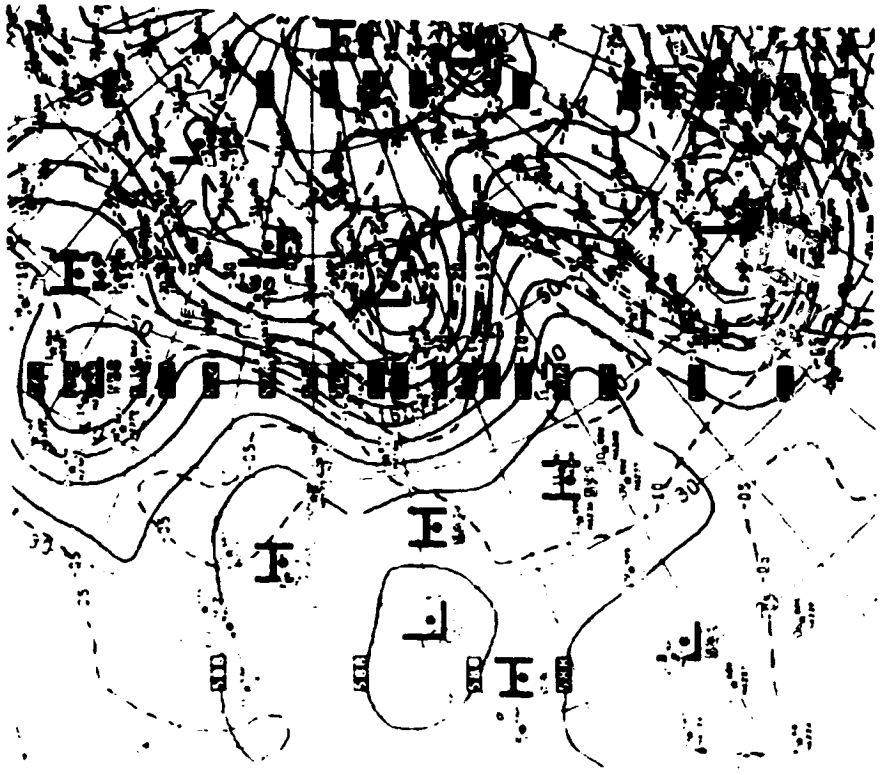

Figure 5b. NMC 500 mb analysis for 0000Z 19 September 1978

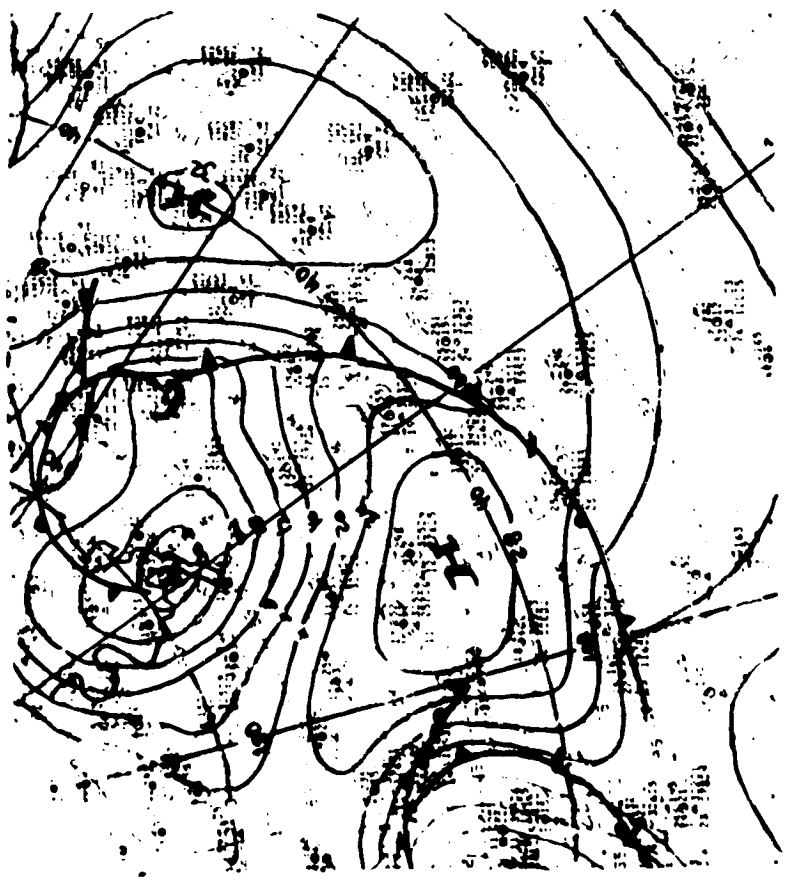

Figure 5a. NMC surface analysis for 0000Z 19 September 1978

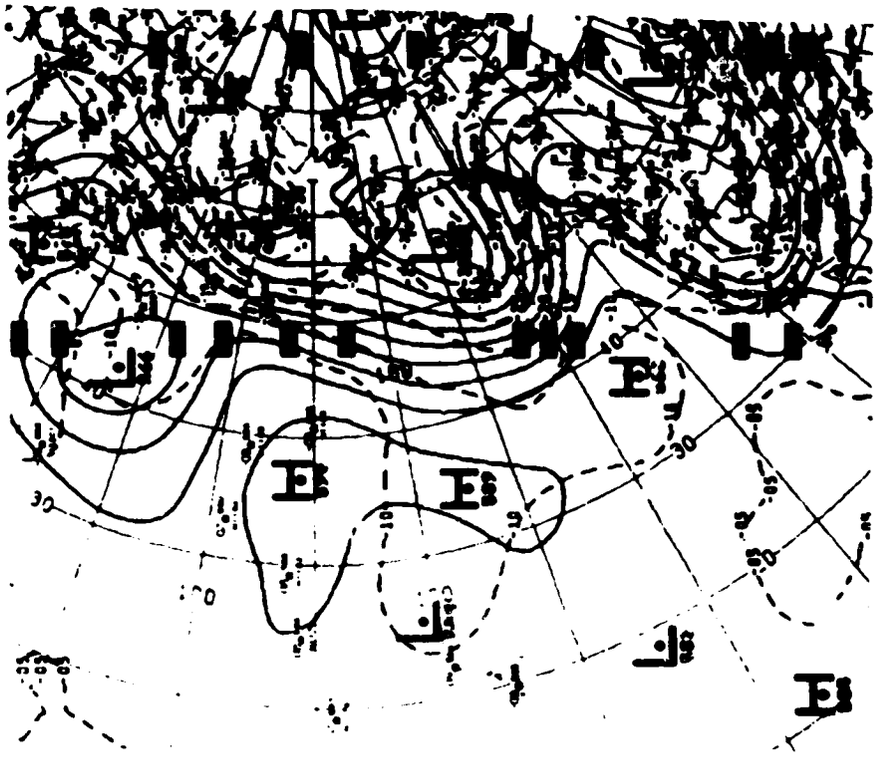

Figure 5d. NMC 500 mb analysis for 1200Z 19 September 1978

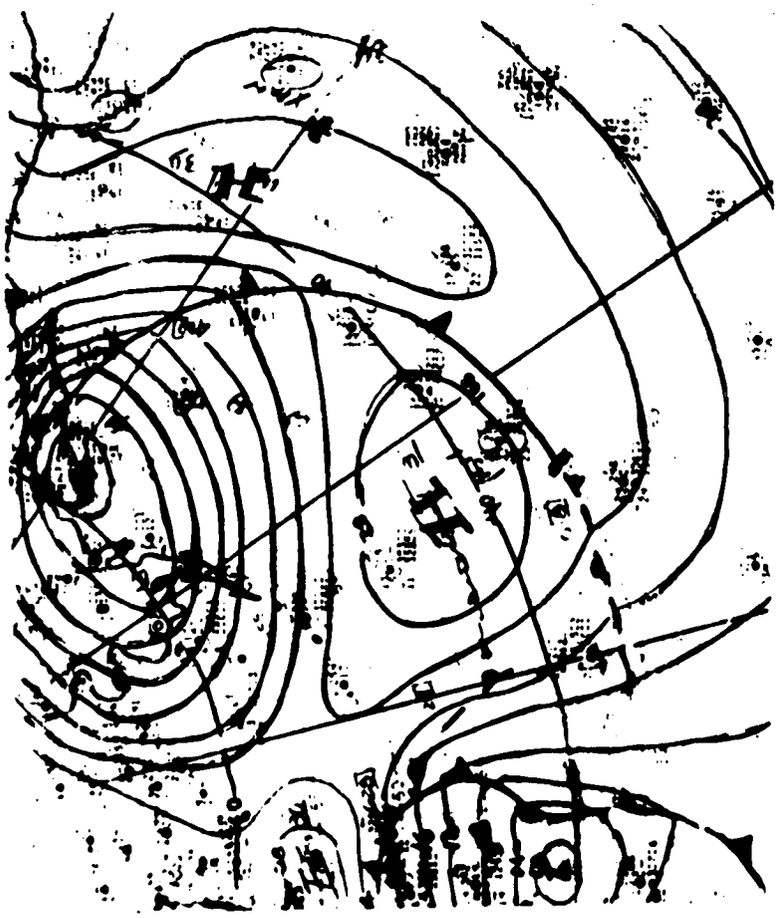

Figure 5c. NMC surface analysis for 1200 Z 19 September 1978

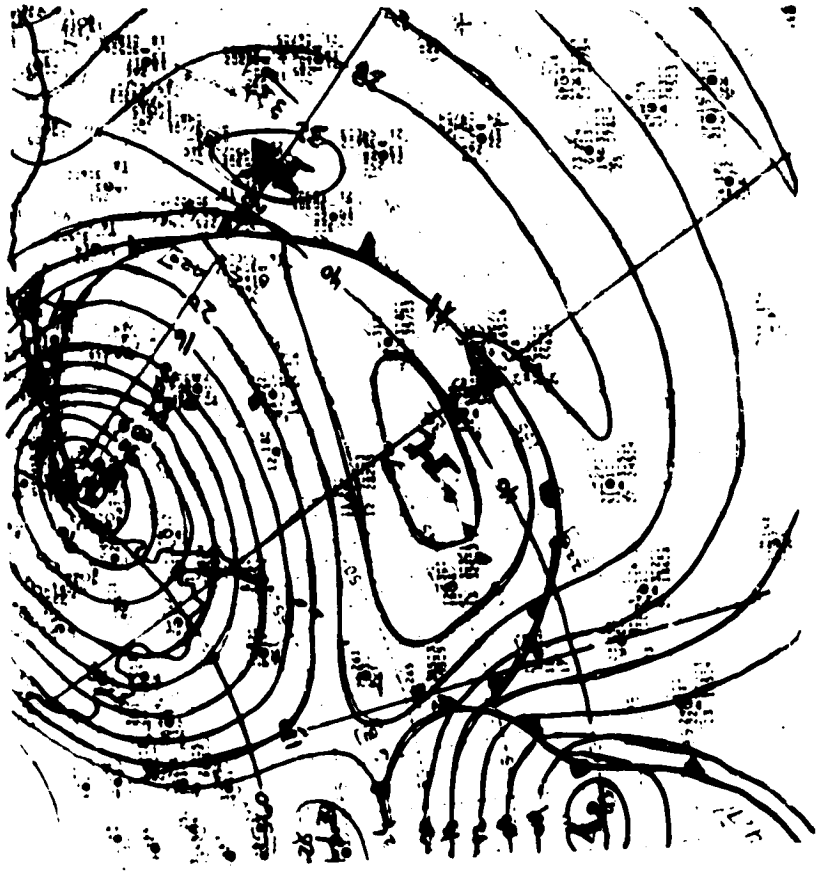

Figure 5e. NMC surface analysis for 1800 Z
19 September 1978

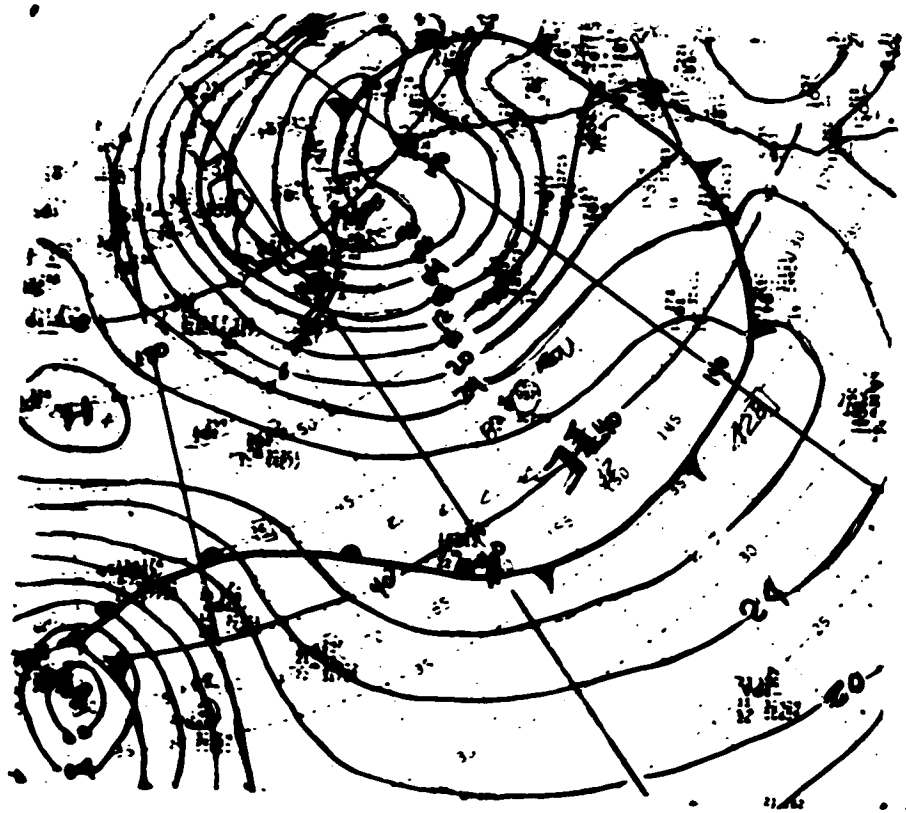

Figure 6a. NMC surface analysis for 1200Z 20 September 1978

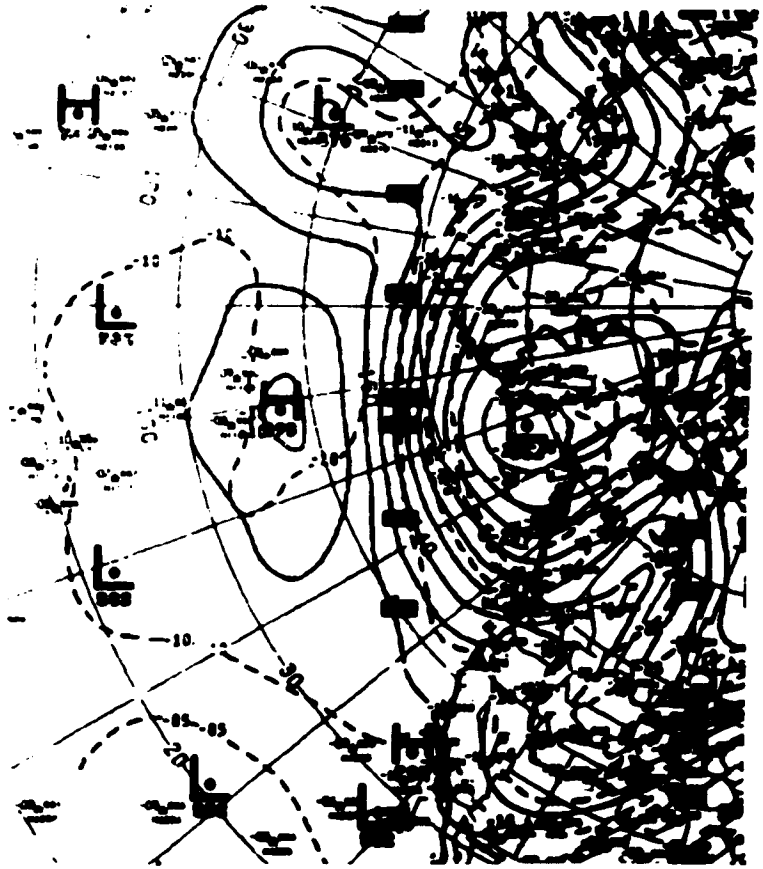

Figure 6b. NMC 500 mb analysis for 1200Z 20 September 1978

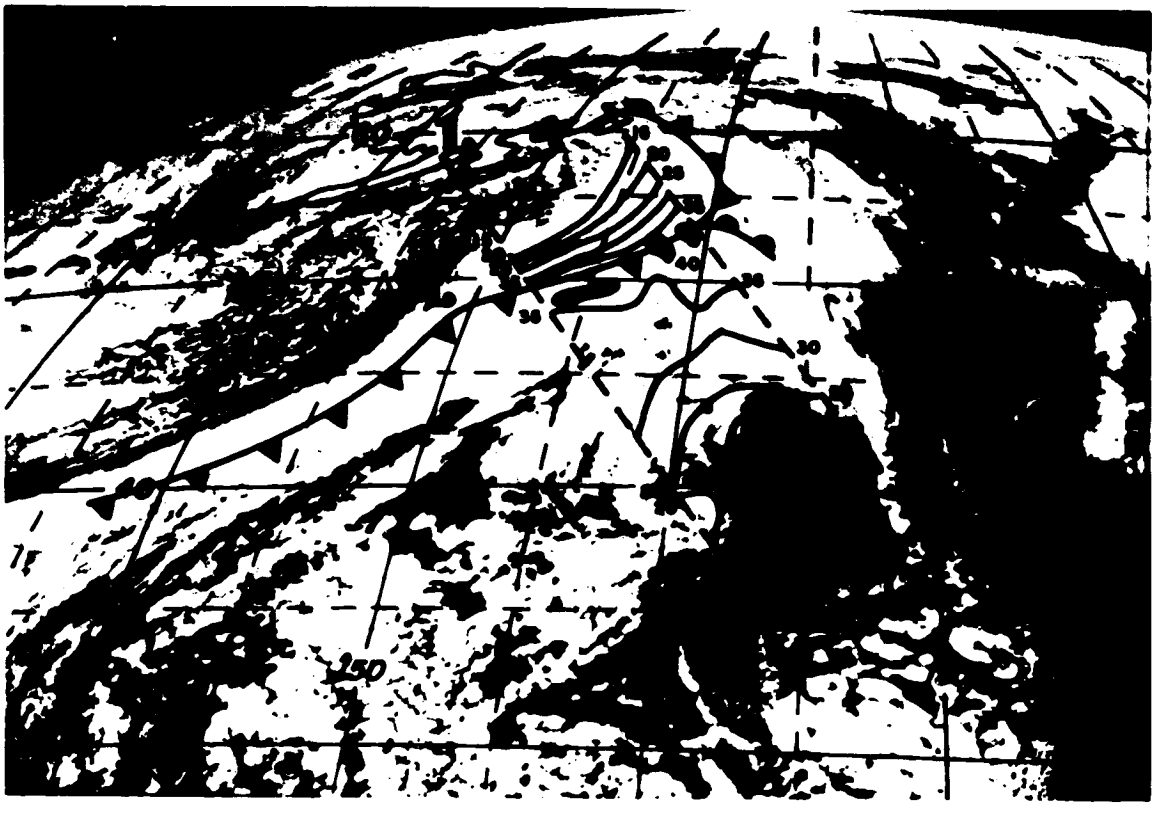

■ > 40 kg/m^2

FIGURE 7A

INTEGRATED WATER VAPOR (KG/M^2) SEPTEMBER 18, 1978
SEASAT REV 1198 GOES-W TIME 1845Z
SEASAT TIME 1830Z NMC ANALYSIS TIME 1800Z

The contours of the integrated water vapor are widely spaced southeast of the front and closely packed northwest of the front within the SMMR swath. The maxima occur just ahead of the front. This pattern shows clearly a boundary between two different air masses.

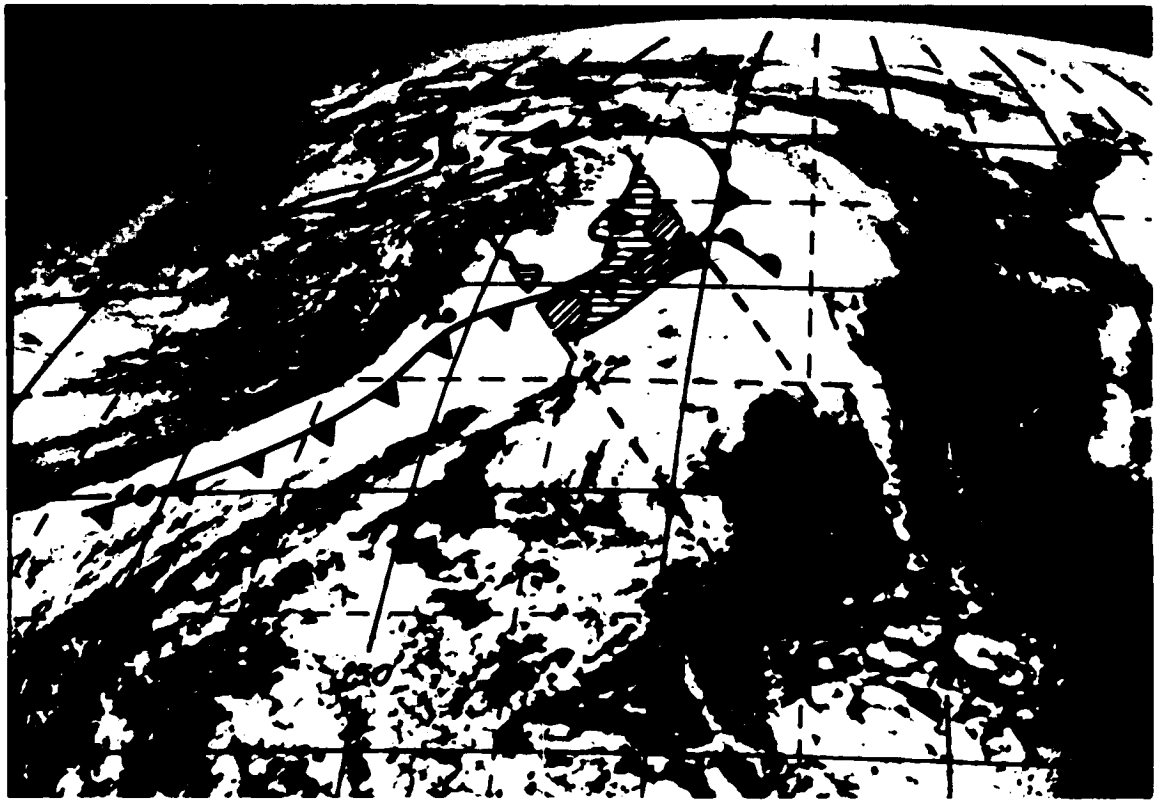

▨ > 1.0 kg/m^2
▨ > 0.6 kg/m^2
▤ > 0.2 kg/m^2

FIGURE 7B

INTEGRATED LIQUID WATER (KG/M^2) SEPTEMBER 18, 1978
SEASAT REV 1198 GOES-W TIME 1845Z
SEASAT TIME 1830Z NMC ANALYSIS TIME 1800Z

The largest amounts of integrated liquid water are concentrated along the front. Two areas of liquid water greater than .2 kg/m^2 are seen north of the front in the vicinity of 55°N 145°W and 50°N 148°W. These areas correspond well with cloudy areas seen on the GOES-W satellite picture.

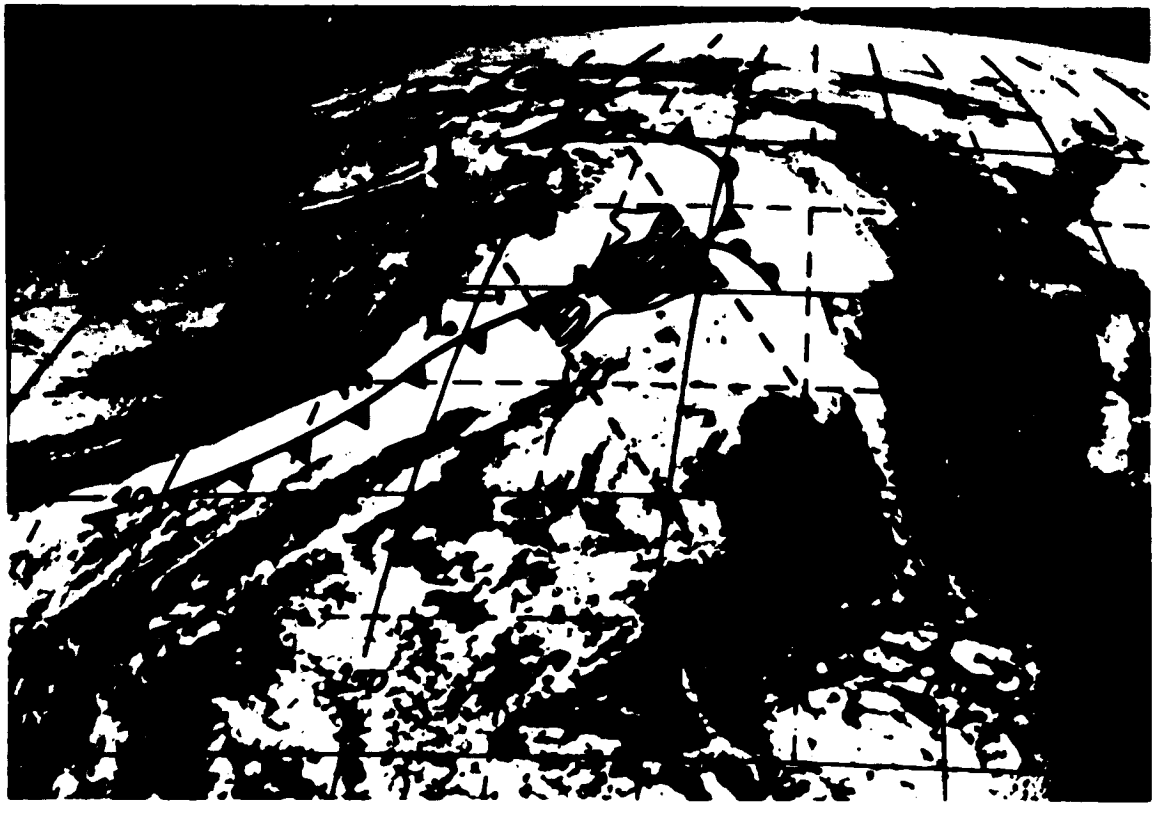

> 2 mm/hr
> 1 mm/hr
> 0.5 mm/hr
> 0.0 mm/hr

FIGURE 7c

RAINFALL RATE (MM/HR)
SEASAT REV 1198
SEASAT TIME 1830Z

SEPTEMBER 18, 1978
GOES-W TIME 1845Z
NMC ANALYSIS TIME 1800Z

Note the two shipments located outside the SMMR swath that are reporting drizzle. The letter P refers to the location of weathership C7P. It reported steady rain from 1500z-2100z. Three distinct areas of steady rain are seen by SMMR.

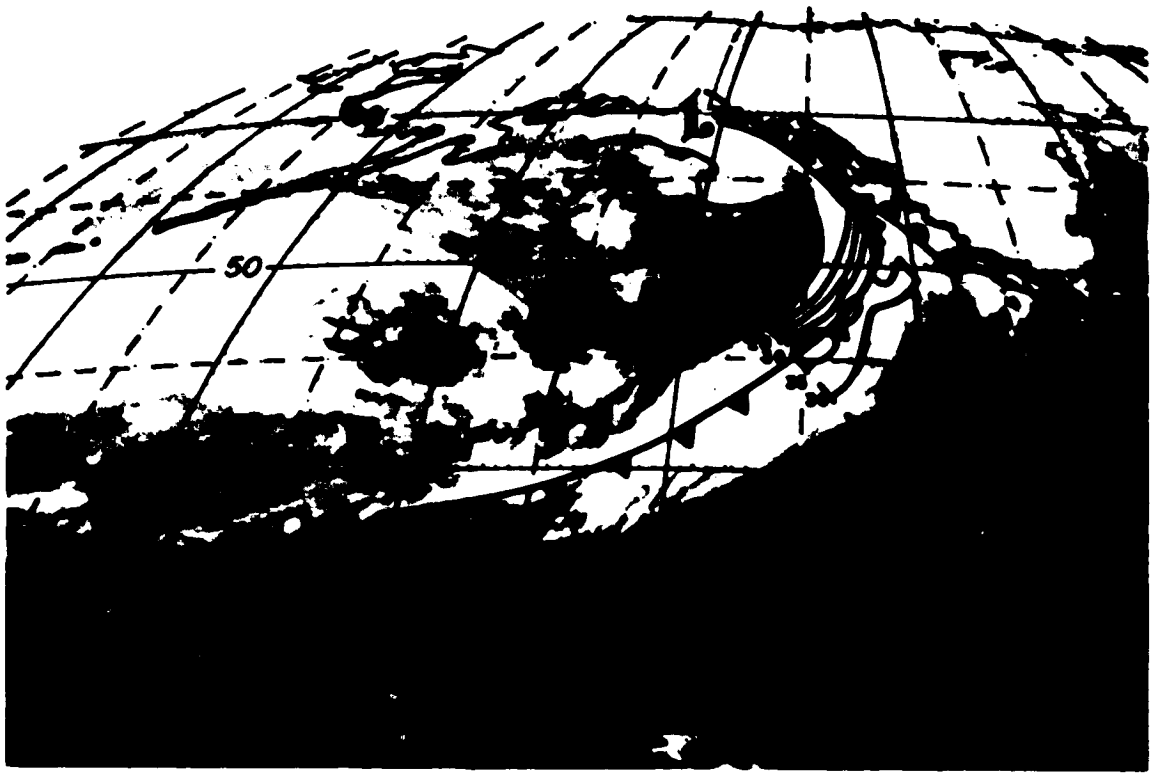

FIGURE 8A

INTEGRATED WATER VAPOR (KG/M^2) SEPTEMBER 19, 1978
SEASAT REV 1212 (IR) GOES-W TIME 1745Z
SEASAT TIME 1810Z NMC ANALYSIS 1800Z

The air ahead and behind the front is somewhat drier than the air in the corresponding area of rev 1198, Figure 7a. But, as in Figure 7a, the maxima in atmospheric water vapor are concentrated along the front.

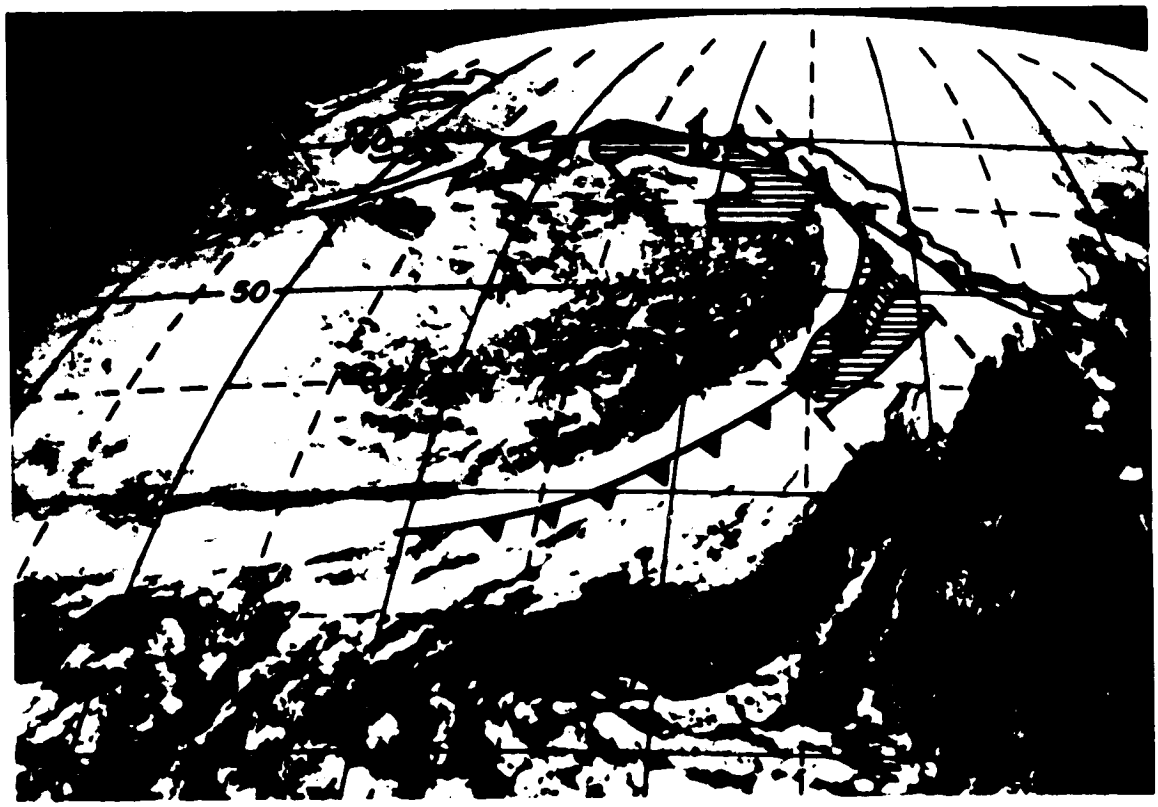

■ > 1.4 kg/m^2
▨ > 1.0 kg/m^2
▨ > 0.6 kg/m^2
▤ > 0.2 kg/m^2

FIGURE 8B

INTEGRATED LIQUID WATER (KG/M^2) SEPTEMBER 19, 1978
SEASAT REV 1212 GOES-W TIME 1745Z
SEASAT TIME 1810Z NMC ANALYSIS TIME 1800Z

The maxima in integrated liquid water are again concentrated along the front. The shaded area behind the occluded front near the surface low corresponds well with brighter clouds as seen in the visible satellite picture.

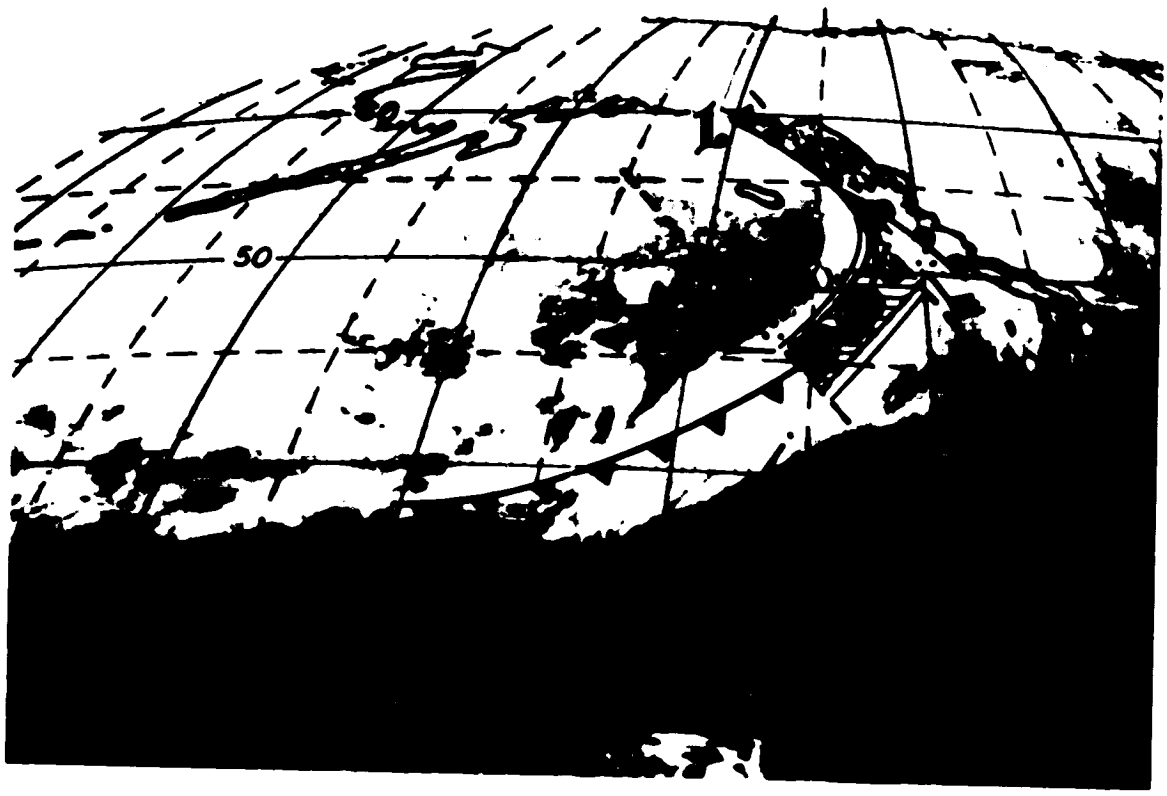

FIGURE 8c

RAINFALL RATE (MM/HR)
SEASAT REV 1212
SEASAT TIME 1810Z

SEPTEMBER 19, 1978
(IR) GOES-W TIME 1745Z
NMC ANALYSIS TIME 1800Z

The areas of rain are along the front in three distinct bands. The middle band snows rainfall rates greater than 3 mm/hr. Two ship reports, one near 45°N, the other near 50°N, lying near SMMR areas of rain, reported steady rain at 1800z.

APPENDIX A.

In OCEANOGRAPHY FROM SPACE
Edited by J. F. R. Gower
(Plenum Publishing Corporation,
1981), 691-706.

QUALITY OF SEASAT SMMR (SCANNING MULTICHANNEL MICROWAVE RADIOMETER) ATMOSPHERIC WATER DETERMINATIONS

Kristina B. Katsaros
Department of Atmospheric Sciences
University of Washington
Seattle, Washington 98195, U.S.A.

Peter K. Taylor
Institute of Oceanographic Sciences
Wormley, Godalming, Surrey GU8 5UB, ENGLAND

John C. Alishouse
S321B, NOAA/NESS, FOB#4
Washington, D.C. 20233, U.S.A.

Richard G. Lipes
Jet Propulsion Laboratory
California Institute of Technology
4800 Oak Grove Drive
Pasadena, California 91106, U.S.A.

1. ABSTRACT

Determinations of total precipitable water vapor in the atmospheric column between SEASAT-A and the ocean surface by two different algorithms applied to the Scanning Multichannel Microwave Radiometer (SMMR) on board this satellite have been evaluated. Comparisons between the SMMR predictions and integrated radiosonde data have been made on three separate data sets. During the three months that SEASAT was functioning, two large scale oceanic experiments took place. The Gulf of Alaska-SEASAT Experiment (GOASEX), September 1978, was especially designed to obtain in situ measurements. The second one, the Joint Air Sea Interaction Experiment (JASIN), which was carried out mid-July to early September 1978 in the North Atlantic, was not designed for SEASAT, but its data set is well suited for testing SEASAT's capabilities. Both GOASEX and JASIN took place in midlatitudes in the Northern Hemisphere. The maximum amount of atmospheric precipitable water vapor which was observed in these two

experiments is 36.8 kg/m^2. A third comparison data set is, therefore, produced from tropical WMO radiosonde stations on small atolls in the Pacific, thereby extending the range to 71.5 kg/m^2. The original algorithms performed very well in midlatitudes on GOASEX data, but overpredicted in the tropics by about 20%. Improved algorithms were then tested at a SEASAT-JASIN workshop held in Pasadena, California in March 1980. Statistics on the JASIN data set plus a new set of tropical soundings show the predictions of the improved algorithms to be within 6% in the JASIN area and 9% in the tropics. An overview of the liquid water and precipitation rate algorithm retrievals is presented. However, this information is still only qualitative.

2. INTRODUCTION

The Scanning Multichannel Microwave Radiometer (SMMR) on the SEASAT experimental satellite, which was launched on 28 June 1978 and expired on 10 October 1978, measured the earth's emission in five narrow frequency bands in both horizontal and vertical polarizations (Table 1). (For a SEASAT mission overview see Born et al, 1979 and Born et al, this volume.) These ten measurements over the ocean surface are utilized in determining the geophysical quantities, sea surface temperature, wind speed, integrated atmospheric water vapor, liquid water, and precipitation rate. The Nimbus-7 project has chosen to utilize measurements over polar regions from an identical instrument to make, in addition, estimates of ice and snow conditions. Attenuation of the active microwave measurements, e.g. altimeter path length corrections, also are calculated from SMMR data.

The inversion algorithms are based on a mix of theory, laboratory measurements and empirical correlation matrices obtained in field tests. Two main algorithms are in use during the evaluation of the SEASAT SMMR performance, one referred to as Wentz (GOASEX Workshop Report, 1979), and one referred to as Wilheit (Wilheit and Chang, 1979). This report covers mainly the evaluation of the determination of integrated atmospheric water vapor but will also touch on the determinations of total columnar liquid water and precipitation rate.

The measurement of atmospheric water vapor and liquid water with passive microwave techniques has had precedent in aircraft experiments (e.g. Rosenkranz et al, 1972) and on the Nimbus-5 and 6 satellites (e.g. Staelin et al, 1976, and Allison et al, 1974), but SEASAT has the finest areal resolution to date (Table 1). In relation to the horizontal variability of these quantities in the atmosphere, the resolution is still very coarse. It is obvious that scattered cloudiness, such as the cumulus convection in the cold air region of midlatitude cyclones, will not be resolved on a 54 x 54 km scale. Precipitation is in most cases concentrated in rain cells or

Table 1

Frequency, Wavelength, Footprint Size, and Principal Geophysical Quantity Predicted by SEASAT's 5 Channel SMMR

Frequency GHz	Microwave Wavelength cm	Seasat's Retrieval Grid at 3dB limit km x km	Principal Predicted Quantity
6.6	4.6	150 x 150	Sea surface temperature
10.7	2.8	85 x 85	Wind speed
18.0	1.7	54 x 54	Precipitation rate (18H) Water vapor, liquid water
21.0	1.4	54 x 54	Water vapor, liquid water
37.0	0.8	27 x 27	Precipitation rate (37H) Windspeed in clear air Water vapor, liquid water

rain bands, whose smallest horizontal dimension is of the order of 35 km (e.g. Matejka et al, 1980).

Since SEASAT was planned as an experimental satellite, an effort was made to obtain in situ data for verification and validation of whether the SEASAT instruments met their design specifications. For SMMR the GOASEX (Gulf of Alaska SEASAT Experiment) was the only experiment specifically planned for this purpose which could be carried out before the power failure which led to SEASAT's premature demise. The data are from September 1978. During the Joint Air Sea Interaction Experiment (JASIN) in the North Atlantic, 14 July - 5 September 1978, some special surface recordings were made during SEASAT overpasses for the benefit of the validation effort, but the experiment as such was not planned for this purpose. The JASIN radiosonde data have, however, turned out to be one of our most valuable data sources for total integrated atmospheric water vapor, q_t. The GOASEX radiosonde data came from weathership PAPA (50°N, 145°W) and R/V OCEANOGRAPHER also at latitudes around 50°N. The JASIN radiosondes used in this study are from a 200 km triangle of research ships stationed at about 60°N. In both these data sets the magnitude of q_t is less than 36.8 kg/m^2. An effort was therefore made to obtain data from the tropics.

Because the SMMR antenna has significant sidelobes and because the emissivity of land is much larger than that of the sea, only weatherships, research ships, and radiosonde stations on tiny atolls could be used. It is further necessary to select satellite and radiosonde observations which are within a few hours of each other and to be sure that the humidity profiles contain enough significant levels for accurate integration. All three radiosonde data sets were evaluated with similar trapezoidal rule integration schemes. The JASIN data set was calculated at the Institute of Oceanographic Sciences, Wormley, England, and the Gulf of Alaska and tropical data

with the NOAA routine in the United States (see Alishouse and Katsaros, 1980, for details). The evaluation of the SEASAT SMMR performance has taken place in a series of workshops reported in the GOASEX I Report (1979) or Lipes et al (1979, SMMR-Mini I Report (1979), SMMR-Mini II Report (1979), and the SEASAT-JASIN Workshop Report (1980). A limited set of SEASAT revolutions were processed for each workshop. Problem areas in algorithms were identified and improvements were made between each workshop.

3. EARLY RESULTS OF SEASAT SMMR WATER VAPOR RETRIEVALS

In the GOASEX I workshop there appeared to be a correlation between sea surface temperature and water vapor predictions. A possible explanation was that the correction for the emission by the water vapor was improperly applied in evaluation of the sea surface temperature. However, the values of total integrated water vapor calculated by both the Wentz and Wilheit algorithms were in excellent agreement with the five available radiosonde estimates. By the SMMR-Mini I workshop (May, 1979) a few tropical intercomparisons were available. While the midlatitude estimates were still good, the satellite overestimated q_t by about 20% in the tropics. Between SMMR-Mini I and SMMR-Mini II (September, 1979) the complete antenna pattern correction, a problem called "cross-track bias", and other corrections had been incorporated from which new brightness temperature values were generated and the geophysical parameters were rederived. In addition, a few more tropical station intercomparisons were obtained. The satellite value corresponding to a raob (radiosonde observation) was interpolated using the four nearest satellite predictions. These results are found in Tables 2 and 3. The calculated mean biases and standard deviations show that there existed a positive bias for the Wilheit algorithm of 20%, both in midlatitudes and in the tropics, and that the Wentz algorithm, which was tuned for midlatitudes, was within 7% there but was off by 24% in the tropics.

4. WATER VAPOR RETRIEVALS AT THE SEASAT JASIN WORKSHOP

During this workshop the algorithm improvements made on the basis of the experience gained in the three previous SMMR workshops were tested against independent high quality data from the JASIN experiment and against new data from the tropical Pacific.

4.1 JASIN Area Evaluations of Integrated Water Vapor (Wentz Algorithm)

The surface truth data sets available to the workshop included, in total, 320 radiosonde flights from the JASIN ships for comparison with 30 selected SEASAT revolutions. Many of the radiosonde flights were designed only to reach 500 mb. Figure 1 shows the mean water vapor content of different layers of the atmosphere for each of the

Table 2

Radiosonde and SMMR Determined Values of Total Atmospheric Water Vapor in the GOASEX Experiment

Date	Station	SEASAT Rev	Raob Time (Z)		Raob kg/m^2	Wentz kg/m^2	Wilheit kg/m^2	Comments
July 31, '78	W/S Papa	495	1500		22	25	27	
Sept 13, '78	R/V Ocean	1120	0747		16	14	17	
Sept 14, '78	W/S Papa	1135	0911		12	12	15	
Sept 16, '78	R/V Ocean	1163	0819		12	11	13	
Sept 17, '78	W/S Papa	1178	0923		13	14	17	
Sept 22, '78	R/V Ocean	1255	1822		17	13	18	
Sept 24, '78	W/S Papa	1284	1903		13	12	16	
Mean					15	14.4	17.6	
Bias						-0.6	2.6	
						(-4%)	(17%)	
Standard deviation					3.7	4.5	4.5	

Table 3

Radiosonde and SMMR Determined Values of Total Atmospheric Water Vapor at Tropical Stations (Results of SMMR Mini-Workshops I and II)

Date	Station	SEASAT Rev	Raob Time (Z)	Satellite overpass Time @ MT	Island area, % of Grid	Raob kg/m^2	Wentz kg/m^2	Wilheit kg/m^2	Comments
Sept 14, '78	Johnston Is	1135	2315,1115	~0921	0.04	48	53	49	
Sept 19, '78	Funafuti	1214-5	2300	22:52:44	0.1	37	50	51	
Sept 19, '78	Majuro	1214-5	2255	22:58:00	0.3	50	63	58	
Sept 19, '78	Kwajalein	1214-5	2300	22:58:30	0.5	66	70	70	
Sept 19, '78	Wake Is	1214-5	2300	23:01:30	0.3	42	52	53	
Sept 20, '78	Guam	1216	2300	0:40:45	19	51	67	62	
Sept 20, '78	W/S Tango	1216	2330	0:44:45	-	63	83	76	probably raining
Mean						51	62.5	59.9	W/S Tango data are not included in statistics.
Bias							11.6	8.9	
							(23%)	(17%)	
Standard deviation						10.5	11.9	10.12	

data sets. It suggests that the water vapor content above 500 mb might be estimated to within ±2.0 kg/m^2. However, initial comparisons suggested that the SEASAT determinations were at least this good. It was therefore decided to limit comparisons to radiosonde flights which reached pressures of 250 mb or less, and which were launched within ±2 hours of the overpass time. These stringent requirements resulted in the set of 19 comparisons shown in Table 4. The mean magnitude of the difference between overpass time and radiosonde launch time was 45 minutes. SEASAT values of the water vapor content were obtained from plots of the Wentz algorithm determina-

Table 4

Comparisons of Surface Truth and SMMR (Wentz Algorithm) Determinations of Total Water Vapor Content in JASIN

	Seasat		Radiosonde					
Day	Rev	Time GMT	Radiosonde Flight	Time GMT	Top Pressure mb	SMMR kg/m^2	Raob kg/m^2	Difference Seasat SMMR Minus Raob
219	590	0622	C104	0557	200	15.0	14.0	+01.0
219	599	2142	J083	2143	207	18.9	14.0	+04.9
233	800	2245	H041	2357	235	21.2	21.9	-00.7
233	800	2245	M(*)	234/ 00	200	21.2	20.5	+00.7
234	805	0653	H042	0608	220	18.1	15.3	+02.8
235	829	2321	C140	236/ 0026	130	16.6	18.2	-01.6
235	829	2321	H061	2358	155	17.0	14.6	+02.4
235	829	2321	M(*)	236/ 00	200	17.3	16.1	+01.2
236	834	0730	C141	0557	135	16.0	15.0	+01.0
236	834	0730	H062	0555	215	15.2	16.1	-00.9
236	843	2250	H077	2347	180	20.5	21.3	-00.8
238	872	2328	M(*)	239/ 00	200	25.8	24.7	+01.1
239	886	2259	H098	2358	170	29.3	27.9	+01.4
242	929	2312	H119	2355	195	31.0	28.2	+02.7
242	929	2312	M(*)	243/ 00	200	36.9	36.8	+00.1
244	944	0022	C221	0009	120	21.0	18.7	+02.9
244	958	2353	C238	2359	180	22.0	20.1	+01.9
244	958	2353	H245	0037	190	21.9	19.6	+02.3
244	958	2353	M(*)	245/ 00	200	22.5	22.1	+00.4
Mean						21.4	20.3	1.2 (6%)
Standard deviation						5.8	5.9	1.6

KEY TO SHIPS: C = Gardline Endurer, H = Hecla, M = Meteor, J = John Murray.

*Indicates Meteor Synoptic Report, the times are then 00Z on the following Julian Day.

tions covering the JASIN area. The actual value used was obtained by linear interpolation between the nearest data points. The differences between the SEASAT and in situ values shown in Table 4 are plotted against the radiosonde water vapor values in Figure 2. There is no obvious relationship.

One point, representing a radiosonde flight from the ship JOHN MURRAY, has considerably greater difference. Examination of spacecraft and the radiosonde data for this comparison shows no reason for its rejection. It has, therefore, been retained in the statistics.

Except for the one JOHN MURRAY value, there is no significant difference between the various ships. The overall mean difference

QUALITY OF SMMR ATMOSPHERIC WATER DETERMINATIONS

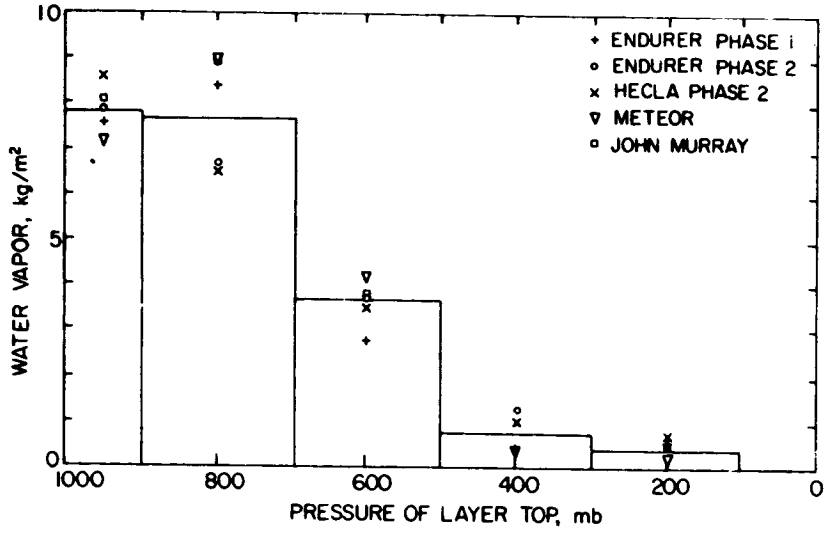

Fig. 1: Mean water vapor content in each atmospheric layer calculated for each data set in JASIN. (The names following the symbols belong to the meteorological ships.)

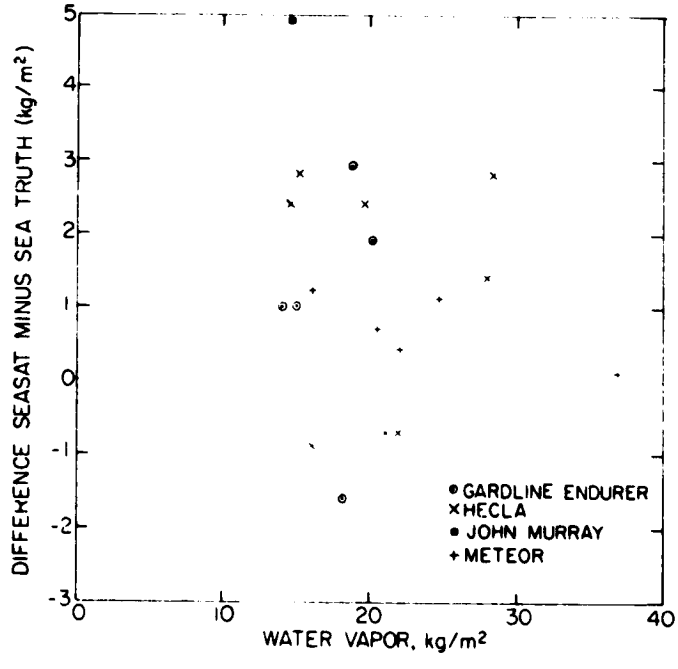

Fig. 2: Integrated water vapor comparisons - SMMR Wentz algorithm versus radiosonde observations.

of 1.2 ± 1.6 kg m^2 compares well with the accuracy of the radiosonde determinations which had been estimated at worst as ±3 kg/m^2.

4.2 Tropical Area Evaluation of Integrated Water Vapor at the SEASAT-JASIN Workshop

The Wentz algorithm determinations were tested on a new, independent data set from tropical islands and W/S TANGO. After elimination of incomplete radiosonde ascents and cases with differences between radiosonde and overpass times much greater than 3 hours, ten comparisons remain. Three of these are for the radiosonde station on the island of Guam, whose area is 541 km^2. This is large compared to the footprint of the SMMR, 2,900 km^2. (See discussion of land effects in SEASAT-JASIN Workshop Report, 1980.)

Table 5 lists the results. The Guam data and the W/S TANGO data for revolution 427 has been left out of the statistics because of possible land or rain contamination. The algorithm "fit" to the in situ data has a mean bias of 4.9 kg/m^2, a 9% error.

5. LIQUID WATER AND PRECIPITATION RATE PREDICTIONS BY THE SMMR ALGORITHMS

No direct measurements of total integrated liquid water in an atmospheric column and only one precipitation rate measurement is

Table 5

Precipitable Water Vapor at Tropical Stations, SEASAT-JASIN Workshop (Wentz Algorithm)

Rev No.	Julian	Mo/Day	Time Hour-Min	Wentz Algorithm kg/m^2	Radiosonde Data Station	Time	Amount kg/m^2	SMMR/Wentz Minus Radiosonde kg/m^2	Comment
384	204	7/23	20:38	30.2	W/S Tango	24:00Z	29.2	1.0	
				66.8*	Guam*	24:00Z	55.0	(11.8)*	
427	207	7/26	20:45	77.6	W/S Tango	24:00Z	56.7	20.9	Rain within 200 km distance (surrounding SMMR numbers all approximately 66.5)
				70.7*	Guam*	24:00Z	57.1	(13.6)*	
542	216	8/4	21:37	80.2	W/S Tango	24:00Z	71.5	8.7	
628	221	8/9	21:51	54.3	W/S Tango	24:00Z	53.9	.4	
				65.0*	Guam*	24:00Z	67.2	(2.8)*	Rain
828	235	8/23	21:06	63.4	Wake	24:00Z	54.4	8.0	SMMR has locally high values by 2.0-4.0 kg/m^2
				62.1	Kwajelein	24:00Z	56.5	5.6	
				64.5	Majuro	24:00Z	58.0	6.5	
Mean				59.1			53.9	4.9 (9%)	Guam and W/S Tango 7/26 eliminated from statistics
Standard deviation				16.5			13.7	3.7	

*Guam is a large island, values probably show land effects.

available for comparisons with SEASAT's predictions. Some general observations and qualitative evaluations can be made, however.

5.1 GOASEX I Results

An encouraging agreement between Wentz algorithm prediction of precipitation bands along a cyclonic frontal system and evaluations of high precipitation probability from visible and infrared satellite data was seen in the GOASEX I workshop (Figure 3). The elongated rain cells are in qualitative agreement with results of the University of Washington CYCLES Project (e.g. Hobbs, 1979. CYCLES is a program to study cyclonic storms as they cross the Washington coast.) A few ships' reports near the frontal zone give corroborating evidence that SMMR can identify frontal precipitation.

The liquid water content calculations had a bias at the time of GOASEX I and gave unintelligible results.

5.2 JASIN Area Evaluations of Liquid Water and Precipitation Rate

The precipitation which occurred in JASIN was typically very light. Of the 30 SMMR revolutions, only a few show coincidence between reported precipitation at the ships and by SMMR, viz., revolutions 355, 432, 929, and 1006. These cases are listed in Table 6. During these revolutions, the rain appears to have been of the type called "widespread" with several ships reporting some form of precipitation. For this situation the Wentz algorithm predicts the rain occurrence very well. In one case, a measurement of the rain rate was available. From the R/V JOHN MURRAY rain gauge measurements between 20:00Z and 21:00Z on July 21, we can estimate a rain rate of 0.2 mm/h. Wentz algorithm calculates 0.0 to 0.2 mm/h at the footprints surrounding this ship location.

There are several occasions when ships report light rain or showers close to the time of the overpass, viz., revolutions 547, 556, 590, 597 and the series on August 21 and 24 (791, 834, and 843) and the algorithm does not predict rain. For these last three revolutions the ships report showers, and the Wentz algorithm gives liquid water contents of 0.04, 0.08, 0.10 kg/m^2, etc., which are all less than the threshold value of 0.5 kg/m^2 used to infer rain. With showery precipitation the footprints of the SMMR would not be filled with the heavy concentrations of liquid water associated with the convective cloud elements producing the showers. This is an inherent limitation of the SMMR resolution, and is not dependent on the algorithm. An interesting case was found where SMMR shows centers of high liquid water and high water vapor content and some ships report thunderstorms while the SEASAT scatterometer wind determinations did not agree with ship measurements within the typical accuracy (Guymer et al, 1981).

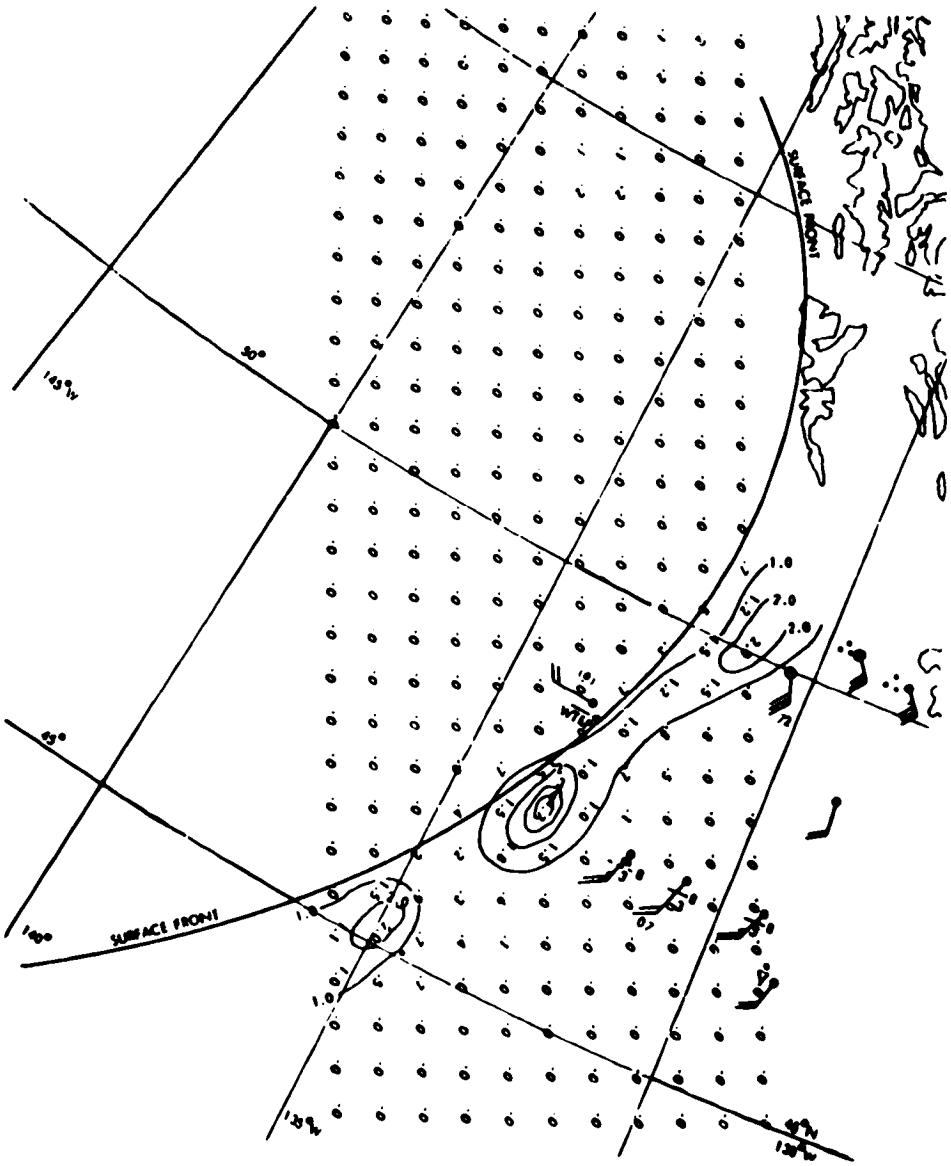

Fig. 3: Rain rate for rev 1212 obtained with the Wentz algorithm with superimposed ship observations. Note the report from R/V OCEANOGRAPHER at 48.7°N, 133.5°W, which reports rain in sight and rain in the previous 3 hours.

Table 6

Rain Rate and Liquid Water Algorithms for Wilheit and Wentz at Ship Locations Reporting Precipitation in the JASIN Experiment. The Accompanying Sketch of the JASIN Meteorological Triangle Shows Designations of Ship Locations Found Under the Location Column

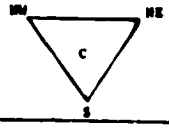

Corresponding Ship and Triangle Locations

Rev #	Rev Time Mo/Day/hr	Wilheit Liquid Water kg/m²	Wilheit Rain mm/hr	Wentz Liquid Water kg/m²	Wentz Rain mm/hr	Location of satellite observ. and ship.	The stations below report precipitation in the WMO code ww or as comments at a time near satellite overpass*.	
355	7/21/20	1.00	1.10	1.20	1.00	(S)	METEOR	616
432	7/27/05	0.44	0.10	0.37	0.00	(NE)	HECLA	606
		0.40	0.10	0.31	0.00	(S)	METEOR	606
		0.49	0.00	0.44	0.00	(S)	TYDEMAN	612,596
547	8/6/06	0.74	0.00	0.20	0.00	(NE)	JOHN MURRAY	605
		0.29	0.10	0.24	0.00			
556	8/6/22	0.14	0.00	0.20	0.00	(S)	CHALLENGER	626
590	8/7/06	0.11	-	0.09	0.00	(NW)	GARDLINE ENDURER	showers
599	8/7/22	0.16	-	0.14	0.00	(S)	DISCOVERY	
633	8/10/06	1.13	0.90	1.51	1.40	No surface reports of precipitation		
		1.19	0.70	1.37	1.20			
		0.93	0.40	1.01	0.70			
642	8/10/22	0.43	0.20	0.39	0.00		ATLANTIS	603
		West of Seasat Path					SHACKELTON	626
676	8/13/07	0.60	0.25	0.60	0.30	(S)	SHACKELTON/HECLA	622
		0.91	0.20	0.94	0.63	(S)		
719	8/16/07	0.46	0.10	0.45	0.00	(NW)		
748	8/18/07	0.35	0.20	2.20	0.00	South of JASIN area		
		6.90	7.00	0.70	0.30	~50°N		
		0.86	0.90	0.99	0.70	350°E		
		1.15	0.80	1.26	1.10			
791	8/21/07	0.04	0.00	0.04	0.00	(C)	JOHN MURRAY	showers
		0.10	0.00	0.08	0.00	(S)	PLANET	showers
834	8/24/07	0.04	0.00	0.06	0.00	(C)	JOHN MURRAY	showers
		0.02	0.00	0.04	0.00	(NW)	GARDLINE ENDURER	showers
		0.08	0.00	0.08	0.00	(S)	SHACKELTON	interm. rain
843	8/24/23	0.00	0.00	0.01	0.00	(S)	SHACKELTON	
929	8/30/23	0.61	0.30	0.61	0.15	(NE)	HECLA	616
		0.70	0.50	0.70	0.30	(NE)	HECLA	
956	9/1/24	0.08	0.00	0.16	0.00		METEOR (23Z)	505
		0.04	0.00	0.05	0.00	- Position	(24Z)	025
		0.01	0.00	0.12	0.00	- above (S)		
		0.01	0.00	0.14	0.00			
1001	9/5/00	1.05	0.60	1.12	0.90			
		0.82	0.80	0.97	0.70	- SW corner of		
		0.59	0.60	0.73	0.30	- large scale area.		
		0.68	0.30	0.64	0.20			
1006	9/5/08	0.04	0.00	0.03	0.00		HECLA	616
		0.77	0.60	0.76	0.37	(S)	GARDLINE & PLANET	608,612
		0.10	0.00	0.12	0.00	between NW & NE	SHACKELTON	602

* ww from 60-65 indicates intermittent light rain to continuous heavy rain. Numbers in the 50's indicate drizzle.
W-6 indicates rain as past weather. W-5 indicates drizzle as past weather.

From the data collected in Table 6, an intercomparison in the JASIN area of the Wentz and Wilheit liquid water algorithms can be made. It reveals a nonlinear relationship for values less than 1.2 kg/m^2 (Figure 4). An intercomparison of the rain algorithms suggests a linear relationship between the two with a standard deviation of less than 0.3 mm/h (Figure 5).

5.3 Tropical Area Liquid Water and Precipitation Rate Algorithm Intercomparison

Since any comparison data for either liquid water or precipitation rate was unavailable in the tropical areas, an intercomparison of the determinations of these quantities by the Wentz and Wilheit algorithms was made. As seen in Figure 6, a relationship between the liquid water algorithms exists for values below 1.2 kg/m. This is similar to the relationship in the JASIN area, except that the intercept is not zero. Above 1.2 kg/m the correlation breaks down. (Data affected by land have not been identified in this correlation.)

The Wentz and Wilheit rain algorithms show a large amount of scatter in their correlation (Figure 7). Wilheit values are typically larger and give in some cases between 0.1 and 1.5 mm/h of rain rate where the Wentz algorithm predicts zero rain rate. This indicates that the algorithm may not yet be depended on to flag regions

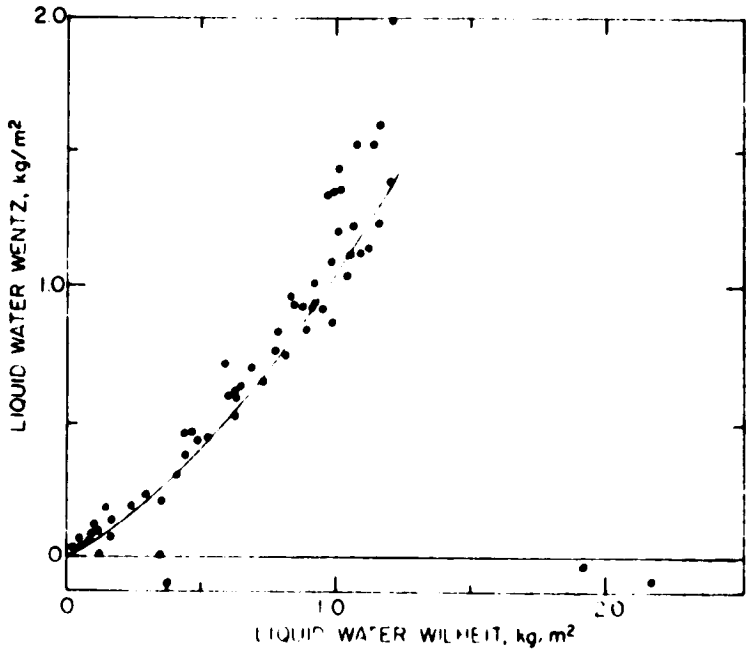

Fig. 4: Wentz versus Wilheit liquid water estimates in JASIN.

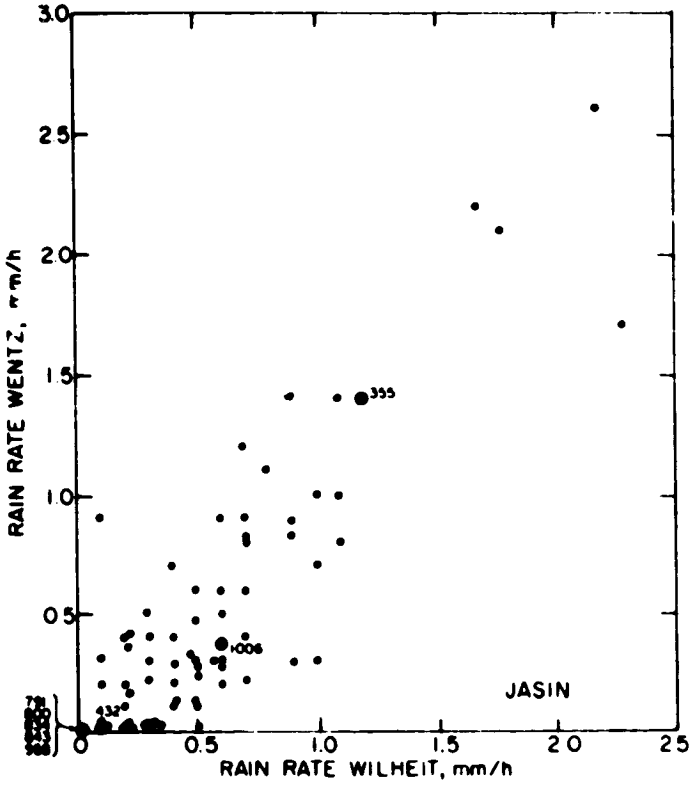

Fig. 5: Wentz versus Wilheit rain rate estimates in JASIN. The circled stations correspond to 355, 1006, widespread rain. 791...958 had shower type precipitation.

where other parameter determinations might be compromised by rain in the field of view.

6. CONCLUSIONS

The integrated water vapor values retrieved with SEASAT SMMR algorithms are as accurate in midlatitudes as integrations of radiosonde data and more representative. When care is taken in selecting data pairs for intercomparisons in the tropics, the Wentz algorithm agrees within 10% with a limited number of radiosondes. The large areal coverage by SMMR is already contributing to a better scientific understanding of the water vapor content and structure of frontal systems affecting the JASIN experiment, particularly since it extends beyond the small meteorological triangle (Taylor et al, 1981). Further, being biased to lower atmospheric levels (Figure 1), the integrated water vapor is a better indicator of surface frontal position, which may be obscured by high clouds in visible and infrared images.

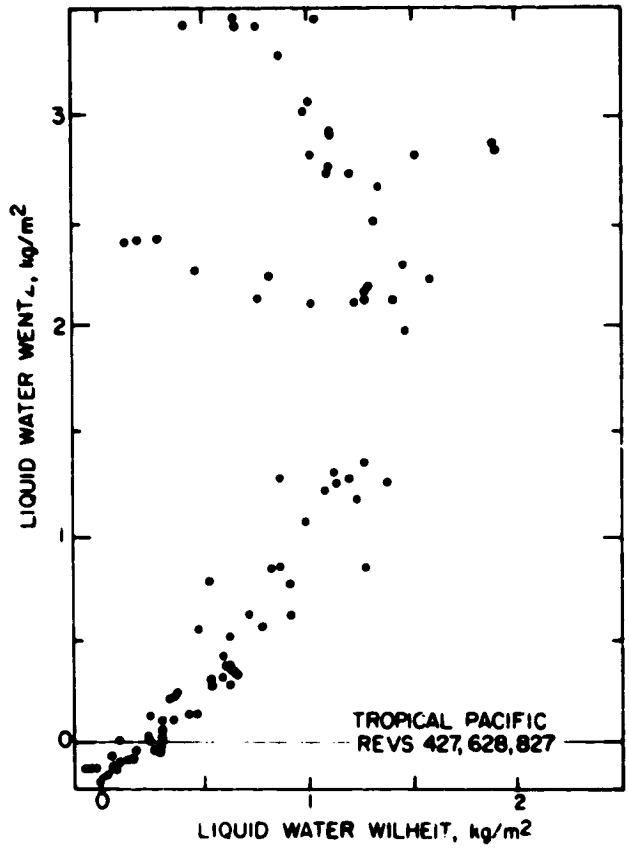

Fig. 6: Wentz versus Wilheit liquid water estimates in tropics.

The integrated liquid water and rain rate values provided by SMMR are essentially unproven to date. These data provide information deep within a synoptic system, but emphasize different levels than the integrated water vapor. The qualitative picture, which emerges from the GOASEX and JASIN plots, is consistent with other observations and quite exciting. The presence of liquid water indicates release of latent heat, vertical motion, and therefore convergence and divergence (e.g. Matejka et al, 1978), which may be used as dynamical input to atmospheric models. The two main algorithms are in poor agreement on absolute values of liquid water content and rain rate, which indicates that much work is needed in this area. Because of the small horizontal scale of many types of cloudiness and precipitation, greater scientific contributions are expected from the future LAMMR (Large Antenna Multichannel Microwave Radiometer), whose resolution will be of the order of 10 km for the atmospheric water related parameters.

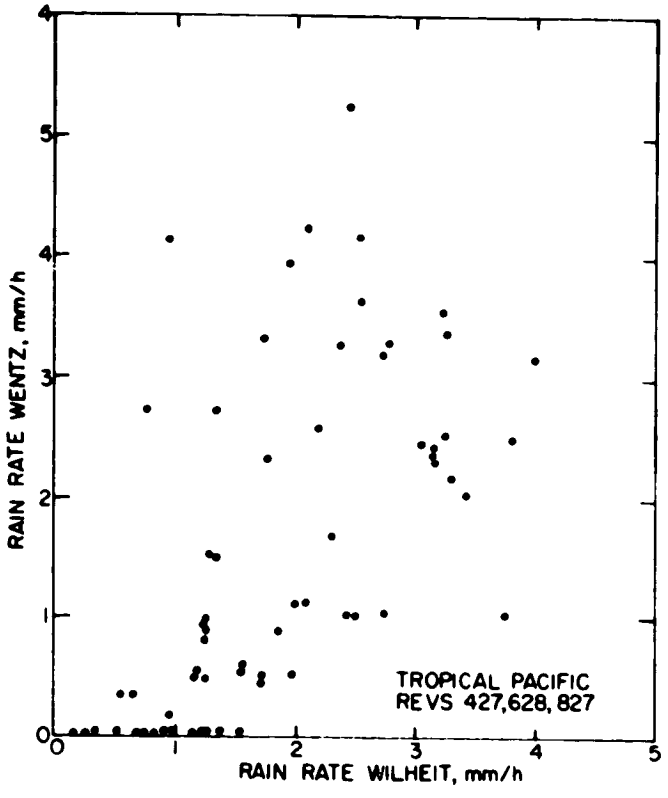

Fig. 7: Wentz versus Wilheit rain rate estimates in tropics.

7. ACKNOWLEDGEMENTS

Many people contribute to a complex undertaking such as the SEASAT SMMR validation effort. The participants in the GOASEX and JASIN experiments who collected the in situ data must be recognized. Dr. John Wilkerson of NOAA and Dr. Trevor Guymer of IOS, Wormley, coordinated the preparation of earth-based data for the SEASAT workship; Mr. Allan Macklin, PMEL/NOAA, Mr. Arnold Hanson, Ms. Lynn McMurdie, and Dr. James Anderson of the University of Washington helped with preparations for the SEASAT-JASIN workshop; Dr. Barbara Wind, Dr. Tom Chester of the Jet Propulsion Laboratory prepared the SEASAT results. Dr. K.B. Katsaros is grateful for support from NOAA under Contract MO-A01-78-00-4102 and from NASA/JPL/JASIN-SEASAT under Contract 955528.

REFERENCES

Alishouse, J.C. and Katsaros, K.B., 1980, "SEASAT SMMR Water Vapor Determinations Status," NOAA Report (to appear).

Allison, L.J., Rodgers, E.B., Wilheit, T.T. and Fett, R.W., 1974, "Tropical Cyclone Rainfall as Measured by the Nimbus 5 Electrically Scanning Microwave Radiometer," Bull. Am. Met. Soc., 55, 1074-1089.

Born, G.H., Dunne, J.A. and Lame, D.B., 1979, "SEASAT Mission Overview," Science, 204, 1405-1406.

Guymer, T., 1981, "Thunderstorm Action in JASIN Registered on SEASAT Microwave Sensors," Nature (to appear).

Hobbs, P.V., 1978, "Organization and Structure of Clouds and Precipitation on the Mesoscale and Microscale in Cyclonic Storms," Rev. of Geophys. and Space Phys., 16, 741-755.

Lipes, R.G., Bernstein, R.L., Cardone, V.J., Katsaros, K.B., Njoku, E.G., Riley, A.L., Ross, D.B., Swift, C.T. and Wentz, F.J., 1979, "SEASAT Scanning Multichannel Microwave Radiometer: Results of the Gulf of Alaska Workshop," Science, 204, 1415-1417.

Matejka, T.J., Houze, Jr., R.A., and Hobbs, P.V., 1980, "Microphysics and Dynamics of Clouds Associated with Mesoscale Rainbands in Extratropical Cyclones," Quart. J. Roy. Met. Soc., 106, 29-56.

Rosenkranz, P.W., Barath, F.T., Blinn III, J.C., Johnston, E.J., Lenoir, W.B., Staelin, D.H. and Waters, J.W., 1972, "Microwave Radiometric Measurements of Atmospheric Temperature and Water from an Aircraft, J. Geophys. Res., 77, 5833-5844.

Royal Society, 1979, "Air Sea Interaction Project. Summary of the 1978 Field Experiment (JASIN, 1978)," The Royal Society, London, pp. 139.

SEASAT Gulf of Alaska Workshop, Report Vol. I and II, JPL-622-101-NASA, Jet Propulsion Laboratory, California Institute of Technology, Pasadena, California, 1979.

SEASAT-JASIN Workshop Report, Jet Propulsion Laboratory, California Institute of Technology, Pasadena, California, 1980 (to appear).

SEASAT SMMR-Mini Workshop I, JPL-622-200-NASA, Jet Propulsion Laboratory, California Institute of Technology, Pasadena, California, 1979.

SEASAT SMMR-Mini Workshop II, JPL-622-212-NASA, Jet Propulsion Laboratory, California Institute of Technology, Pasadena, California, 1979.

Staelin, D.H., Kunzi, K.F., Pettyjohn, R.L., Poon, R.K.L. and Wilcox, R.W., 1976, "Remote Sensing of Atmospheric Water Vapor and Liquid Water with the Nimbus 5 Microwave Spectrometer," J. Appl. Met., 15, 1204-1214.

Taylor, P.K., 1981, "Identification of Frontal Features in JASIN using SEASAT Water Vapor, Liquid Water, and Rain Rate Maps, Nature (to appear).

Wilheit, T.T. and Chang, A.T.C., 1979, "An Algorithm for Retrieval of Ocean Surface and Atmospheric Parameters from the Observations of the Scanning Multichannel Microwave Radiometer (SMMR)," NASA Tech. Mem. 80277 Goddard SFC, Greenbelt, Md.

Nature Vol. 294 24/31 December 1981, 737-739.

Determinations by Seasat of atmospheric water and synoptic fronts

P. K. Taylor

Institute of Oceanographic Sciences, Wormley, Godalming, Surrey GU8 5UB, UK

K. B. Katsaros

Department of Atmospheric Sciences, University of Washington, Seattle, Washington 98195, USA

R. G. Lipes

Jet Propulsion Laboratory, Pasadena, California 91103, USA

The Seasat Scanning Multichannel Microwave Radiometer (SMMR)[1,2] determined the total atmospheric water vapour, q_t, over 600-km wide swaths with a resolution of 54 km. Using radiosonde data from the Joint Air–Sea Interaction experiment, JASIN[3], we show here that the SMMR q_t distributions can be used to detect the position of atmospheric fronts in the lower troposphere. Unlike visible and IR radiometry these SMMR determinations are not hampered by extensive cirrus or by lack of frontal cloud. Advantages of the SMMR over previous passive microwave instruments on satellites such as Nimbus 5 and 6 (refs 4–9) are: the use of more channels, allowing better discrimination between the effects of liquid water, water vapour and sea state; and improved spatial resolution. The SMMR performance has been evaluated at several workshops[10–14]. Our results[15] show that the SMMR q_t determinations have similar accuracy to *in situ* radiosonde measurements.

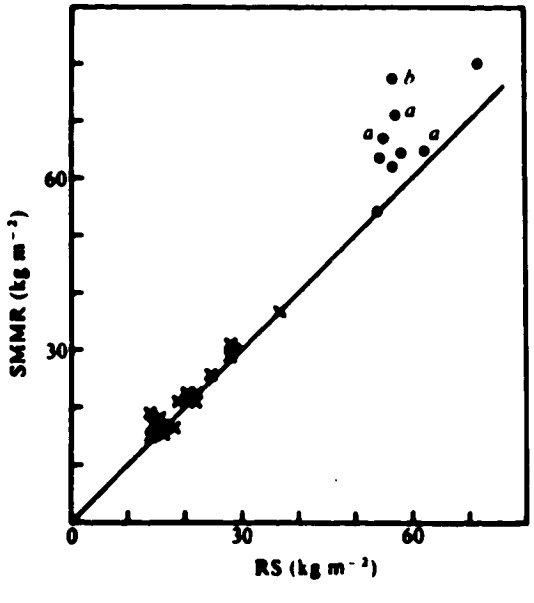

Fig. 1 Comparison of integrated atmospheric water vapour q_t as measured by the SMMR and by radiosondes. ×, JASIN values; ●, tropical soundings. *a* indicates tropical soundings for which SMMR values may be too high due to the island of Guam being within the field of view. *b*, SMMR values may have been affected by heavy rain.

Independently evaluated SMMR and radiosonde estimates of q_t were compared at the Seasat–JASIN Workshop[13] (Fig. 1). The SMMR results were evaluated using the Wentz algorithm[10], the nearest grid values being linearly interpolated to the radiosonde launch position. Radiosonde data from the JASIN experiment, conducted in the North Atlantic (60 °N, 12 °W) during July to September 1978[3], are shown. Specially calibrated fast sampling radiosondes were used and comparisons restricted to flights launched within ±2 h of Seasat overpass time. Estimated accuracy of the radiosonde q_t value was $\sim\pm1.7\,kg\,m^{-2}$ (ref. 13). The mean difference, SMMR minus radiosonde, was $1.2\pm1.6\,kg\,m^{-2}$. To provide comparison at higher q_t values

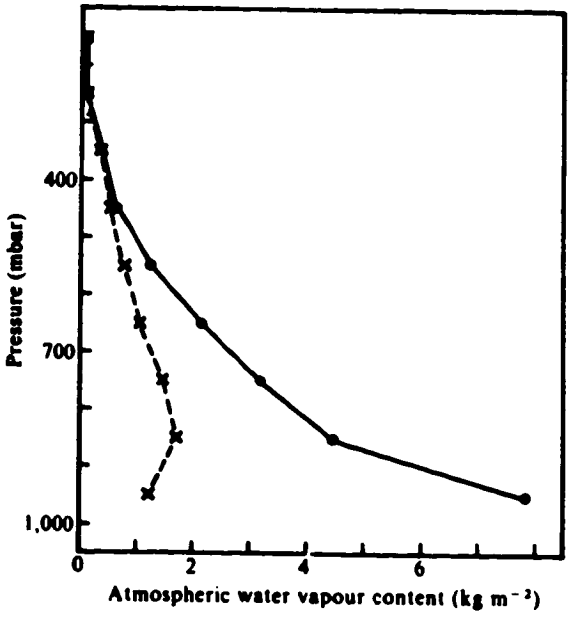

Fig. 2 Mean atmospheric water vapour content of 100-mbar layers during JASIN. Solid line shows the mean value and the dashed line the standard deviation of individual observations for some 200 radiosonde flights of which 110 reached 400 mbar.

radiosonde flights from tropical islands and weather ship Tango are also plotted. These are standard synoptic ascents within 3 h of overpass time. Estimates of q_t cannot be obtained over land and the tropical island of Guam, being significant in size compared with the SMMR resolution, may have affected the data for three flights marked. One comparison may be affected by local heavy rain. Eliminating these flights the mean difference is $4.9\pm3.7\,kg\,m^{-2}$. Radiosonde errors would be expected to be greater in these ascents and, as for JASIN, the actual error due to the SMMR is not known. However, changes to the SMMR evaluation procedures following the Seasat–JASIN workshop have shown reduced biases[14].

The SMMR also provided liquid water and rain rate estimates; however, no quantitative evaluation was possible because of the difficulty of obtaining reliable *in situ* measurements. The horizontal variation of liquid water content was

Fig. 3 NOAA 5 IR satellite photograph at 10.37 GMT on 5 September 1978 showing a front stretching from Ireland and Scotland (lower left) to Iceland (upper right). SMMR derived values of q_l are shown in kg m^{-2}. The dashed line marks the maximum in these values. (Photograph: University of Dundee.)

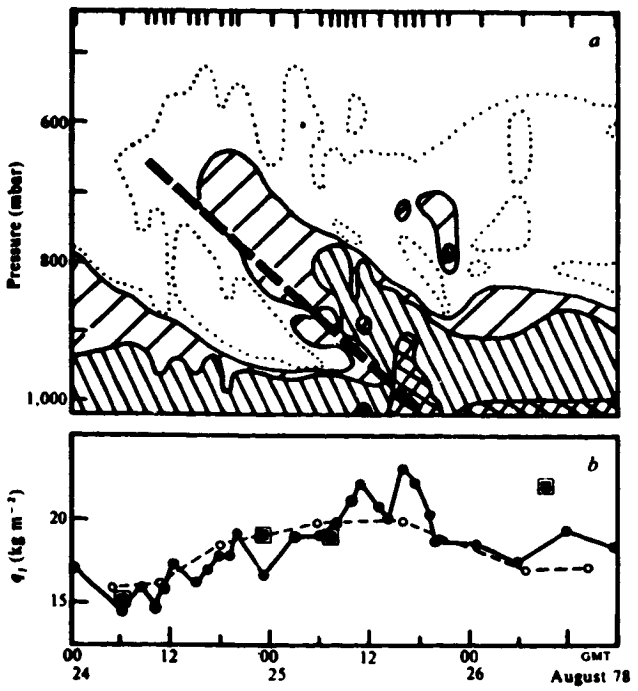

Fig. 4 *a*, Time–height atmospheric cross-section showing the variation of specific humidity with the passage of a warm front. Values shown are 2 g per kg (dotted), 4–6 g per kg (wide diagonals), 6–8 g per kg (close diagonals), above 8 g per kg (cross-hatched). The section is based on 31 radiosonde flights at the times marked at the top. The dashed line marks the approximate region of the frontal surface. *b*, Values of q_l from the radiosonde data (solid line), SMMR (■) and SMMR q_l distribution at 07.30 GMT on 24 August. The moist air ascending the front results in an increase in q_l with time to a maximum at about the time of surface frontal passage. Following the front there is a decrease to the warm air boundary layer value. .

qualitatively consistent with the meteorological conditions (see ref. 16). For JASIN, SMMR indicated rain when precipitation was 'widespread'—reported by several JASIN ships. Light scattered showers were not detected probably because such showers have horizontal dimensions very much less than the SMMR resolution. Although difficult to obtain[17], quantitative determination of rainfall would have obvious meteorological value. Rain detection is also needed to flag doubtful q_l values (Fig. 1). However, two different rain rate algorithms used in SMMR evaluation gave different quantitative results showing that much more work is needed on this variable.

The accurate horizontal distributions of q_l provided by SMMR are useful not only for the calculation of atmospheric water budgets[18], but also for determining the position of synoptic scale fronts in the lower troposphere. To demonstrate this we need to consider the vertical distribution of water vapour in the atmosphere. Figure 2 shows the mean water vapour content of each 100-mbar atmospheric layer for the whole of the JASIN experiment. The water vapour content falls rapidly with decreasing pressure and temperature, ~80% of the total occurring in the lowest 250 mbar. In contrast the variability of water vapour content is a maximum not at the surface but in the 900–800 mbar layer, and decreases less rapidly, 80% of the variation being spread over the lowest 400 mbar. Thus for this mid-latitude area, although the surface boundary layer is typically 1–2 km deep and contains much of the water vapour, the variability of q_l is not dominated by boundary layer processes but reflects changes in humidity at levels up to 5 km. Synoptic scale fronts cause moistening at these levels and hence result in significant variations of q_l. For example, Fig. 3 shows a NOAA 5 satellite IR image in which an occluded front is marked by a 250-km wide band of cirrus which masks any lower level clouds. The variation of q_l measured by SMMR showed a strong maximum associated with the front, marked in Fig. 3 by the broken line. The position of this maximum was well defined to within the 54-km SMMR resolution, except in one area where a more complicated frontal structure was indicated.

The actual position of the surface front relative to the q_l maximum will vary from case to case. As an example Fig. 4*a* shows a radiosonde derived time–height cross-section of specific humidity during the passage of a warm front. Although the front was a significant feature of the radiosonde data, lack of frontal cloud prevented its detection in visible or IR satellite images. The corresponding variation of q_l is shown in Fig. 4*b*. SMMR values are in reasonable agreement with the radiosonde values. A difference on the 26 August was probably caused by larger values of q_l occurring just outside the JASIN area but within the SMMR resolution cell. Radiosonde observations from other JASIN ships show that the front propagated through the area with little change in structure and hence the SMMR horizontal q_l distribution for 07.30 GMT on 24 August has been transformed

to the time variation shown by the dashed line in Fig. 4. Both radiosondes and SMMR show that, in spite of a marked reduction in boundary layer height, there was a gradual increase of q_t with the approach of the front. The surface passage of the front was marked by a sharp decrease of q_t to the warm air boundary layer value. By mapping these q_t variations in the SMMR data from several Seasat orbits the changing position and alignment of the front have been determined more precisely than was possible using the conventional meteorological observations.

Detection of synoptic fronts in the lower troposphere using SMMR q_t measurements offers an important new aid for meteorological analysis which is already proving valuable in the interpretation of the JASIN data.

K.B.K. acknowledges support by NOAA/NASA contract NA 78 SAC 04102 and the Jet Propulsion Laboratory.

Received 22 June, accepted 6 October 1981.

1. Born, G. H., Dunne, J. A. & Lame, D. B. *Science* **204**, 1405–1406 (1979).
2. Njoku, E. G., Stacey, J. M. & Barath, F. T. *IEEE J. ocean. Engng* **OE-5**, 100–115 (1980).
3. *Air–Sea Interaction Project* (The Royal Society, London, 1979).
4. Wilhelt, T. T. *Boundary Layer Met.* **13**, 277–293 (1978).
5. Staelin, D. H. *et al. J. appl. Met.* **15**, 1204–1214 (1976).
6. Rosenkranz, P. W., Staelin, D. H. & Grody, N. C. *J. geophys. Res.* **83**, 1857–1868 (1978).
7. Viezee, W., Shigeishi, H. & Chang, A. T. C. *J. appl. Met.* **18**, 1151–1157 (1979).
8. Rodgers, E., Siddalingaiah, H., Chang, A. T. C. & Wilheit, T. T. *J. appl. Met.* **18**, 978–991 (1979).
9. Grody, N. C., Gruber, A. & Shen, W. C. *J. appl. Met.* **19**, 986–996 (1980).
10. *Rep. Seasat Gulf of Alaska Workshop* Vols I, II (JPL-622-101-NASA, Jet Propulsion Laboratory, Pasadena, 1979).
11. *Seasat SMMR Mini-Workshop I* (JPL-622-208-NASA, Jet Propulsion Laboratory, Pasadena, 1979).
12. *Seasat SMMR Mini-Workshop II* (JPL-622-212-NASA, Jet Propulsion Laboratory, Pasadena, 1979).
13. *Rep. Seasat-JASIN Workshop* Vol. 1 (JPL-[illegible], Jet Propulsion Laboratory, Pasadena, 1980).
14. *Seasat SMMR Mini-Workshop III* (JPL-622-224-NASA, Jet Propulsion Laboratory, Pasadena, 1980).
15. Katsaros, K. B., Taylor, P. K., Alishouse, J. C. & Lipes, R. G. *Boundary Layer Met.* (in the press).
16. Guymer, T. H., Businger, J. A., Jones, W. L. & Stewart, R. H. *Nature* **294**, 735–737 (1981).
17. Lovejoy, S. & Austin, G. L. *Q. Jl R. met. Soc.* **106**, 255–276 (1980).
18. Viezee, W., Davis, P. A. & Wolf, D. E. *Mon. Weath. Rev.* **106**, 1627–1633 (1978).

APPENDIX C.

In Proceedings of the Global Water Budget Symposium, 10-15 August 1981, Oxford, England, 1982.

Atmospheric water distributions determined by the Seasat Multichannel Microwave Radiometer

P.K. Taylor (Institute of Oceanographic Sciences, Wormley) T.H. Guymer (IOS, Wormley), K.B. Katsaros (University of Washington, Seattle), R.G. Lipes (Jet Propulsion Laboratory, Pasadena).

Abstract

The Seasat Scanning Multichannel Microwave Radiometer (SMMR) provided determinations of total atmospheric water vapour q_v and liquid water q_l and estimates of rain rate. During the life of Seasat the Joint Air Sea Interaction Experiment, JASIN, took place in the North Atlantic. JASIN radiosonde data show that variations in q_v and q_l reflect changes of structure in the first 500mb of the atmosphere. For JASIN q_v had values between 10 and 30 kg/m² and varied by 15 kg/m² for a given near surface humidity value, hence surface humidity was a poor predictor of q_v. Comparisons show that the SMMR measures q_v at least as accurately as the JASIN radiosondes. SMMR q_l and rain rate values are in qualitative agreement with JASIN observations. Quantitative evaluation is hampered by lack of independent measurements; for those few comparisons which can be made, agreement is good.

Examples are given of the use of SMMR data in the detection of atmospheric fronts, the mapping of areas of widespread rainfall, and the detection of a mesoscale thunderstorm area. The SMMR is shown to be a valuable research tool contributing to the analysis of the JASIN data.

1. Introduction

Seasat, the first oceanographic satellite using microwave sensors, was launched on 28 June 1978 and failed on 10 October 1978. The satellite (Born, Dunne & Lame, 1979) carried five instruments including a Scanning Multichannel Microwave Radiometer, SMMR (Njoku, Stacey & Barath, 1980) a similar instrument to that currently in operation on Nimbus 7. The SMMR measured microwave radiation from the earth at five frequencies between 6.6 and 37 GHz for both vertical and horizontal polarizations (Table 1). This allows estimation of sea surface temperature and wind speed; and atmospheric water vapour, liquid water and rain rate (Wilheit, 1978; Wilheit, Chang & Milman, 1980). This paper will consider the last three variables which represent major components of the atmospheric water budget.

Passive microwave radiometry has been previously used to measure atmospheric water from satellites such as Nimbus 5 and Nimbus 6. Both the Nimbus 5 Microwave Spectrometer, NEMS (Staelin, Kunzi, Pettyjohn, Poon, Wilcox & Waters, 1976), and the Scanning Microwave Spectrometer, SCAMS (Rozenkranz, Staelin & Grody, 1978), used a 22 GHz water vapour channel and 31 GHz window channel for atmospheric water vapour determinations (e.g. Viezee, Davis & Wolf, 1978; Liou & Duff, 1979). Electrically Scanning Microwave Radiometers, ESMR, carried on Nimbus 5 (Allison, Rodgers, Wilheit & Fett, 1974; Wilheit, Chang, Rao, Rodgers & Theon, 1977) and Nimbus 6 (Rodgers, Siddalingaiah, Chang & Wilheit, 1979) were designed to map rainfall areas. The advantages of the SMMR over these previous instruments are the incorporation of additional channels to

allow better discrimination between the effects of liquid, water, water vapour and sea state and improved spatial resolution (Table 1).

Seasat was an experimental satellite and the performance of the sensors has required validation by comparison with *in situ* measurements. For the SMMR the Gulf of Alaska Experiment, GOASEX, was designed for this purpose. The results have been evaluated at a number of workshops and reported in GOASEX I Report (1979), Lipes *et al.* (1979), SMMR-Mini I Report (1979), SMMR-Mini II Report 1979 and GOASEX II Report (1980). The results for atmospheric water are summarized by Katsaros, Taylor, Alishouse and Lipes (1981).

During the life of Seasat a large, independently organized field experiment, the Joint Air Sea Interaction experiment, JASIN (Royal Society, 1979) took place in the North Atlantic Ocean. Comparisons of Seasat data and JASIN measurements are reported in the Seasat-JASIN Report (1980) and SMMR-Mini III Report (1980). The JASIN radiosonde data has been particularly valuable in evaluating the SMMR atmospheric water determinations (Katsaros *et al.*, 1981).

The aim of the present paper is to demonstrate the value of SMMR derived atmospheric water distributions for scientific analysis of atmospheric structure by presenting examples from the JASIN experiment. SMMR data will be used to detect the position of atmospheric fronts, to map rainfall regions, and in the detection of mesoscale features. However, first it will be necessary to consider how two quantities measured by SMMR, the total atmospheric water vapour content q_v and the total liquid water content q_l, relate to the vertical structure

of the atmosphere and to consider the accuracy of the SMMR measurements of these quantities.

2. Radiosonde and SMMR determinations of atmospheric water

2.1 The JASIN radiosonde observations

During JASIN radiosonde ascents were released from three ships which formed a triangle of approximately 200km sides centred at about 59½°N, 12½°W in the North Rockall Trough region of the North Atlantic. The ships were on station between 23rd July and 8th August and 22nd August to 4th September, 1978. During certain periods a fourth radiosonde ship was positioned at the triangle centre. Radiosondes were released from each ship at intervals of at most six hours and at approximately hourly intervals during the daylight hours of chosen intensive days. VIZ 1220 and 1223 radiosondes were used with factory calibrated "premium" sensors of U.S. National Weather Service type sampled every 0.8 seconds. The resulting data set provides a uniquely detailed description of the troposphere at a midlatitude open ocean site during a summer time period. The data will be used to show the variability of the observed atmospheric water amounts and to provide comparisons with the SMMR measurements.

2.2 Atmospheric water vapour variations

The variability of the integrated atmospheric water vapour content q_v during JASIN has been summarized by Taylor, Katsaros & Lipes (1981) but will be discussed here in more detail. Figure 1 shows mean values of q_v for 5mb layers for all the JASIN radiosonde flights evaluated to date, about 600 ascents. As is well known, the decrease of temperature with height results in a rapid decrease of q_v; some 80% of

q_v occurring in the range $p^* = 0$ to $p^* = 250$mb where

$$p^* = p_o - p_j$$

with p_o the surface pressure and p_j the pressure at the level of interest. In contrast the standard deviation of q_v for each 5mb layer is a maximum not at the surface but in the p^* range 120mb to 230mb. This is due to the relative uniformity of the surface boundary layer and the large fluctuations in q_v for those layers which are sometimes within the boundary layer and at other times within the drier air above. The standard deviation remains comparable to the surface value to about $p^* = 550$mb and 80% of the variation is spread over the p^* range 0 to 400mb. Thus despite the maximum of q_v at the surface, variations of q_v may reflect changes in at least the first 500mb of the atmosphere.

An important consequence of the above is that the use of surface humidity measurements together with a standard model atmosphere to calculate the moist tropospheric radio range correction for satellite radar altimeter measurements (e.g. Saastamoinen, 1971) is subject to significant error. This is demonstrated by Figure 2 which shows the JASIN radiosonde q_v values plotted against the observed near surface specific humidity. The dashed lines represent limits within which the points may, a priori, be expected to lie. The right hand cutoff simply represents 100% near surface relative humidity for the mean observed air temperature, points to the right represent higher air temperatures. The sloping dashed lines have been calculated using a simple model atmosphere. This contains a surface boundary layer in which the surface specific humidity and potential temperature are constant with height (i.e. well mixed) until saturation is reached at the

lifting condensation level (LCL). Above the LCL, 100% humidity and constant equivalent potential temperature are assumed until a specified inversion height p^*_i above which a mean JASIN temperature profile and constant relative humidity are assumed. The lower dashed line represents a boundary layer to p^*_i = 100mb and 20% relative humidity above (or equivalently p^*_i = 170mb and 10% above). This is approximately the minimum q_v model for JASIN. The upper dashed line represents p^*_i = 0mb, that is 100% relative humidity from the LCL upwards. The observed points however are not bounded by this line but lie beneath the sloping chain line which has been taken nominally to be p^*_i = 120mb and a relative humidity above the boundary layer equal to the near surface value. The inference is that drier air does not occur at the surface without drier air being present above the boundary layer. The final bounding line, the left hand vertical chain line, represents surface humidity of 65% the lowest values observed during JASIN.

The variation of q_v with near surface humidity is therefore more limited than might be expected, particularly for lower values of the latter. However, the maximum range, at near saturation surface values, was 15kg/m^2. This would represent an error of about 11cm in a radar altimeter measurement, a significant error in detecting the sea surface slope associated with ocean currents by satellite altimetry.

2.3 Comparison of SMMR and radiosonde q_v measurements.

The comparison of SMMR and radiosonde determinations of q_v at the Seasat JASIN workshop has been reported by Katsaros et al. (1980) and Taylor et al. (1981) and will only be summarized here. Figure 3 shows comparisons for JASIN ascents

(crosses) and tropical soundings (circles). For JASIN the mean difference, SMMR minus radiosonde, was 1.2 $\pm$ 1.6kg/m² which compares very favourably with the estimated accuracy of the radiosondes of $\pm$ 1.7kg/m².

In the tropics radiosonde errors would be expected to be greater, and, after elimination of values contaminated by land effects or, in one case, heavy rain, the mean difference was 4.9 $\pm$ 3.7kg/m². Changes in the SMMR evaluation procedures following the Seasat-JASIN workshop have removed this bias (SMMR-Mini III, 1980), and it appears that SMMR can measure atmospheric water vapour at least as accurately as radiosonde ascents.

2.4 Radiosonde determinations of liquid water.

Radiosondes do not measure liquid water and the only direct measurements available for JASIN were obtained by aircraft equipped with Johnson-Williams type instruments (Slingo, Nicholls & Schmetz, 1981). These measurements were limited in space and time and in order to attempt to provide comparisons with Seasat estimates an attempt has been made to extend the data by inferring liquid water content from the radiosonde flights. Fortunately Slingo et al. 1981 show that, for the marine stratocumulus layer which frequently occurred during JASIN, the liquid water content was very close to that calculated by adiabatic ascent of a parcel of air from cloud base. The level at which the radiosonde balloon was observed to enter cloud was noted during JASIN and hence, for stratocumulus, the specific liquid water content Q_l is given by

$$Q_l = Q_{CB} - Q_j$$

where Q_{CB} and Q_j represent the specific humidity at cloud base

and at the level of interest. The total liquid water content is therefore obtained by integrating between cloud base and the cloud top. For the JASIN radiosondes the mean relative humidity at cloud entry was 98 $\pm$ 3% and a fall to 95% or less was arbitarily chosen as marking cloud top. This gave good agreement with the aircraft measurements where these were available. Upper cloud layers were assumed if the relative humidity rose above 98%, extending until values less than 95% were encountered, and the calculations were performed for all ascents irrespective of cloud type; the justification for the latter being to attempt to make some estimate of q_l however approximate.

The resulting radiosonde derived liquid water data is represented in Figure 4. The continuous line shows the number of ascents reporting "cloud" at each level from a total of about 600 ascents of which all but 50 reached 500mb. The maximum occurs just below the maximum variation of q_v (Figure 1), that is below the mean boundary layer top. The dashed line shows the mean liquid water content for each 5mb layer where the mean is taken over only those ascents reporting liquid water at that level. This increases through the boundary layer and then remains high as long as "clouds" are present. This behaviour probably reflects the adiabatic assumption used as much as the real atmospheric distribution, however it does suggest that all layers to 500mb could make a significant contribution to liquid water content. The dotted line shows the number of ascents reporting cloud if only the lowest cloud layer, that which the balloon was observed to enter, is included. The liquid water content (not shown) was similar to that for all layers except that the cutoff was at about $p^* = 300$mb.

2.5 SMMR determinations of liquid water

Katsaros et al. (1981) present comparisons of two different algorithms used in evaluating the SMMR data. For JASIN the agreement was within about 0.06kg/m² for q_1 less than 1kg/m². For higher q_1 values and in the tropics agreement was less good with the Wentz algorithm (GOASEX I Report, 1979) giving higher values than that of Wilheit (Wilheit & Chang, 1979). Under certain circumstances both algorithms exhibited negative values suggesting a bias, (SMMR-Mini III, 1980) however this was not evident in the Wentz determination for the JASIN area which will be used in this report.

2.6 Comparison of SMMR and Radiosonde q_1 values.

A comparison of SMMR q_1 measurements and in situ estimates is shown in Figure 5. The SMMR values represent the mean liquid water content for all passes on a given day for the area 58.5°N to 61°N and 9°W to 16°W. The radiosonde values represent the mean for all flights on a given day for all of the ships, different symbols indicating the magnitude of the standard deviation between the three ships. Solid symbols represent those days on which a relatively uniform stratocumulus layer covered the area. The aircraft measured values are shown by squares. That shown in parentheses was derived from a single profile (S. Nicholls, personal communication), the other being a mean of several profiles (Slingo et al. 1981). For both aircraft measurements there was a uniform stratocumulus cover. The figure shows that for q_1 less than 0.2kg/m² the standard deviation of the radiosonde values was small and the agreement with SMMR was good, particularly for the stratocumulus cases. At higher

q_1 values the radiosondes showed high variability and tended to overestimate compared to SMMR. This would be expected, both because the adiabatic assumption is less likely to hold for deeper cloud layers, and because of the assumption that a higher cloud layer always occurred when over 98% relative humidity was observed. Figure 6 shows the comparison if only the first, observed, cloud layer is allowed. The standard deviation of many of the radiosonde values is decreased and more cases are in agreement with the SMMR. There is a possible tendency for the radiosondes to underestimate for the non-stratocumulus low q_1 days (open circles). This again is reasonable since these represent broken small cumulus cloud cover which is badly sampled by the radiosondes.

In summary, for those cases where the radiosonde liquid water measurements should be reliable agreement with SMMR is good. For the other cases the differences between SMMR and radiosondes are physically reasonable. The comparison further emphasises the difficulty of obtaining liquid water data by means other than microwave radiometry.

2.7 SMMR measurements of rain rate.

SMMR rain rate determinations are discussed by Katsaros et al. (1981) and SMMR-Mini III (1980). For JASIN the Wentz and Wilheit algorithms (section 2.5) showed a scatter of about 0.5mm/hr in rain rate. For the tropics the scatter was much greater. The Wilheit algorithm predicted rain for more cases than did the Wentz. Qualitatively, for JASIN, SMMR predicted rain when precipitation was "widespread", i.e. reported by several JASIN ships. Light scattered showers, with horizontal dimensions very much less than the SMMR resolution, were not detected. Lack of surface truth has prevented a quantitative comparison, however section 3.2 below presents a single example

in which SMMR and ship measured rain rates were in reasonable agreement.

3. Examples of SMMR atmospheric water distributions for the JASIN area.

3.1 The detection of atmospheric fronts.

Taylor et al. (1981) have shown that the position of atmospheric fronts could be detected by SMMR on occasions where lack of distinct cloud structures made detection by visible or infra-red imagery difficult. Figure 7, taken from their paper is a time height cross-section showing the variation of specific humidity with the passage of the warm front based on radiosonde ascents from the ship Endurer at the northwest corner of the JASIN triangle. The values of q_v for the 31 radiosonde flights used is shown in the lower part of the figure. The ascending warm moist air results in an increase of q_v to a maximum at about the time of frontal passage. There is then a sharp fall to the warm air boundary layer value. It is now possible to superimpose SMMR values on the figure (square symbols). These show good agreement with the radiosondes except on the 26th. The disagreement at this time is probably due to strong gradients of q_v near the JASIN area and within the SMMR resolution cell.

Figure 8 shows the SMMR q_v distribution at 0730 gmt 24th August 1978, that is near the start of the period shown in Figure 7, superimposed on the NOAA 5 VHRR infra-red image for 1138 gmt. Values of q_v measured by the JASIN radiosonde ship triangle (shown in boxes) are in good agreement with the SMMR data. The JASIN radiosonde observations indicate little change in the frontal structure with time. Hence the horizontal distribution in Figure 8 can be transformed into a time variation of q_v at Endurer using the appropriate

propagation speed, taken as 2 m/s toward 005°. The resulting time variation of q_v is shown by the dashed line in the lower part of Figure 7 and agrees reasonably with the radiosonde values.

Thus the surface frontal position has been marked on Figure 8 by reference to the SMMR q_v distribution and the frontal movement has been calculated using succeeding SMMR passes. This was not possible using visible and infra-red imagery because of the lack of any distinct cloud band associated with the front (Figure 8). Nor was the frontal position detectable in the standard synoptic surface data and the front was shown as discontinuous in the U.K. Meteorological Office analysis. Frontal detection by SMMR will considerably aid interpretation of the JASIN radiosonde data.

3.2 Detection of rainfall areas.

During the evening of 30th August 1978 an occluding frontal system passed over the JASIN area. SMMR rainfall rates measured at 2311 gmt are shown in Figure 9 superimposed on the NOAA 5 VHRR Infra-Red image from 2030 gmt. The approximate positions of the surface fronts were marked by reference to the VHRR and SMMR data and corresponds approximately to the U.K. Meteorological Office analysis except that the latter placed the occlusion point about 100km to the West. The SMMR q_v and q_l distributions are shown in Figure 10. The warm air sector ahead of the cold front had q_v values greater than 3[illegible]kg/m² compared to a minimum in the cold air to the east of the frontal system of less than 12kg/m². Liquid water content was generally less than 0.2kg/m² except in the occlusion point region where a large area had q_l greater than 0.6kg/m² with a maximum of over 0.8kg/m².

The area of over 0.4mm/hour rain is shaded. The figure may be interpreted in terms of the ascent of warm moist air in the occlusion region with condensation to liquid water and the production of rain.

The SMMR data on the 30th and 31st suggested that the main rain area moved at 12m/s towards 110°. Using these values rain would be predicted at HMS Hecla at the northeast corner of the JASIN triangle between 1600 and 2300 gmt with a mean SMMR rain rate of 0.4mm/hour. Figure 11 shows the rainfall as measured at HMS Hecla. Rain occurred between 1600 and 2400 gmt with a mean of 0.7mm/hour. Considering the difficulty of making accurate shipboard measurements of rainfall this is in reasonable agreement with the SMMR.

Quantitative rainfall measurements were not available from the other JASIN ships, however Figure 12 shows the present weather types, reported in standard meteorological code, plotted in a frame of reference moving with the SMMR rain area. Observations of rain generally lie within the 0.2mm/hour SMMR contour while SMMR values between 0.1 and 0.2mm/hour correspond to drizzle. However, the distinctions between moderate and slight rain and whether intermittent or continuous do not correspond with SMMR rain rate values.

This example shows that the SMMR rainfall rates can be used to map areas of widespread rain over the ocean. It is hoped to use the SMMR data quantitatively to estimate total rainfall amounts and latent heat release in the occlusion point region, however this awaits a complete trajectory analysis for the situation.

3.3 Mesoscale features

The SMMR can resolve atmospheric structures having

length scales of 100km and upwards and the last example shows the detection of a thunderstorm area on 4th August 1978. This feature was detected by several of the Seasat sensors and has been discussed in more detail by Guymer, Businger, Jones & Stewart (1981). Figure 13 shows the synoptic situation at about 2100 gmt. A near stationary cold front lay to the southwest while a cold occluded front moved southwestward through the JASIN area at about 5m/s. Radiosonde ascents showed that between these fronts boundary layer convection was prevented from penetrating above about 2km height by a strong temperature inversion with marked the warm front surface of the occlusion. The air above this inversion was potentially unstable and could support deep convection extending from 2 to 6km if lifted by a small amount. The SMMR derived q_v and q_l distributions are shown in Figure 14. There was a region of high q_v between the fronts with low values in the cold air sectors. A maximum in q_l occurred at the cold front presumably indicating ascent of the warm air over the frontal surface. Maxima in q_v and q_l occurred to the southeast of the JASIN area at a position marked by deep convective cloud in the NOAA 5 VHRR and Seasat Visible and Infra-Red Radiometer imagery. Assuming that this feature was steered with the mid-tropospheric flow (Newton & Katz, 1958), it would have passed over the southern part of the JASIN triangle at about 2330 gmt. Three of the JASIN ships in that region reported thunderstorm activity between 2100 gmt and midnight.

Thus a mesoscale region of midlevel thunderstorm

activity was detected in the SMMR data as a maximum in q_v and q_l. Despite the deep convection the ships reported little precipitation at the surface during the period and SMMR indicated zero rain rate over the area.

4. Summary

For a midlatitude deep ocean area variations in integrated water vapour, q_v, and liquid water, q_l, reflect changes in the structure of the lower 500mb of the atmosphere. Surface humidity is a poor prediction of q_v however SMMR measurements of q_v are at least as accurate as radiosonde values. SMMR values of q_l agree with radiosonde estimates for uniform marine stratocumulus cloud cover. For other cases the SMMR estimates appear reasonable but lack independent confirmation. Similarly for rain rate the SMMR estimates appear qualitatively correct and quantitatively reasonable for cases of widespread rainfall however good independent measurements are lacking. This was demonstrated for the ascent of the warm air at an occlusion.

SMMR derived q_v distributions may be used to position synoptic scale fronts even in cases where this is not possible from visible or infra-red imagery. A mesoscale region of midlevel thunderstorm activity was detected in the SMMR data as maxima in q_v and q_l.

The examples which have been shown represent the first stages in the use of SMMR measurements in analysis of the JASIN data. The JASIN radiosondes, JASIN surface observations and SMMR measurements are complementary data sets with which it is hoped to improve our understanding

of the midlatitude atmosphere over the ocean. Despite its short life the Seasat SMMR has graduated from a sensor validation project to an actively used research tool.

References

Allison, L.J., Rodgers, E.B., Wilheit, T.T. & Fett, R.W. 1974 Tropical cyclone rainfall as measured by the Nimbus 5 Electrically Scanning Microwave Radiometer. Bull. Am. meteorol. Soc., 55, 1074-1089.

Born, G.H., Dunne, J.A. & Lame, D.B. 1979 Seasat Mission Overview. Science, N.Y., 204, 1405-1406.

GOASEX I Report 1979 Seasat Gulf of Alaska Workshop Report, JPL-622-101-NASA, Vol.1., Pasadena: Jet Propulsion Laboratory, California Inst. of Technology.

GOASEX II Report 1980 Seasat Gulf of Alaska Workshop II Report, JPL-622-107-NASA, Pasadena: Jet Propulsion Laboratory, California Inst. of Technology.

Guymer, T.H., Businger, J.A., Jones, W.L. & Stewart, R.H. 1981 Anomalous wind estimates from the Seasat Scatterometer, (letter submitted to Nature).

Katsaros, K.B., Taylor, P.K., Alishouse, J.C., & Lipes, R.G. 1981 Quality of Seasat SMMR (Scanning Multi-Channel Microwave Radiometer) atmospheric water determinations. Boundary-Layer meteorol. (accepted for publication).

Liou, K-N. & Duff, A.D. 1979 Atmospheric liquid water content derived from parameterization of Nimbus 6 Scanning Microwave Spectrometer data. J. appl. meteorol., 18, 99-103.

Lipes, R.G., Bernstein, R.L., Cardone, V.J., Katsaros, K.B., Njoku, E.G., Riley, A.L., Ross, D.B., Swift, C.T., & Wentz, F.J. 1979 Seasat Scanning Multichannel Microwave Radiometer: Results of the Gulf of Alaska Workshop. Science, N.Y., 204, 1415-1417.

Newton, C.W. & Katz, S. 1958 Movement of large convective rainstorms in relation to winds aloft. Bull. Am. meteorol. Soc., 39, 129-136.

Njoku, E.G., Stacey, J.M. & Barath, F.T. 1980 The Seasat Scanning Multichannel Microwave Radiometer (SMMR): instrument description and performance. IEEE J. Oceanic Eng., OE-5, 100-115.

Rodgers, E., Siddalingaiah, H., Chang, A.T.C. & Wilheit, T.T. 1979 A statistical technique for determining rainfall over land employing Nimbus 6 ESMR measurements. J. appl. meteorol., 18, 978-991.

Royal Society 1979 Air-Sea Interaction Project: Summary of the 1978 Field Experiment (JASIN 1978) 139 pp. London: The Royal Society.

Rozenkranz, P.W., Staelin, D.H. & Grody, N.C. 1978 Typhoon June (1975) viewed by a Scanning Microwave Spectrometer. J. geophys. Res., 83, 1857-1868.

Saastamoinen, J. 1971 Use of artificial satellites for geodesy; atmospheric correction for the troposphere and stratosphere in radio ranging for satellites. In: Proc. of 3rd Intern.Symp., Am. Geophys. Union.

Seasat-JASIN Report 1980 Seasat-JASIN Workshop Report Volume 1: Findings and Conclusions. JPL 80-62, Pasadena: Jet Propulsion Laboratory, California Inst. of Technology.

SMMR-Mini I 1979 Seasat SMMR-Mini Workshop I, JPL-622-208-NASA, Pasadena: Jet Propulsion Laboratory, California Inst. of Technology.

SMMR-Mini II 1979 Seasat SMMR-Mini Workshop II, JPL-622-212-NASA, Pasadena: Jet Propulsion Laboratory, California Inst. of Technology.

SMMR-Mini III 1980 Seasat SMMR-Mini Workshop III, JPL-622-224-NASA, Pasadena: Jet Propulsion Laboratory, California Inst. of Technology.

Slingo, A., Nicholls, S., & Schmetz, J. 1981 Aircraft observations of marine stratocumulus during JASIN, (submitted for publication).

Staelin, D.H., Kunzi, K.F., Pettyjohn, R.L., Poon, R.K.L., Wilcox, R.W. & Waters, J.W. 1976 Remote sensing of atmospheric water vapour and liquid water with the Nimbus 5 microwave spectrometer. J. appl. meteorol., 15, 1204-1214.

Taylor, P.K., Katsaros, K.B. & Lipes, R.G. 1981 Seasat Multichannel Microwave Radiometer atmospheric water determinations and the detection of synoptic fronts, (letter submitted to Nature).

Wilheit, T.T., Chang, A.T.C., Rao, M.S.V., Rodgers, E.B. & Theon, J.S. 1977 A satellite technique for quantitatively mapping rainfall rates over the oceans. J. appl. meteorol., 16, 551-560.

Wilheit, T.T., 1978 A review of applications of microwave radiometry to oceanography. Boundary-Layer meteorol., 13, 277-293.

Wilheit, T.T. & Chang, A.T.C 1979 An Algorithm for Retrieval of Ocean Surface and Atmospheric Parameters

from the Observations of the Scanning Multichannel Microwave Radiometer (SMMR), NASA Tech. Memorandum 80277, Greenbelt: NASA Goddard Space Flight Center.

Wilheit, T.T., Chang, A.T.C. & Milman, A.S. 1980 Atmospheric corrections to passive microwave observations of the ocean. Boundary-Layer meteorol., 18, 65-77.

Viezee, W., Shigeishi, H., & Chang, A.T.C. 1979 Relation between West Coastal Rainfall and Nimbus 6 SCAMS Liquid Water data over the Northeastern Pacific Ocean. J. appl. meteorol., 18, 1151-1157.

Frequency GHz	Wavelength cm	Retrieval Grid km x km	Principal Predicted Quantity
6.6	4.6	150 x 150	Sea surface temperature
10.7	2.8	85 x 85	Wind speed
18.0	1.7	54 x 54	Precipitation rate (18H), Water vapour, liquid water
21.0	1.4	54 x 54	Water vapour, liquid water
37.0	0.8	27 x 27	Precipitation rate (37H), Windspeed in clear air, Water vapour, liquid water

Table 1. Characteristics of the Seasat SMMR channels.
The retrieval grid is referred to a 3dB limit.

FIGURE LEGENDS

Figure 1. Mean atmospheric water vapour content during JASIN for 5mb layers and the standard deviation of individual radiosonde observations for each layer. Data was available for about 600 ascents.

Figure 2. Integrated atmospheric water vapour content q_v for individual radiosonde flights plotted against the near surface specific humidity at the time of launch. The top scale shows approximately the equivalent near surface relative humidity. For further explanation see text.

Figure 3. (after Taylor et al. 1981) Seasat-JASIN workshop comparison of integrated atmospheric water vapour q_v as measured by the SMMR and by radiosondes. JASIN values are shown by crosses, tropical soundings by circles. (1) - indicates tropical soundings for which SMMR values may be too high due to the island of Guam being within the field of view. (2) - SMMR values may have been affected by heavy rain. Processing changes since the workshop have removed the tropical data bias.

Figure 4. Number of radiosonde ascents for which cloud is inferred for 5mb layers of the atmosphere (full line: multiple cloud layers; dotted line: first layer only). Also shown is the mean liquid water content for cases reporting cloud in each layer (dashed line).

Figure 5. Comparison of SMMR, aircraft, and radiosonde estimates of total liquid water q_l where radiosonde estimates include all cloud layers. ■ = Aircraft, other symbols indicate radiosonde values with standard deviation (kg/m^2) as follows: ●, ○ < 0.05; ▽ < 0.1, △ < 0.5. Full symbols indicate stratocumulus cases.

Figure 6. As Figure 5 but radiosonde values include the first cloud layer only.

Figure 7. (above) Time-height atmospheric cross-section showing the variation of specific humidity with the passage of a warm front. Values shown are 2g/kg (dotted), 4 to 6 g/kg (wide diagonals), 6 to 8 g/kg (close diagonals), above 8 g/kg (cross-hatched). The section is based on 31 radiosonde flights at the times marked at the top of the figure. The dashed line marks the approximate region of the frontal surface. (below) Values of integrated water vapour q_v from the radiosondes (full line), SMMR (squares), and from the SMMR q_v distribution at 0730 gmt 24 August (dashed line). (Adapted from Taylor et al. 1981)

Figure 8. SMMR q_v distribution (kg/m^2) at 0730 gmt 24 August 1978 superimposed on NOAA 5 Infra-Red image for 1138 gmt. Radiosonde q_v values are shown in boxes. (Photo: University of Dundee).

Figure 9. SMMR rain rate values (mm/hour) at 2311 gmt 30 August 1978 superimposed on NOAA 5 Infra-Red image for 2030 gmt. (Photo: University of Dundee).

Figure 10. SMMR values of q_v (full lines, kg/m²) and q_l (dashed lines with values in boxes, kg/m²) at 2311 gmt, 30 August 1978. The region of over 0.4mm/hour rain rate is shaded.

Figure 11. Rainfall measurements from HMS Hecla for the evening of 30 August 1978.

Figure 12. Comparison of SMMR rain rate measurements (as Figure 9) and W.M.O. present weather codes reported from the three JASIN ships assuming that the rainfall area propagated at 12 m/s toward 110°.

Figure 13. Synoptic chart for 2100 gmt on 4 August 1978, full arrows show the near surface flow, open arrowheads the middle level flow. The NOAA 5 Infra-Red image was obtained at 2010 gmt. (Photo: University of Dundee).

Figure 14. SMMR distributions of q_v (full lines kg/m²) and water vapour (shading, kg/m²) for 2134 gmt. The thunderstorm symbol marks the region of deep convective activity. Note that the maximum in the region of 62°N, 7°W probably represents an erroneous SMMR value due to the presence of land (Faeroe Islands).

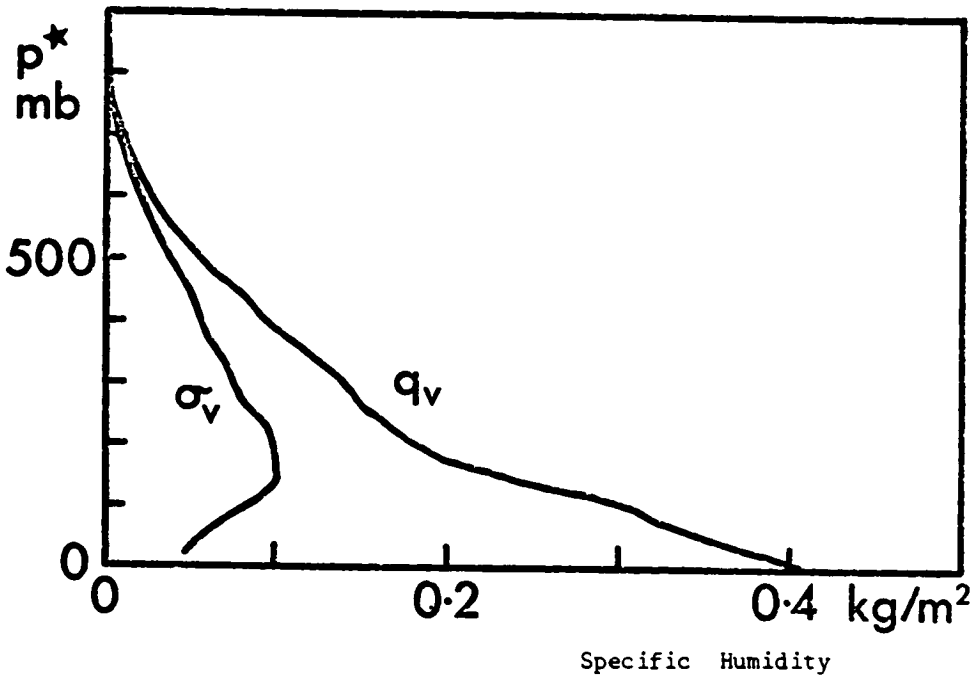

Figure 1. Mean atmospheric water vapour content during JASIN for 5mb layers and the standard deviation of individual radiosonde observations for each layer. Data was available for about 600 ascents.

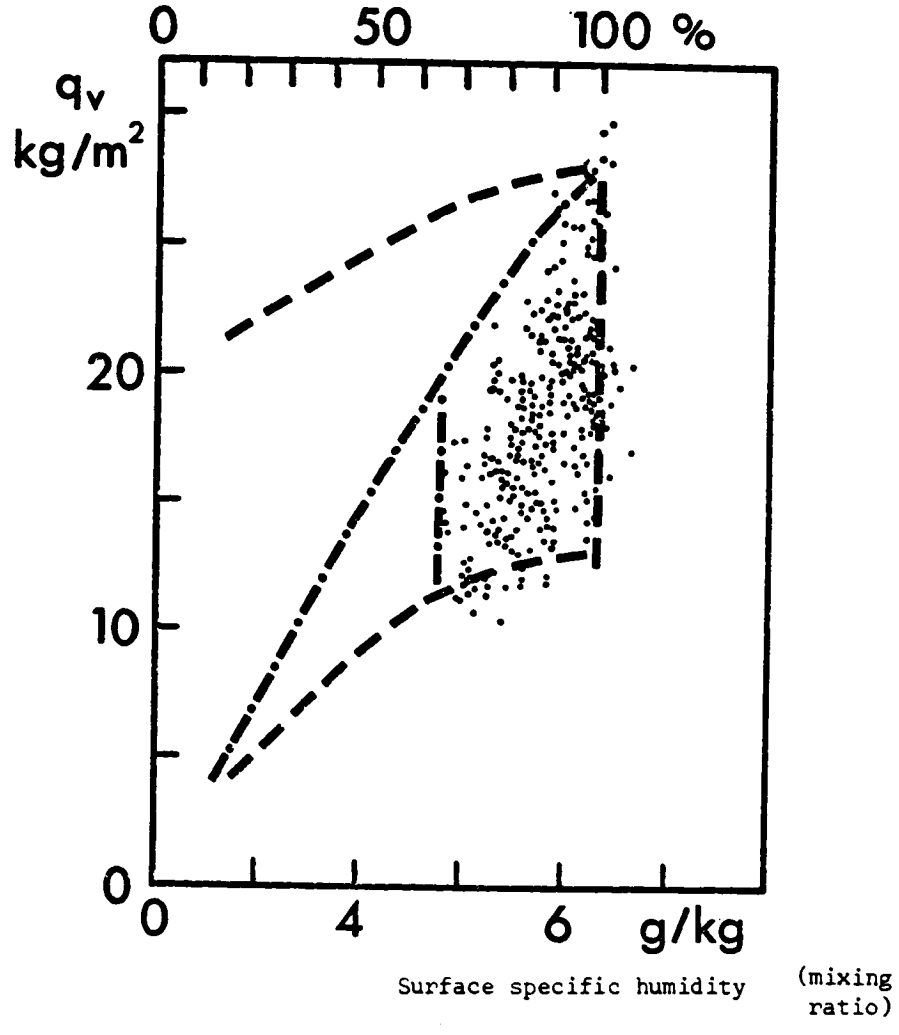

Figure 2. Integrated atmospheric water vapour content q_v for individual radiosonde flights plotted against the near surface specific humidity at the time of launch. The top scale shows approximately the equivalent near surface relative humidity. For further explanation see text.

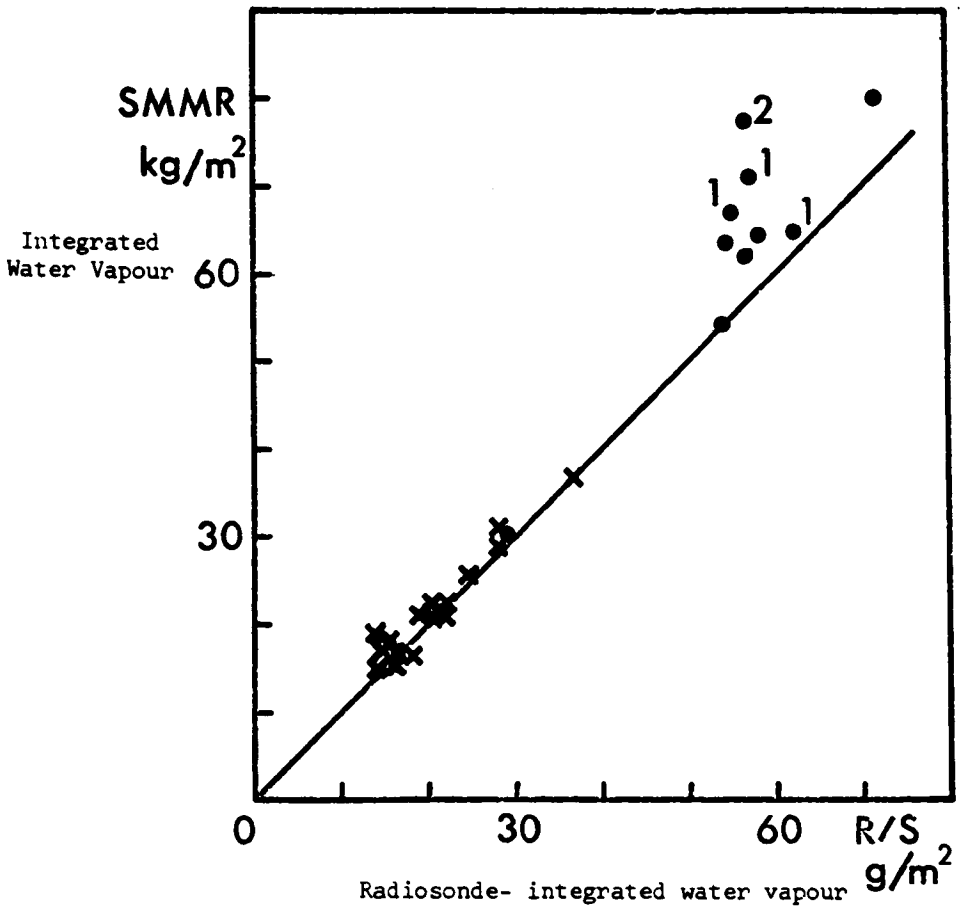

Figure 3. (after Taylor et al. 1981) Seasat-JASIN workshop comparison of integrated atmospheric water vapour q_v as measured by the SMMR and by radiosondes. JASIN values are shown by crosses, tropical soundings by circles. 1 - indicates tropical soundings for which SMMR values may be too high due to the island of Gaum being within the field of view. 2 - SMMR values may have been affected by heavy rain. Processing changes since the workshop have removed the tropical data bias.

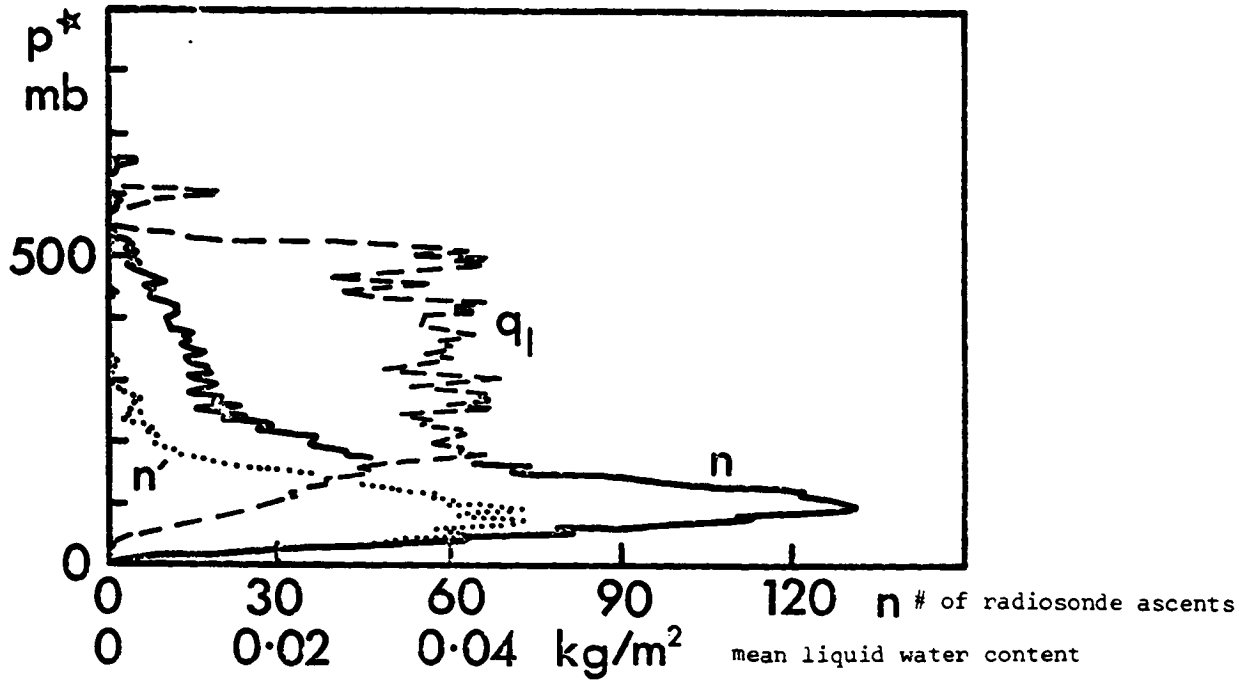

Figure 4. Number of radiosonde ascents for which cloud is inferred for 5mb layers of the atmosphere (full line: multiple cloud layers; dotted line: first layer only). Also shown is the mean liquid water content for cases reporting cloud in each layer (dashed line).

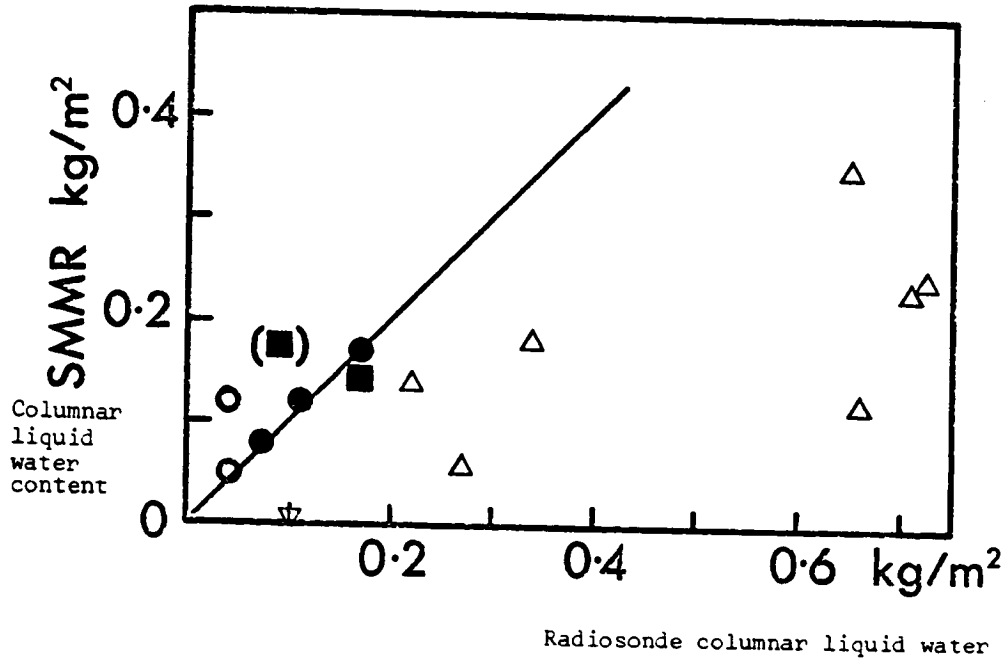

Figure 5. Comparison of SMMR, aircraft, and radiosonde estimates of total liquid water q_l where radiosonde estimates include all cloud layers. □ = Aircraft, other symbols indicate radiosonde values with standard deviation (kg/m²) as follows: ○,● <0.0 5; ▽< 0. 1, △ < 0. 5. Full symbols indicate stratocumulus cases.

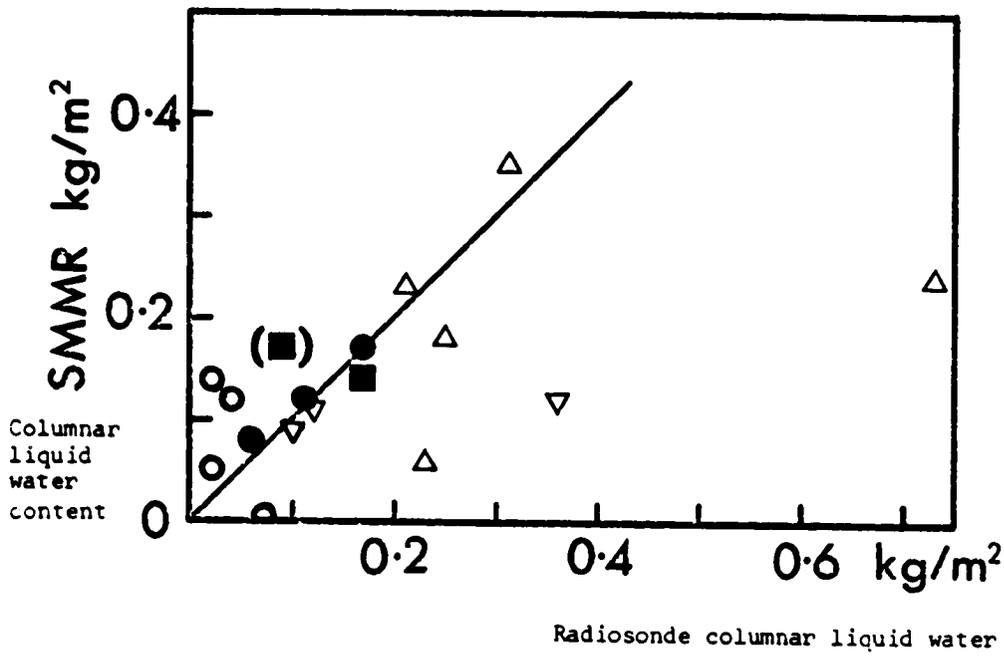

Figure 6. As Figure 5 but radiosonde values include the first cloud layer only.

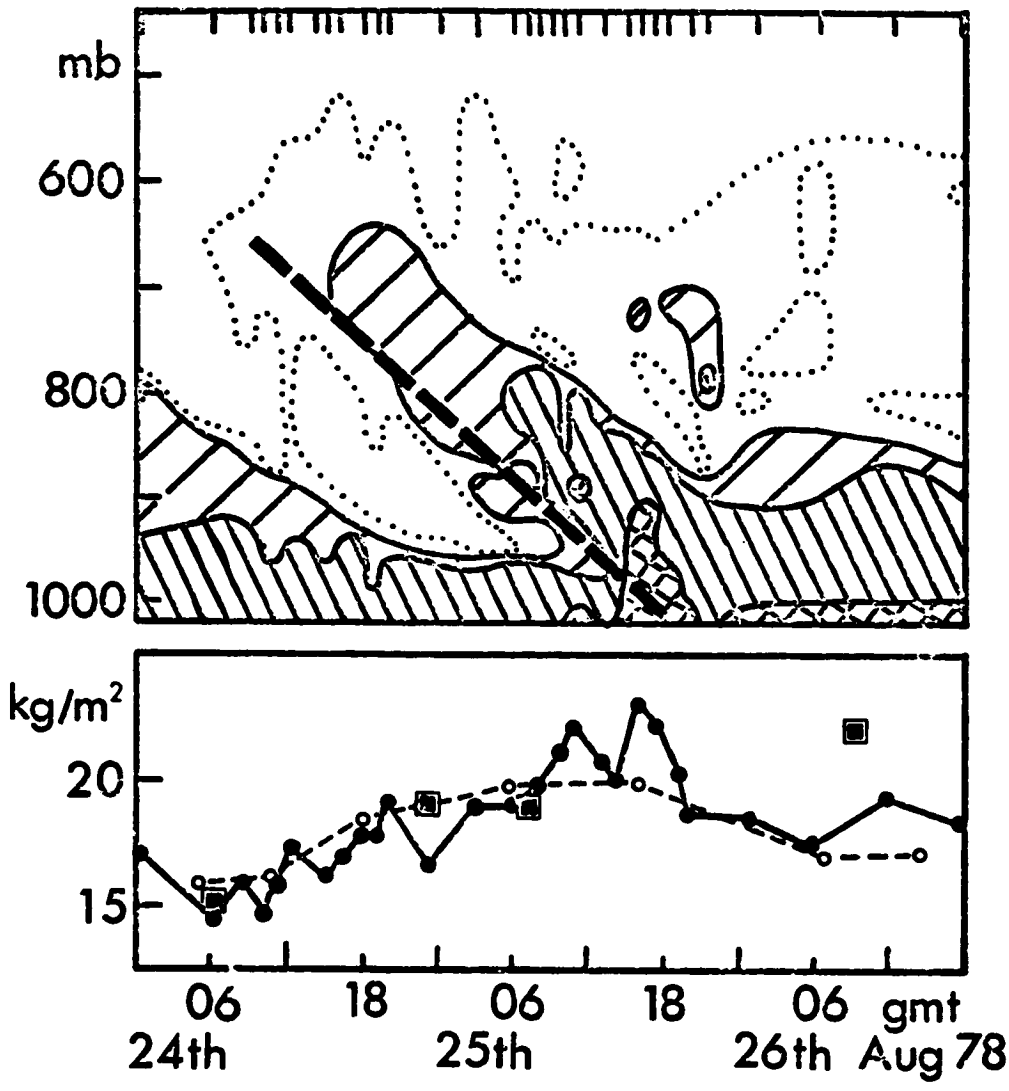

Figure 7. (above) Time-height atmospheric cross-section showing the variation of specific humidity with the passage of a warm front. Values shown are 2g/kg (dotted), 4 to 6 g/kg (wide diagonals), 6 to 8 g/kg (close diagonals), above 8 g/kg (cross-hatched). The section is based on 31 radiosonde flights at the times marked at the top of the figure . The dashed line marks the approximate region of the frontal surface. (below) Values of integrated water vapour q_v from the radiosondes (full line), SMMR (squares), and from the SMMR q_v distribution at 0730 gmt 24 August (dashed line).

(Adapted from Taylor et al. 1981)

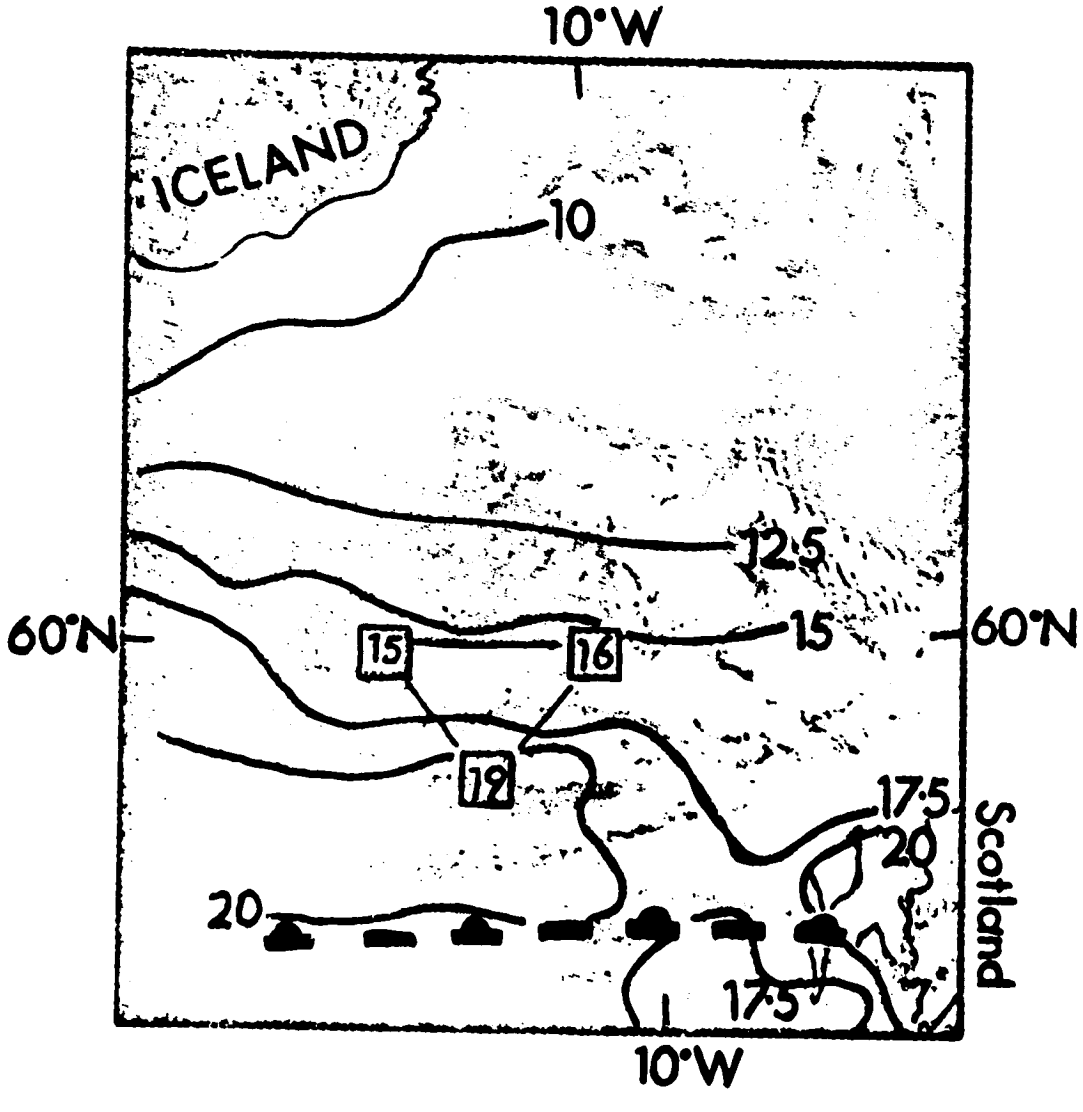

Figure 8. SMMR q_v distribution (kg/m²) at 0730 gmt 24 August 1978 superimposed on NOAA 5 Infra-Red image for 1138 gmt. Radiosonde q_v values are shown in boxes. (Photo: University of Dundee).

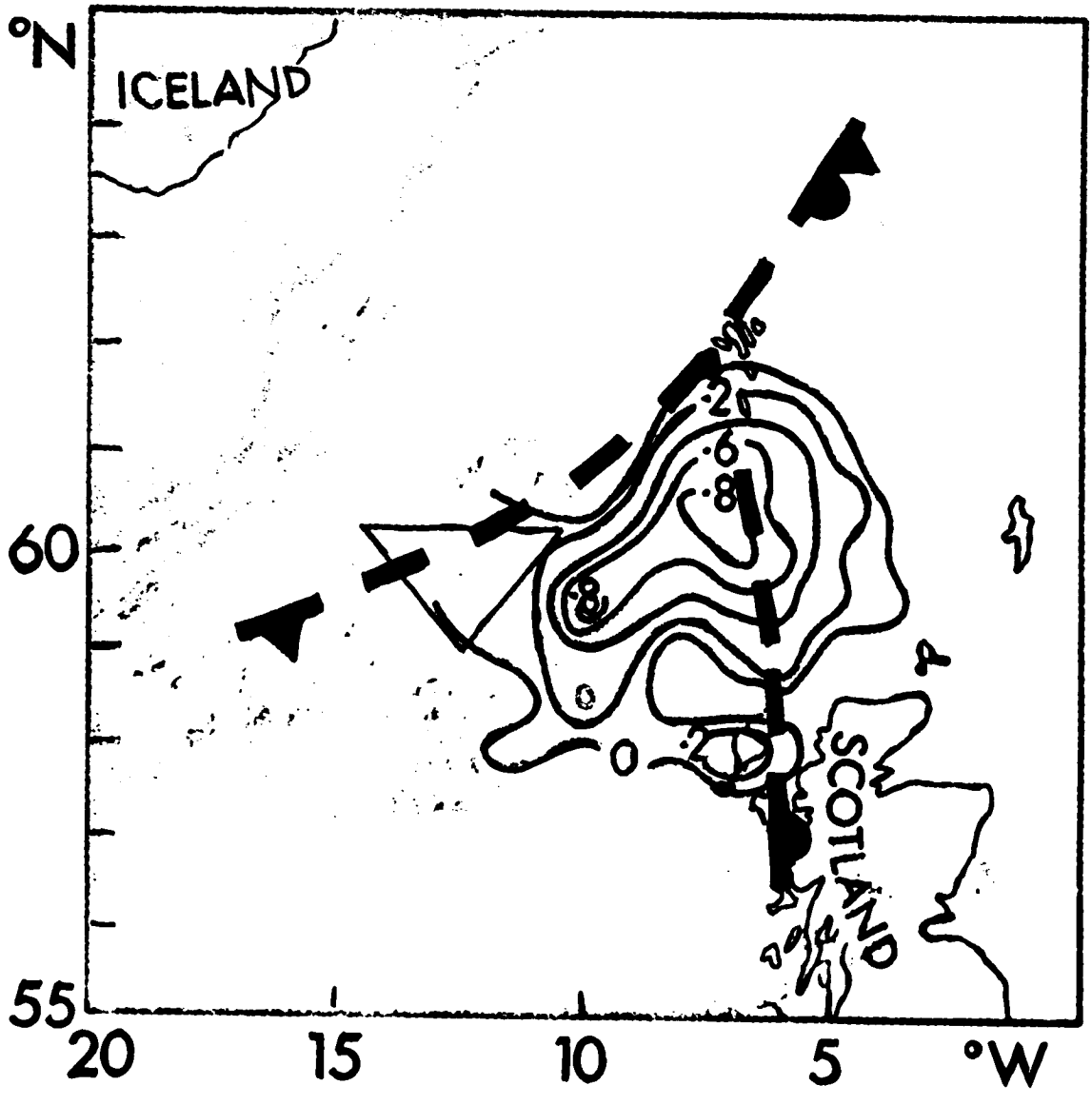

Figure 9. SMMR rain rate values (mm/hour) at 2311 gmt 30 August 1978 superimposed on NOAA 5 Infra-Red image for 2030 gmt. (Photo: University of Dundee).

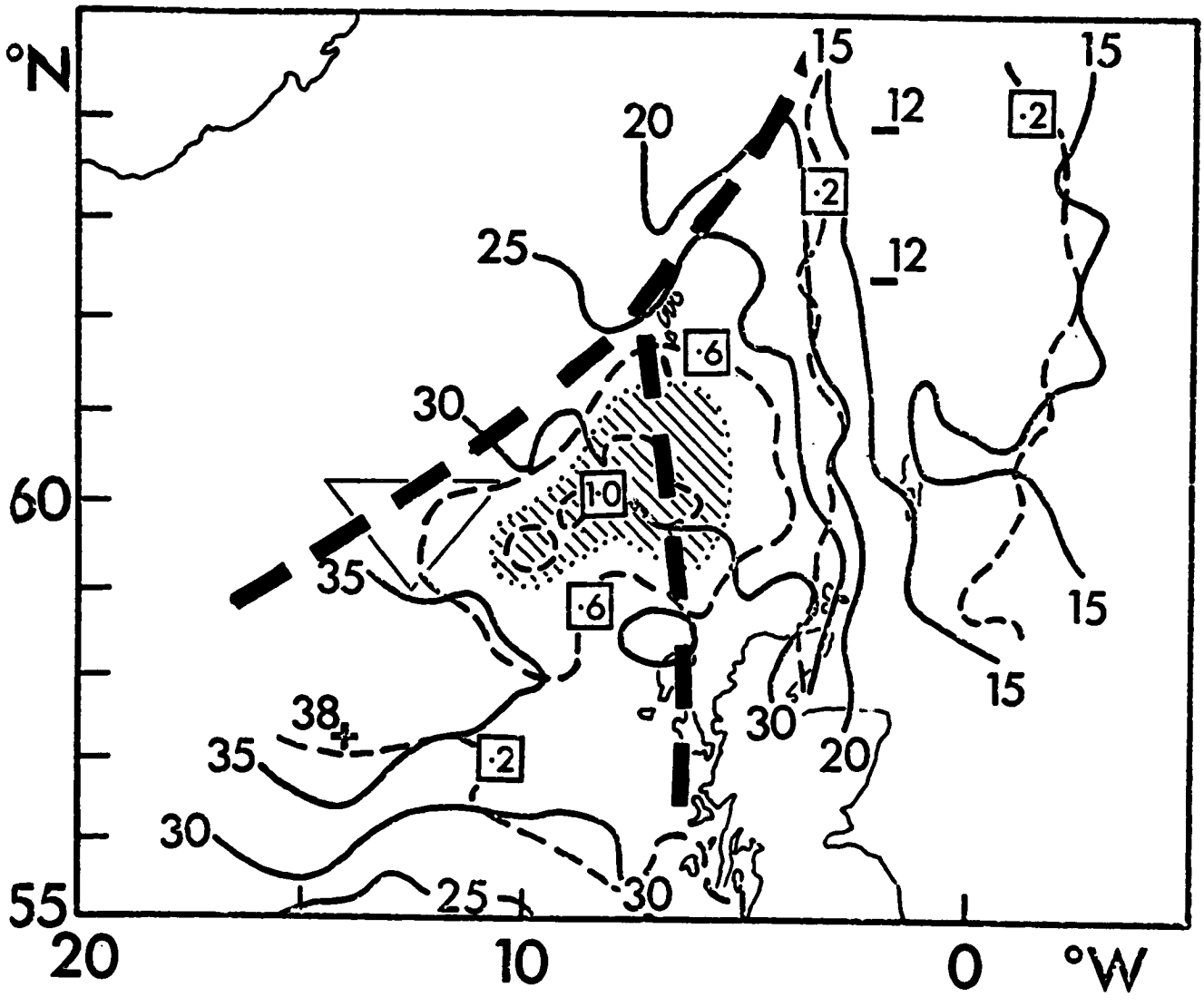

Figure 10. SMMR values of q_v (full lines, kg/m²) and q_l (dashed lines with values in boxes, kg/m²) at 2311 gmt, 30 August 1978. The region of over 0.4mm/hour rain rate is shaded.

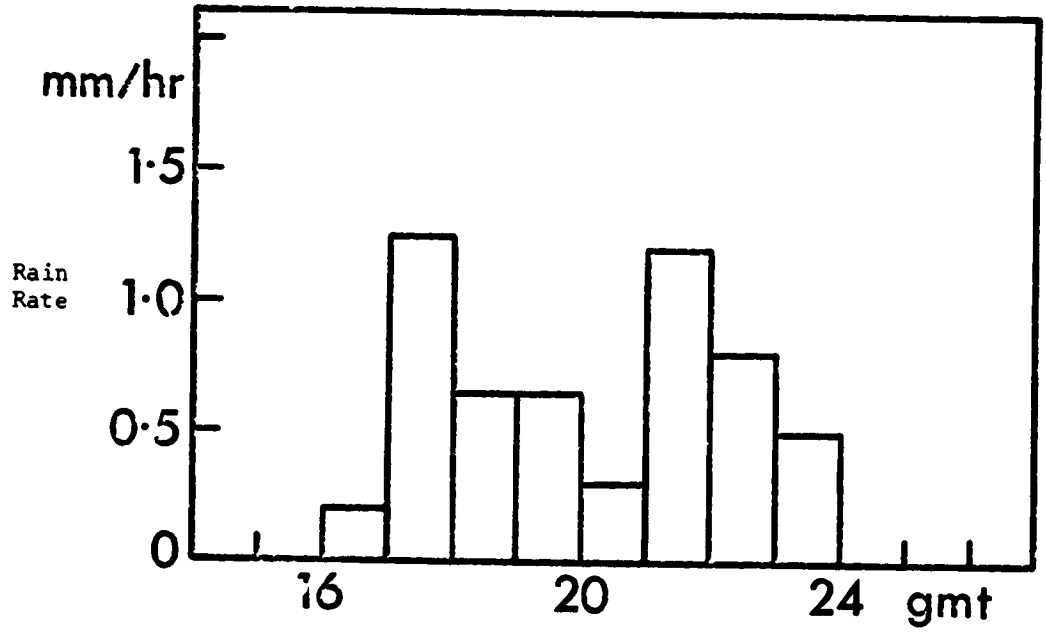

Figure 11. Rainfall measurements from HMS Hecla for the evening of 30 August 1978.

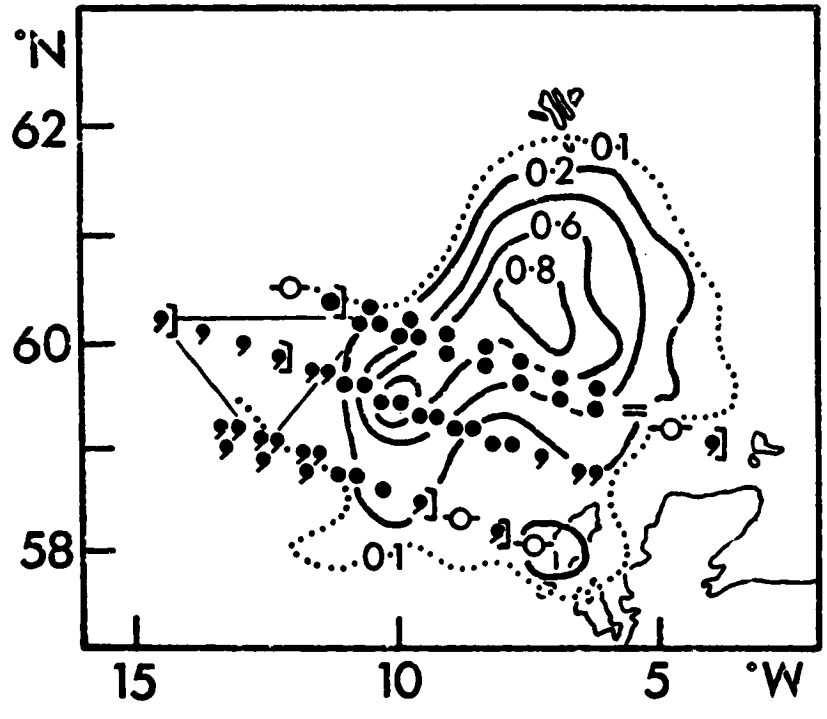

Figure 12. Comparison of SMMR rain rate measurements (as Figure 9) and W.M.O. present weather codes reported from the threo JASIN ships assuming that the rainfall area propagated at 12 m/s toward 110°.

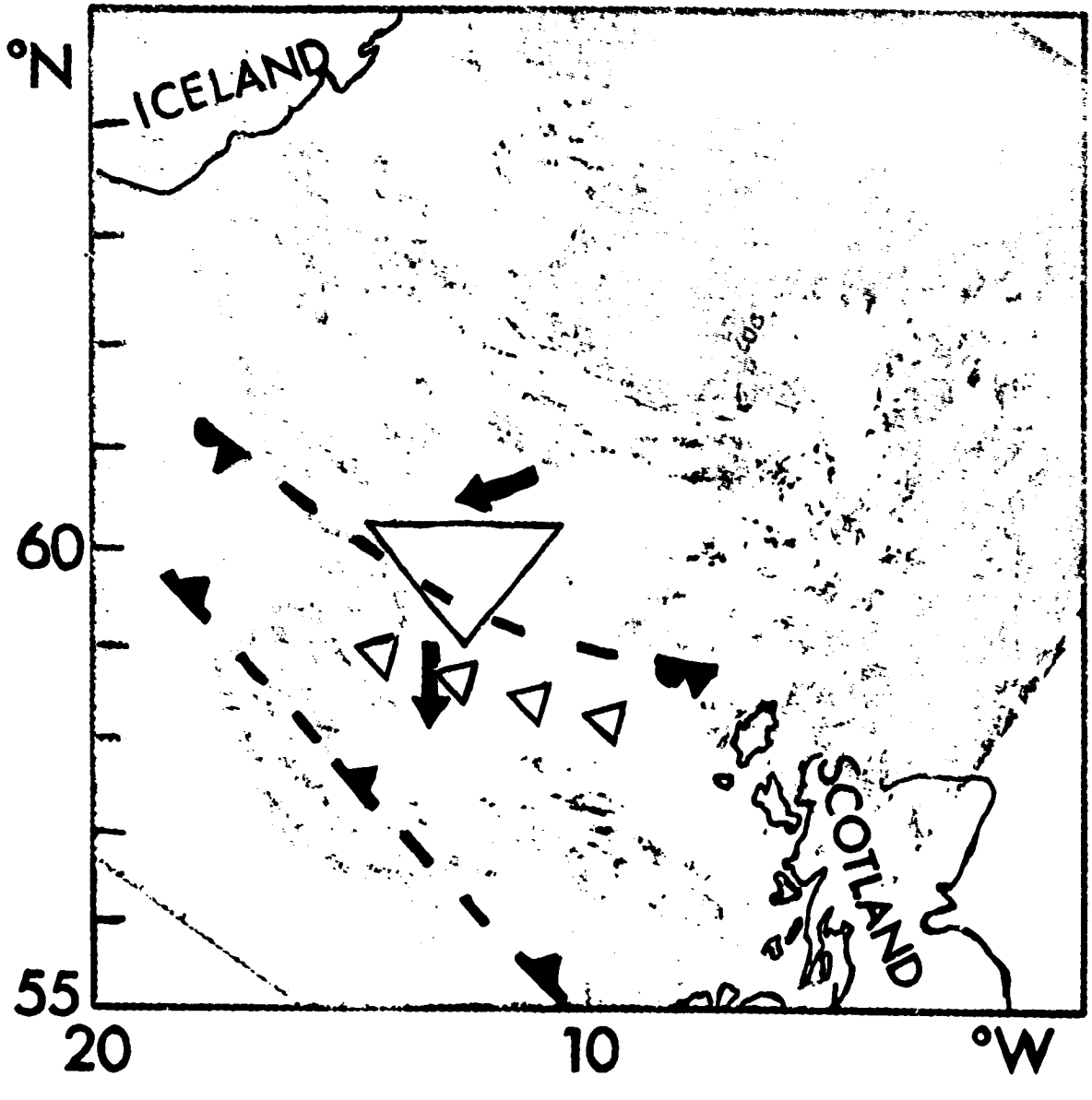

Figure 13. Synoptic chart for 2100 gmt on 4 August 1978, full arrows show the near surface flow, open arrowheads the middle level flow. The NOAA 5 Infra-Red image was obtained at 2010 gmt. (Photo: University of Dundee).

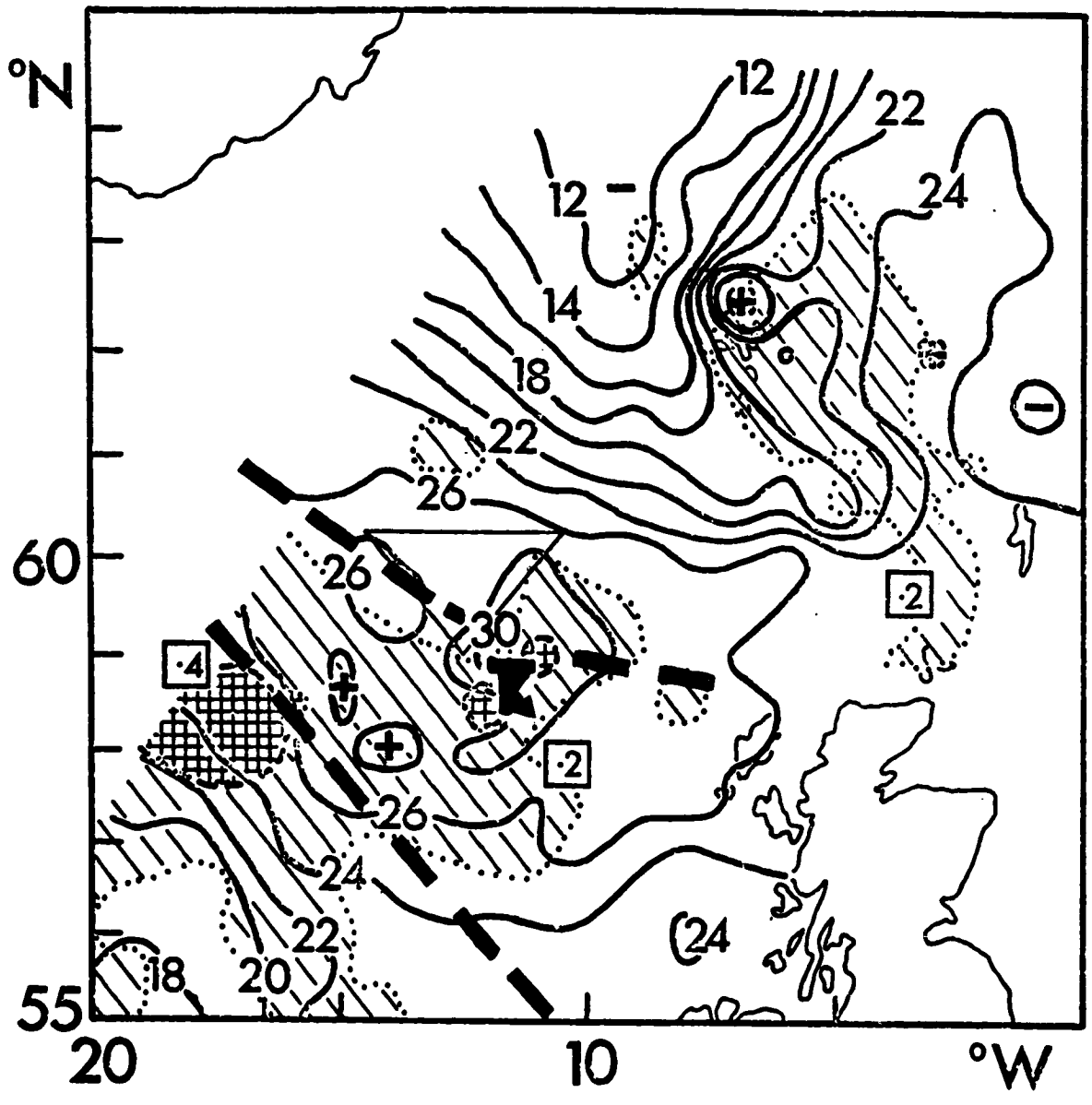

Figure 14. SMMR distributions of q_v (full lines kg/m²) and water vapour (shading, kg/m²) for 2134 gmt. The thunderstorm symbol marks the region of deep convective activity. Note that the maximum in the region of 62°N, 7°W probably represents an erroneous SMMR value due to the presence of land (Faeroe Islands).

In Proceedings of a Workshop on Applications of Existing Satellite Data to the Study of the Ocean Surface Energetics, 19-21 November 1980, University of Wisconsin-Madison (Ed. C. Gautier), 145-149.

SEASAT SMMR'S ATMOSPHERIC WATER DETERMINATIONS

APPENDIX D.

Kristina B. Katsaros
Department of Atmospheric Sciences
University of Washington
Seattle, Washington 98195

Introduction

Over the open ocean three of the five frequencies in the Scanning Multichannel Microwave Radiometers (SMMR) on Seasat and Nimbus 7 are primarily used for determination of the water in the atmospheric column (see Table 1). The algorithms developed for interpretation of these signals provide values of total integrated water vapor, total integrated liquid water, and from sampling the larger drops that would be precipitating, also an estimate of the rain rate. This type of information mapped over large areas with rather fine resolution is providing something totally new and, I believe, potentially very powerful. These data provide sources for research on storm systems, and perhaps in the not too distant future input on the thermodynamics and dynamics of the atmosphere for forecast models.

Table 1

Frequency, Wavelength, Footprint Size, and Principal Geophysical Quantity Predicted by Seasat's 5 Channel SMMR.

Frequency GHz	Microwave Wavelength cm	Seasat's Retrieval Grid at 3dB limit km x km	Principal Predicted Quantity
6.6	4.6	150 x 150	Sea surface temperature
10.7	2.8	85 x 85	Wind speed
18.0	1.7	54 x 54	Precipitation rate (18H) Water vapor, liquid water
21.0	1.4	54 x 54	Water vapor, liquid water
37.0	0.8	27 x 27	Precipitation rate (37H) Windspeed in clear air Water vapor, liquid water

Present status

First a taste of what we have learned from Seasat's SMMR (the Nimbus 7 SMMR data are still being corrected for engineering type problems and an unexplained large bias). The Seasat SMMR products were checked against surface truth collected in the Gulf of Alaska (the Gulf of Alaska Experiment, September 1978), in the North Atlantic (the Joint Air Sea Interaction Experiment, July-August 1978), and from the tropical Pacific (radiosonde measurements from weatherships and small atolls). A summary of the integrated water vapor results is seen in Table 2 (for further details see Katsaros et al., 1980). The r.m.s. errors are of about the same magnitude for the two techniques of obtaining total integrated atmospheric water vapor. Alishouse (1980) has made intercomparisons with a larger number of radiosonde integrations without substantial change in the percent agreement.

Table II. Summary of the Water Vapor Retrievals Considered at the JASIN/Seasat Workshop.

Data set	No points	Raob Mean σ kg/m²		Wentz algo. Mean bias σ kg/m²			Wilheit algo. Mean bias σ kg/m²		
COASEX	7	15		14	-1 (7%)	2.3	18	+3	1.7
JASIN	19	20.3	5.9	21.4	1.2 (6%)	5.8			
Tropics	6	53.9	16.5	59.1	4.9 (9%)	16.5			

Being that the SMMR produced water vapor data is available as a map, it has been found to provide more precise information about the position of the weather fronts during the JASIN experiment than would be ascertained from synoptic maps or 3-hourly radiosonde observations from the three ships in the meteorological triangle with legs ≈ 200 km in length (Taylor, personal communication, 1980).

For the other two products, integrated atmospheric liquid water and precipitation rate, there exists virtually no surface intercomparison data, in part because of the difficulties in measuring these quantities, in part because the emphasis with the SMMR's has been on ocean surface parameters and sea ice. However, even though the algorithms are probably only relatively correct and even though the resolution of the present instruments is coarse compared to the scale of the phenomena, they too look promising. In Katsaros et al. (1980) the two algorithms are compared. They are found to be in agreement

in mid latitudes (low values) of total liquid water content, but differ over tropical areas. One of the algorithms ("Wilheit") has an upper limit to the amount of liquid water it can produce. Gautier (1980) has compared plots of GOES visible data with SMMR's liquid water with qualitative agreement.

For precipitation rate the two algorithms are in fairly good agreement at low rain rates, but differ for large values. In the JASIN experiment, one intercomparison with a ship observation was obtained with good agreement. The Wentz algorithm predicted 2 mm/hr, and over an hour's time 2 mm of rain had been caught by a rain gauge. Wher the JASIN ships reported showers, the satellite retrievals gave no indication of rain, while the occurrence of wide spread rain verified well against the Seasat SMMR.

An exciting portrayal of a frontal rain band is given by the rain rate map calculated from Seasat's SMMR data on rev. 1212 over the eastern Pacific (Figure 1). The presence of multiple cells is very reminiscent of the description of cyclonic rainbands given by Hobbs (1978).

Looking ahead

If one allows one's imagination a bit of freedom in considering ways in which future microwave radiometer data on atmospheric water parameters may aid atmospheric and oceanic research and improve numerical forecast models, one can find good cause for optimism. Figure 2 is a flow chart of how these parameters may be employed. The solid boxes show importance mainly for the atmosphere, the dashed ones for the sea. Simply obtaining data on the distribution of these parameters is, of course, valuable. The deduced "E" and the "P" for the ocean are the time averaged evaporation and precipitation terms, which determine water density and thereby geostrophic currents. The latent heat involved in formation and dissolution of clouds and the net heating, where precipitation occurs, influence the atmospheric energetics and dynamics. Atmospheric motions in turn influence circulations in the upper ocean. The total liquid water in an atmospheric column is, at least for simple cloud structures, the parameter which determines transmittance of shortwave radiation and emittance of longwave radiation. Thus, the satellite measurement of liquid water could be used to predict the radiative heat budget at the sea surface. Having all these relationships parameterized, we feed the real time satellite data into coupled atmosphere/ocean numerical models.

Summary

Information about the water in the atmosphere can be determined from 3 channels on the Scanning Multichannel Microwave Radiometer

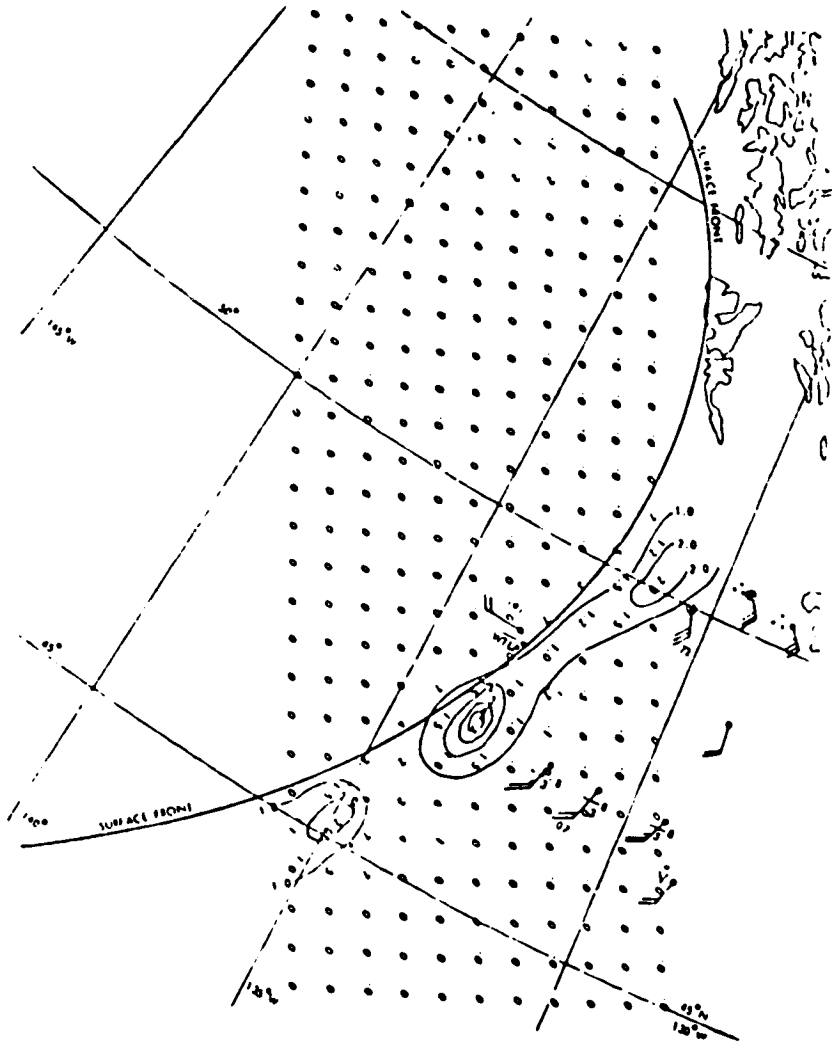

Fig. 1. Seasat SMMR rain rate retrieval from rev. 1212 with corroborating ship reports. (Wentz).

(SMMR) on Seasat and Nimbus 7. The existing algorithms interpret the signals as 1) total integrated water vapor in the column, 2) total liquid water, and 3) precipitation rate.

During several workshops for evaluation of Seasat's SMMR, it has been found that total atmospheric water vapor is determined by SMMR to an accuracy comparable to that of the radiosondes from ships and small tropical atolls. The total liquid water and rain rate determinations have virtually no in situ verification, but look qualitatively very promising. Rain rate determinations are corroborated by standard synoptic frontal analysis and conventional satellite data.

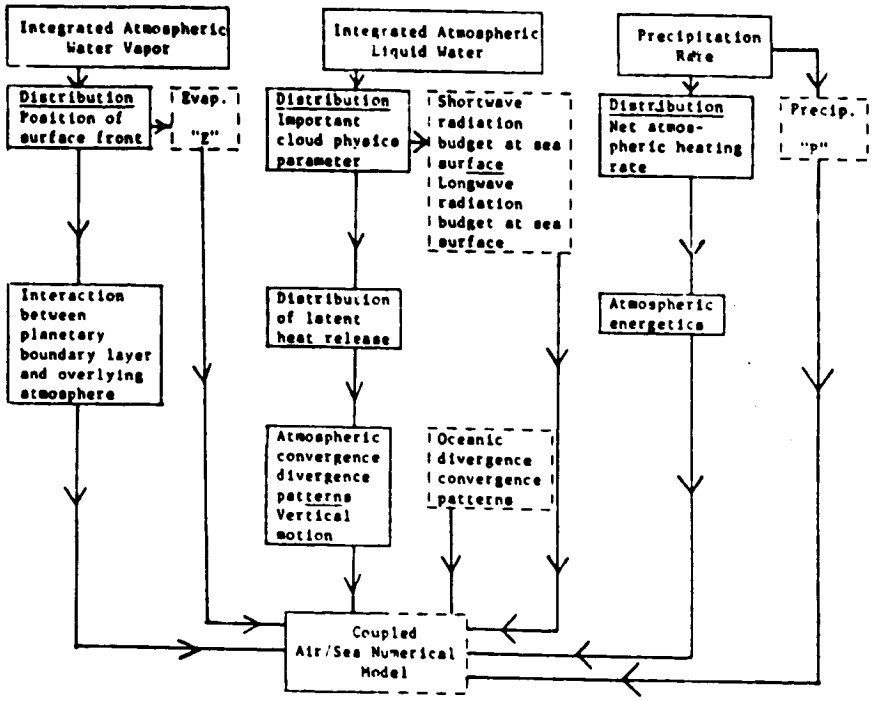

Figure 2. Potential Uses of SMMR Water Vapor Channels.

REFERENCES

Alishouse,J., 1980: Atmospheric water determinations, SMMR Mini-Workshop III, 26-27 August 1980, NASA, Jet Propulsion Laboratory Report 622-224, pp. 7-1 - 7-4.

Gautier, C., 1980: Comparison of SMMR liquid water retrievals with GOES data, SMMR Mini-Workshop III, 26-27 August 1980, NASA, Jet Propulsion Laboratory Report 622-224, pp. 9-1 - 9-5.

Hobbs, P. V., 1978: Organization and structure of clouds and precipitation on the mesoscale and microscale in cyclonic storms, Rev. of Geophys. and Space Phys., 16, 741-755.

Katsaros, K. B., P. K. Taylor, J. C. Alishouse, and R. G. Lipes, 1980: Quality of Seasat SMMR (Scanning Multichannel Microwave Radiometer) atmospheric water determinations, Boundary Layer Meteorol. (in press).

END